ABSTRACT

Title of dissertation:	LEFT-RIGHT SYMMETRIC MODEL AND ITS TEV-SCALE PHENOMENOLOGY
	Chang-Hun Lee, Doctor of Philosophy, 2017
Dissertation directed by:	Professor Rabindra N. Mohapatra Department of Physics

The Standard Model of particle physics is a chiral theory with a broken parity symmetry, and the left-right symmetric model is an extension of the SM with the parity symmetry restored at high energies. Its extended particle content allows us not only to find the solution to the parity problem of the SM but also to solve the problem of understanding the neutrino masses via the seesaw mechanism. If the scale of parity restoration is in the few TeV range, we can expect new physics signals that are not present in the Standard Model in planned future experiments. We investigate the TeV-scale phenomenology of the various classes of left-right symmetric models, focusing on the charged lepton flavour violation, neutrinoless double beta decay, electric dipole moments of charged leptons, and leptogenesis.

LEFT-RIGHT SYMMETRIC MODEL AND ITS TEV-SCALE PHENOMENOLOGY

by

Chang-Hun Lee

Dissertation submitted to the Faculty of the Graduate School of the
University of Maryland, College Park in partial fulfillment
of the requirements for the degree of
Doctor of Philosophy
2017

Advisory Committee:
Professor Rabindra N. Mohapatra, Chair/Advisor
Professor Kaustubh Agashe
Professor Sarah Eno
Professor Niranjan Ramachandran
Professor Raman Sundum

Table of Contents

List of Abbreviations

CLFV	Charged lepton flavour violation
EDM	Electric dipole moment
LH	Left-handed
LHC	Large Hadron Collider
LRSM	Left-right symmetric model
MLRSM	Minimal left-right symmetric model
PMNS	Pontecorvo-Maki-Nakagawa-Sakata
RH	Right-handed
SM	Standard Model
TeV	Teraelectron-Volts
$0\nu\beta\beta$	Neutrinoless double beta decay

Chapter 1: Introduction

The Standard Model (SM) of particle physics is the theoretical framework to explain the fundamental principles of nature. The gauge group of the SM before the spontaneous symmetry breaking is

$$\mathrm{SU}(2)_L \otimes \mathrm{U}(1)_Y. \tag{1.1}$$

The representations of the leptons are

$$L_i = \begin{pmatrix} \nu_{Li} \\ \ell_{Li} \end{pmatrix} \sim (\mathbf{2}, -1), \qquad \ell_{Ri} \sim (\mathbf{1}, -2), \tag{1.2}$$

and for quarks, we have

$$Q_i = \begin{pmatrix} u_{Li} \\ d_{Li} \end{pmatrix} \sim (\mathbf{2}, 1/3), \qquad u_{Ri} \sim (\mathbf{1}, 4/3), \qquad d_{Ri} \sim (\mathbf{1}, -2/3) \tag{1.3}$$

where i is the generation index. In addition, the scalar doublet field is given by

$$\Phi = \begin{pmatrix} \phi^+ \\ \phi^0 \end{pmatrix} \sim (\mathbf{2}, 1). \tag{1.4}$$

The Yukawa interaction Lagrangian is written as

$$\mathcal{L}_Y = -f^{\ell}_{ij}\overline{L_i}\Phi\ell_{Rj} - f^{u}_{ij}\overline{Q_i}\widetilde{\Phi}u_{Rj} - f^{d}_{ij}\overline{Q_i}\Phi d_{Rj} \tag{1.5}$$

where $\widetilde{\Phi} \equiv i\sigma_2\Phi^*$. After spontaneous symmetry breaking of the electroweak gauge group $\mathrm{SU}(2)_L \otimes \mathrm{U}(1)_Y$ to $\mathrm{U}(1)_{\mathrm{em}}$ via the vacuum expectation value (VEV) of Higgs

$$\langle\Phi\rangle = \begin{pmatrix} 0 \\ v_{\mathrm{EW}}/\sqrt{2} \end{pmatrix} \tag{1.6}$$

where $v_{\mathrm{EW}} = 246$ GeV, the Yukawa interaction Lagrangian can be written as

$$\langle\mathcal{L}_Y\rangle = -\frac{1}{\sqrt{2}} f^{\ell}_{ij} v_{\mathrm{EW}} \overline{\ell_{Li}} \ell_{Rj} - \frac{1}{\sqrt{2}} f^{u}_{ij} v_{\mathrm{EW}} \overline{u_{Li}} u_{Rj} - \frac{1}{\sqrt{2}} f^{d}_{ij} v_{\mathrm{EW}} \overline{d_{Li}} d_{Rj}. \tag{1.7}$$

In other words, the charged leptons and quarks acquire masses, and neutrinos remain massless in the SM.

The observation of nonzero neutrino masses and mixing has provided the first experimental evidence for physics beyond the SM. Since the origin of mass for all charged fermions in the SM appears to have been clarified by the discovery of the Higgs boson with mass of 125 GeV at the LHC [1, 2], an important question is whether the same Higgs field is also responsible for neutrino masses. If we simply add three right-handed (RH) neutrinos ν_R to the SM, Yukawa coupling terms of the form

$$\mathcal{L}^{\ell}_Y = -\frac{1}{\sqrt{2}} f^{\ell}_{ij} \overline{L_i} \Phi \nu_{Rj} + \mathrm{H.c.} \tag{1.8}$$

can be written in the lepton sector. After spontaneous symmetry breaking, this Yukawa term gives masses of the form $f^{\ell} v_{\mathrm{EW}}/\sqrt{2}$ to the neutrinos. However, to get sub-eV neutrino masses as observed, it requires $f^{\ell} \lesssim 10^{-12}$ which is an unnaturally small number. This provides sufficient reason to believe that there is new physics behind neutrino masses beyond adding just three RH neutrinos to the SM, thereby providing the first clue to the nature of physics beyond the SM.

A simple paradigm for understanding the small neutrino masses is the type-I seesaw mechanism [3–6] where the RH neutrinos alluded to above have a Majorana mass of the form $m_N \nu_R^\mathsf{T} \nu_R$, in addition to having Dirac masses like all charged fermions in the SM. Neutrinos being electrically neutral allow for this possibility, distinguishing them from the charged fermions, and this feature might be at the heart of such diverse mass and mixing patterns for leptons in contrast with the quark sector. The seesaw mechanism leads to the generic 6×6 neutrino mass matrix

$$M_{\nu N} = \begin{pmatrix} 0 & M_D \\ M_D^\mathsf{T} & M_R \end{pmatrix} \tag{1.9}$$

where the 3×3 Dirac mass matrix M_D mixes the ν_L and ν_R states and is generated by the SM Higgs field, while M_R is the Majorana mass for ν_R which embodies the new neutrino mass physics. In the usual seesaw approximation where $|(M_D M_N^{-1})_{ij}| \ll 1$, the light neutrino mass matrix is given by the seesaw formula

$$M_\nu \approx -M_D M_N^{-1} M_D^\mathsf{T}. \tag{1.10}$$

Seesaw mechanism provides a very simple way to understand the smallness of neutrino mases. Two main ingredients of this mechanism are: (i) the introduction of RH neutrinos ν_R to the SM, and (ii) endowing the ν_R's with a Majorana mass which breaks the accidental $B-L$ symmetry of the SM. In the context of the SM gauge group, these two features do not follow from any underlying principle, but are rather put in by hand. There is, however, a class of theories where both these ingredients of seesaw emerge in a natural manner: the left-right symmetric theories of weak interactions [7–9] based on the gauge group $\mathrm{SU}(2)_L \otimes$ $\mathrm{SU}(2)_R \otimes$ $\mathrm{U}(1)_{B-L}$. The existence of the RH neutrinos is guaranteed by the gauge symmetry in both cases and their Majorana masses are connected to the breaking scale of local $B-L$ symmetry, which is a subgroup of the above gauge groups. Furthermore they also predict the number of ν_R's to be three. Thus, the essential ingredients of seesaw are no more adhoc but are rather connected to symmetries of the extended theory. It is then important to explore how new features of these symmetries can be probed in laboratory experiments. Our focus is on the low-scale left-right symmetric model (LRSM) where the seesaw scale can be in the few TeV range and be accessible to the LHC, while satisfying the observed charged lepton and neutrino mass spectra.

The first question for such models is how the small neutrino masses can be understood if the seesaw scale is indeed in the TeV range, since by naive expectations, the Dirac masses are expected to be similar to the charged lepton masses, which after seesaw would give rise to too large tau neutrino mass. In the context of the minimal LRSM, this question becomes specially important since the Higgs sector relates the neutrino Yukawa couplings with charged lepton ones. There are three ways to fit both charged lepton and neutrino masses in such TeV scale LRSM: (i) by choosing one set of the Yukawa couplings to be $\lesssim 10^{-5.5}$ for a particular VEV assignment for the SM-doublet Higgs fields; (ii) by choosing larger Yukawa couplings and invoking cancellations between Yukawa couplings in the Dirac neutrino mass matrix to get smaller Dirac masses for neutrinos to get seesaw to work and (iii) by choosing particular textures for the Yukawa couplings that guarantees the leading order seesaw contribution to neutrino masses to vanish. We call these models Class

I, II, and III models respectively.

Chapter 2: Minimal left-right symmetric model

2.1 Introduction

In the lepton sector of the minimal left-right symmetric model (MLRSM), we have four mass matrices: the charged lepton mass matrix M_ℓ, the Dirac neutrino mass matrix M_D, and the left-handed and RH Majorana neutrino mass matrices M_L and M_R. The light neutrino mass matrix M_ν is determined by M_D, M_L, and M_R through the seesaw mechanism $M_\nu \approx M_L - M_D M_R^{-1} M_D^\intercal$. Since we have experimental data on the masses of charged leptons and the squared-mass differences of neutrinos as well as their mixing angles, M_ℓ is completely known in the charged lepton mass basis and M_ν is also partially determined in its own mass basis and in the charged lepton mass basis. The neutrino mass matrices M_D, M_L, and M_R are nonetheless completely unknown, and constructing those matrices compatible with experimental data is a nontrivial problem, not only because M_ℓ and M_D in the MLRSM are determined from common Yukawa couplings and electroweak VEV's, but also because those Yukawa coupling matrices have a specific structure (i.e. Hermitian or symmetric) in a specific basis (i.e. symmetry basis) due to the discrete symmetry (i.e. parity or charge conjugation symmetry) of the model that realizes the manifest left-right symmetry at high energies.

For simplicity, we may assume that the electroweak VEV's are all real, in which case M_ℓ and M_D have the same structure (i.e. Hermitian or symmetric) as the Yukawa coupling matrices. Since M_ℓ in that case is diagonalized by a similarity transformation (i.e. $V_R^\ell = V_L^\ell$ for Hermitian M_ℓ, and $V_R^\ell = V_L^{\ell *}$ for symmetric M_ℓ), the mass matrices in the charged lepton mass basis maintain that structure. Hence, we can work in that basis where M_ℓ is completely determined so that we can practically forget about it while keeping the structure of mass matrices. Now using that structure itself, we can find M_R from known M_D [10] or alternatively find M_D from known M_R [11]. Without loss of generality, however, we can make only one of two electroweak VEV's real by gauge transformation. Furthermore, for the TeV-scale MLRSM, M_D assumed or constructed in such ways usually requires fine-tuning of Yukawa couplings and VEV's, and it would be rather difficult to make natural predictions for the TeV-scale phenomenology of the MLRSM using those mass matrices.

Here, we develop a different approach appropriate for the case of type-I dominance (i.e. $M_L = 0$) with complex electroweak VEV's: (i) the Yukawa coupling matrices with a desired structure are constructed from M_ℓ in the symmetry basis; (ii) M_D is determined from those Yukawa couplings as well as the electroweak VEV's, and M_R is calculated from M_D we have found. Since Yukawa couplings are explicitly constructed and M_D is calculated from them, fine-tuned M_D can only appear rarely. With this method, we collect a huge amount of data points that satisfy all the major experimental constraints, and conduct a comprehensive study of the TeV-scale phenomenology of the model, focusing on the CLFV, $0\nu\beta\beta$, and EDM's of charged leptons.

There are several works which studied CLFV and $0\nu\beta\beta$ in the MLRSM: in reference [12], those effects were discussed in the type-I or type-II seesaw dominance, and several processes of $0\nu\beta\beta$ were examined in detail; in reference [13], CLFV and $0\nu\beta\beta$ processes were investigated also in type-I or type-II dominance with emphasis on the allowed masses of doubly charged scalar fields; in reference [14], the type-I+II seesaw contributions were simultaneously considered as in references [10] and [11], but with richer results on the phenomenology; in reference [15], the CLFV effects were studied in detail also in the type-I+II seesaw cases by a slightly different method from the one originally proposed by reference [10]. However, the common features of those works are: (i) real electroweak VEV's were explicitly or implicitly assumed, and (ii) M_D or M_R was chosen for numerical analysis without considering the issue of fine-tuning. Even though we can still obtain meaningful results focusing on specific regions of parameter space with rich phenomenologies, it is important to investigate the predictions of the model in a more natural situation. Furthermore, some works assumed that the tree-level contribution to $\mu \to eee$ is always dominant over the type-I contribution in their analyses. We will also see that this is an inadequate assumption.

2.2 Review of the minimal left-right symmetric model

In this section, we briefly review the MLRSM. The gauge group of the MLRSM is

$$\mathrm{SU}(2)_L \otimes \mathrm{SU}(2)_R \otimes \mathrm{U}(1)_{B-L}, \tag{2.1}$$

and the representations of the leptons are

$$L'_{Li} = \begin{pmatrix} \nu'_{Li} \\ \ell'_{Li} \end{pmatrix} \sim (\mathbf{2}, \mathbf{1}, -1), \qquad L'_{Ri} = \begin{pmatrix} \nu'_{Ri} \\ \ell'_{Ri} \end{pmatrix} \sim (\mathbf{1}, \mathbf{2}, -1) \tag{2.2}$$

where i is the flavour index. The bi-doublet scalar field is given by

$$\Phi = \begin{pmatrix} \phi_1^0 & \phi_2^+ \\ \phi_1^- & \phi_2^0 \end{pmatrix} \sim (\mathbf{2}, \mathbf{2}, 0), \tag{2.3}$$

and the triplet scalar fields are

$$\Delta_L = \begin{pmatrix} \delta_L^+/\sqrt{2} & \delta_L^{++} \\ \delta_L^0 & -\delta_L^+/\sqrt{2} \end{pmatrix} \sim (\mathbf{3}, \mathbf{1}, 2), \quad \Delta_R = \begin{pmatrix} \delta_R^+/\sqrt{2} & \delta_R^{++} \\ \delta_R^0 & -\delta_R^+/\sqrt{2} \end{pmatrix} \sim (\mathbf{1}, \mathbf{3}, 2). \tag{2.4}$$

The Lagrangian terms of Yukawa interactions are written as

$$\mathcal{L}_Y^\ell = -\overline{L'_{Li}}(f_{ij}\Phi + \widetilde{f}_{ij}\widetilde{\Phi})L'_{Rj} - h_{Lij}\overline{L'^c_{Li}}i\sigma_2\Delta_L L'_{Lj} - h_{Rij}\overline{L'^c_{Ri}}i\sigma_2\Delta_R L'_{Rj} + \text{H.c.} \tag{2.5}$$

where

$$\widetilde{\Phi} \equiv \sigma_2\Phi^*\sigma_2 = \begin{pmatrix} \phi_2^{0*} & -\phi_1^+ \\ -\phi_2^- & \phi_1^{0*} \end{pmatrix}. \tag{2.6}$$

Here, $\psi^c \equiv \mathsf{C}\psi^*$, and thus $\overline{\psi^c} = -\psi^\mathsf{T}\mathsf{C}$ where $\mathsf{C} = i\gamma^2\gamma^0$ is the charge conjugation operator in the Dirac-Pauli representation. Note that h_L and h_R are symmetric matrices. Without loss of generality, we can write the VEV's of scalar fields as

$$\Phi = \begin{pmatrix} \kappa_1/\sqrt{2} & 0 \\ 0 & \kappa_2 e^{i\alpha}/\sqrt{2} \end{pmatrix}, \quad \Delta_L = \begin{pmatrix} 0 & 0 \\ v_L e^{i\theta_L}/\sqrt{2} & 0 \end{pmatrix}, \quad \Delta_R = \begin{pmatrix} 0 & 0 \\ v_R/\sqrt{2} & 0 \end{pmatrix}. \tag{2.7}$$

After spontaneous symmetry breaking, the mass matrix of charged leptons is written as

$$M_\ell = \frac{1}{\sqrt{2}}(f\kappa_2 e^{i\alpha} + \widetilde{f}\kappa_1), \tag{2.8}$$

and the neutrino mass term is given by

$$\mathcal{L}_\nu^{\text{mass}} = -\frac{1}{2}(\overline{\nu'_L}\ \overline{\nu'^c_R}) \begin{pmatrix} M_L & M_D \\ M_D^\intercal & M_R \end{pmatrix} \begin{pmatrix} \nu'^c_L \\ \nu'_R \end{pmatrix} + \text{H.c.} \tag{2.9}$$

where

$$M_D = \frac{1}{\sqrt{2}}(f\kappa_1 + \widetilde{f}\kappa_2 e^{-i\alpha}), \qquad M_L = \sqrt{2} h_L^* v_L e^{-i\theta_L}, \qquad M_R = \sqrt{2} h_R v_R. \tag{2.10}$$

When $v_L \ll \kappa_1, \kappa_2 \ll v_R$, the light neutrino mass matrix is given by the seesaw mechanism

$$M_\nu \approx M_L - M_D M_R^{-1} M_D^\intercal. \tag{2.11}$$

In this paper, we only consider the case of type-I dominance by assuming $v_L = 0$, and the light neutrino mass matrix is given by the type-I seesaw formula

$$M_\nu \approx -M_D M_R^{-1} M_D^\intercal. \tag{2.12}$$

We denote the mass eigenstates of the light and heavy neutrinos as ν_i and N_i ($i = 1, 2, 3$), respectively. The charged gauge bosons W_L^-, W_R^- in the gauge basis can be written in terms of the mass eigenstates W_1^-, W_2^- as

$$\begin{pmatrix} W_L^- \\ W_R^- \end{pmatrix} = \begin{pmatrix} \cos\xi & \sin\xi e^{i\alpha} \\ -\sin\xi e^{-i\alpha} & \cos\xi \end{pmatrix} \begin{pmatrix} W_1^- \\ W_2^- \end{pmatrix} \tag{2.13}$$

where ξ is the W_L-W_R mixing parameter given by

$$\xi \approx -\frac{\kappa_1 \kappa_2}{v_R^2}. \tag{2.14}$$

The masses of charged gauge bosons are

$$m_{W_1}^2 \approx \frac{1}{4} g^2 v_{\mathrm{EW}}^2, \qquad m_{W_2}^2 \approx \frac{1}{2} g^2 v_R^2 \tag{2.15}$$

where $v_{\mathrm{EW}} = \sqrt{\kappa_1^2 + \kappa_2^2} = 246$ GeV is the VEV of the SM. In addition, the masses of neutral gauge bosons Z_1, Z_2, A are given by

$$m_{Z_1}^2 \approx \frac{g^2 v_{\mathrm{EW}}^2}{4 \cos^2 \theta_W}, \qquad m_{Z_2}^2 \approx \frac{g^2 \cos^2 \theta_W v_R^2}{\cos 2\theta_W}, \qquad m_A^2 = 0 \tag{2.16}$$

where θ_W is the Weinberg angle. We can identify W_1, Z_1, A as W, Z, the photon of the SM, respectively. The neutral gauge bosons W_L^3, W_R^3, B in the gauge basis are expressed in terms of the mass eigenstates as

$$\begin{pmatrix} W_L^3 \\ W_R^3 \\ B \end{pmatrix} = \begin{pmatrix} 1 & 0 & 0 \\ 0 & \cos\zeta_1 & \sin\zeta_1 \\ 0 & -\sin\zeta_1 & \cos\zeta_1 \end{pmatrix} \begin{pmatrix} \cos\zeta_2 & 0 & \sin\zeta_2 \\ 0 & 1 & 0 \\ -\sin\zeta_2 & 0 & \cos\zeta_2 \end{pmatrix} \begin{pmatrix} \cos\zeta_3 & \sin\zeta_3 & 0 \\ -\sin\zeta_3 & \cos\zeta_3 & 0 \\ 0 & 0 & 1 \end{pmatrix} \begin{pmatrix} Z_1 \\ Z_2 \\ A \end{pmatrix} \tag{2.17}$$

where

$$\zeta_1 = \sin^{-1}(\tan\theta_W), \qquad \zeta_2 \approx \theta_W, \qquad \zeta_3 \approx -\frac{g^2 \sqrt{\cos 2\theta_W} v_{\mathrm{EW}}^2}{4\cos^2\theta_W m_{Z_2}^2}. \tag{2.18}$$

For the MLRSM with a manifest left-right symmetry before spontaneous symmetry breaking, we need a discrete symmetry which could be either the parity symmetry or the charge conjugation symmetry. In case of the parity symmetry, we have the relationships of fields and Yukawa couplings given by

$$L'_{Li} \leftrightarrow L'_{Ri}, \qquad \Delta_L \leftrightarrow \Delta_R, \qquad \Phi \leftrightarrow \Phi^\dagger, \qquad f = f^\dagger, \qquad \widetilde{f} = \widetilde{f}^\dagger, \qquad h_L = h_R, \tag{2.19}$$

and in case of the charge conjugation symmetry

$$L'_{Li} \leftrightarrow L'^c_{Ri}, \qquad \Delta_L \leftrightarrow \Delta_R^*, \qquad \Phi \leftrightarrow \Phi^\mathsf{T}, \qquad f = f^\mathsf{T}, \qquad \widetilde{f} = \widetilde{f}^\mathsf{T}, \qquad h_L = h_R^*. \tag{2.20}$$

We consider only the parity symmetry here. This symmetry is manifest in a specific basis in the flavour space, which we call the symmetry basis. The scalar potential invariant under the parity symmetry is written as

$$\begin{aligned}
V = &-\mu_1^2 \mathrm{Tr}\big[\Phi^\dagger\Phi\big] - \mu_2^2\left(\mathrm{Tr}\big[\Phi^\dagger\widetilde{\Phi}\big] + \mathrm{Tr}\big[\widetilde{\Phi}^\dagger\Phi\big]\right) - \mu_3^2\left(\mathrm{Tr}\big[\Delta_L^\dagger\Delta_L\big] + \mathrm{Tr}\big[\Delta_R^\dagger\Delta_R\big]\right) \\
&+ \lambda_1 \mathrm{Tr}\big[\Phi^\dagger\Phi\big]^2 + \lambda_2\left(\mathrm{Tr}\big[\Phi^\dagger\widetilde{\Phi}\big]^2 + \mathrm{Tr}\big[\widetilde{\Phi}^\dagger\Phi\big]^2\right) + \lambda_3 \mathrm{Tr}\big[\Phi^\dagger\widetilde{\Phi}\big]\mathrm{Tr}\big[\widetilde{\Phi}^\dagger\Phi\big] + \lambda_4 \mathrm{Tr}\big[\Phi^\dagger\Phi\big]\left(\mathrm{Tr}\big[\Phi^\dagger\widetilde{\Phi}\big] + \mathrm{Tr}\big[\widetilde{\Phi}^\dagger\Phi\big]\right) \\
&+ \rho_1\left(\mathrm{Tr}\big[\Delta_L^\dagger\Delta_L\big]^2 + \mathrm{Tr}\big[\Delta_R^\dagger\Delta_R\big]^2\right) + \rho_2\left(\mathrm{Tr}\big[\Delta_L^\dagger\Delta_L^\dagger\big]\mathrm{Tr}\big[\Delta_L\Delta_L\big] + \mathrm{Tr}\big[\Delta_R^\dagger\Delta_R^\dagger\big]\mathrm{Tr}\big[\Delta_R\Delta_R\big]\right) \\
&+ \rho_3 \mathrm{Tr}\big[\Delta_L^\dagger\Delta_L\big]\mathrm{Tr}\big[\Delta_R^\dagger\Delta_R\big] + \rho_4\left(\mathrm{Tr}\big[\Delta_L^\dagger\Delta_L^\dagger\big]\mathrm{Tr}\big[\Delta_R\Delta_R\big] + \mathrm{Tr}\big[\Delta_L\Delta_L\big]\mathrm{Tr}\big[\Delta_R^\dagger\Delta_R^\dagger\big]\right) \\
&+ \alpha_1 \mathrm{Tr}\big[\Phi^\dagger\Phi\big]\left(\mathrm{Tr}\big[\Delta_L^\dagger\Delta_L\big] + \mathrm{Tr}\big[\Delta_R^\dagger\Delta_R\big]\right) + \left\{\alpha_2 e^{i\delta_2}\left(\mathrm{Tr}\big[\Phi^\dagger\widetilde{\Phi}\big]\mathrm{Tr}\big[\Delta_L^\dagger\Delta_L\big] + \mathrm{Tr}\big[\widetilde{\Phi}^\dagger\Phi\big]\mathrm{Tr}\big[\Delta_R^\dagger\Delta_R\big]\right) + \mathrm{H.c.}\right\} \\
&+ \alpha_3\left(\mathrm{Tr}\big[\Phi\Phi^\dagger\Delta_L\Delta_L^\dagger\big] + \mathrm{Tr}\big[\Phi^\dagger\Phi\Delta_R\Delta_R^\dagger\big]\right) + \beta_1\left(\mathrm{Tr}\big[\Phi^\dagger\Delta_L^\dagger\Phi\Delta_R\big] + \mathrm{Tr}\big[\Phi^\dagger\Delta_L\Phi\Delta_R^\dagger\big]\right) \\
&+ \beta_2\left(\mathrm{Tr}\big[\Phi^\dagger\Delta_L^\dagger\widetilde{\Phi}\Delta_R\big] + \mathrm{Tr}\big[\widetilde{\Phi}^\dagger\Delta_L\Phi\Delta_R^\dagger\big]\right) + \beta_3\left(\mathrm{Tr}\big[\widetilde{\Phi}^\dagger\Delta_L^\dagger\Phi\Delta_R\big] + \mathrm{Tr}\big[\Phi^\dagger\Delta_L\widetilde{\Phi}\Delta_R^\dagger\big]\right).
\end{aligned} \tag{2.21}$$

In this paper, we study the TeV-scale MLRSM without fine-tuning, for which $\kappa_1 \gg \kappa_2$ is one of the sufficient conditions, as we will see in section 2.4. The physical scalar fields and their masses when $v_L = 0$ and $v_R \gg \kappa_1 \gg \kappa_2$ are summarized in table 2.1 [16].

2.3 Construction of lepton mass matrices

Now, we discuss the procedure to construct lepton mass matrices that satisfy the experimental constraints in the light lepton sector (i.e. light neutrino masses and mixing angles) in case of type-I dominance. The Yukawa coupling matrices f, $\widetilde{f}$ in the symmetry basis are Hermitian due to the parity symmetry before spontaneous symmetry breaking. However, the mass matrices M_ℓ and M_D in the same basis do not have such structures when the electroweak VEV's are complex, and it is therefore a non-trivial problem to construct mass matrices that would give Yukawa couplings with the right structure in the symmetry basis and simultaneously satisfy all the constraints in the light lepton sector.

The procedure to construct such lepton mass matrices is as follows: (i) first, we find M_ℓ in the symmetry basis that gives the right masses of charged leptons, and build up f, $\widetilde{f}$, and VEV's out of it. The solutions are not unique; (ii) M_D is constructed in the straightforward way from the Yukawa couplings and VEV's we have obtained, and M_R can also be easily calculated from this M_D and the type-I seesaw formula of equation 2.12.

Since the masses of charged leptons are already known, M_ℓ in the symmetry basis can be easily constructed from

$$M_\ell = V_L^\ell M_\ell^c V_R^{\ell\dagger} \tag{2.22}$$

where V_L^ℓ and V_R^ℓ are arbitrary unitary matrices and M_ℓ^c is the diagonal matrix which has charged lepton masses as its entries. The superscript c denotes mass matrices in the charged lepton mass basis, and we always assume that matrices without any superscript are in the symmetry basis. Note that V_L^ℓ and V_R^ℓ are totally different matrices in general even with a manifest discrete symmetry when the electroweak VEV's are complex. With the parity symmetry, we have $M_\ell = Ae^{i\alpha} + B$ ($A \equiv f\kappa_2/\sqrt{2}$, $B \equiv \widetilde{f}\kappa_1/\sqrt{2}$) where A, B are Hermitian matrices. Therefore, for the rest of step (i), we claim that, for an arbitrary matrix M, it is always possible to find Hermitian matrices A, B such that $M = Ae^{i\alpha} + B$.

In order to prove it, we explicitly construct Hermitian matrices A, B that satisfy $M = Ae^{i\alpha} + B$. First, we write $A_{ij} = |A_{ij}|e^{i\theta_{ij}}$ and $B_{ij} = |B_{ij}|e^{i\phi_{ij}}$ where $\theta_{ji} = -\theta_{ij}$ and $\phi_{ji} = -\phi_{ij}$. Then, we have $M_{ij} = |A_{ij}|e^{i(\alpha+\theta_{ij})} + |B_{ij}|e^{i\phi_{ij}}$ and $M_{ji} = |A_{ij}|e^{i(\alpha-\theta_{ij})} + |B_{ij}|e^{-i\phi_{ij}}$. From these expressions, it is straightforward to derive

$$2|A_{ij}|\sin\alpha = \pm\sqrt{\mathrm{Re}[M_{ji} - M_{ij}]^2 + \mathrm{Im}[M_{ji} + M_{ij}]^2} \tag{2.23}$$

and

$$\tan\theta_{ij} = \frac{\mathrm{Re}[M_{ji} - M_{ij}]}{\mathrm{Im}[M_{ji} + M_{ij}]}. \tag{2.24}$$

Note that two different values of θ_{ij} are allowed in the range $-\pi < \theta_{ij} < \pi$ for each pair of i, j. In addition, since $|\sin\alpha| \leq 1$, we must have

$$|A_{ij}| \geq \frac{1}{2}\sqrt{\mathrm{Re}[M_{ji} - M_{ij}]^2 + \mathrm{Im}[M_{ji} + M_{ij}]^2} \tag{2.25}$$

which sets the lower bound of $|A_{ij}|$ for given M. If $|A_{ij}| \neq 0$, we can write

$$\sin\alpha = \pm\frac{1}{2|A_{ij}|}\sqrt{\mathrm{Re}[M_{ji} - M_{ij}]^2 + \mathrm{Im}[M_{ji} + M_{ij}]^2}. \tag{2.26}$$

Now we choose an arbitrary real number $|A_{11}|$ that satisfies

$$|A_{11}| > \big|\mathrm{Im}[M_{11}]\big|, \tag{2.27}$$

and determine α from

$$\sin\alpha = \pm\frac{\big|\mathrm{Im}[M_{11}]\big|}{|A_{11}|}. \tag{2.28}$$

Note that four different values of α are allowed in the range $-\pi < \alpha < \pi$. We can find all the other $|A_{ij}|$ from

$$|A_{ij}| = \frac{1}{2|\sin\alpha|}\sqrt{\mathrm{Re}[M_{ji} - M_{ij}]^2 + \mathrm{Im}[M_{ji} + M_{ij}]^2} \tag{2.29}$$

$$= \frac{|A_{11}|}{2\big|\mathrm{Im}[M_{11}]\big|}\sqrt{\mathrm{Re}[M_{ji} - M_{ij}]^2 + \mathrm{Im}[M_{ji} + M_{ij}]^2}. \tag{2.30}$$

By equations 2.30 and 2.24, A is completely determined. Alternatively we can write

$$A_{ij} = \pm\frac{1}{2|\sin\alpha|}\big(\mathrm{Im}[M_{ji} + M_{ij}] + i\mathrm{Re}[M_{ji} - M_{ij}]\big) \tag{2.31}$$

$$= \pm\frac{|A_{11}|}{2\big|\mathrm{Im}[M_{11}]\big|}\big(\mathrm{Im}[M_{ji} + M_{ij}] + i\mathrm{Re}[M_{ji} - M_{ij}]\big). \tag{2.32}$$

It is now trivial to find B from $B = M - Ae^{i\alpha}$, and explicitly

$$\begin{aligned}\mathrm{Re}[B_{ij}] &= \frac{1}{2}\mathrm{Re}[M_{ji} + M_{ij}] - \mathrm{Re}[A_{ij}]\cos\alpha,\\ \mathrm{Im}[B_{ij}] &= -\frac{1}{2}\mathrm{Im}[M_{ji} - M_{ij}] - \mathrm{Im}[A_{ij}]\cos\alpha,\end{aligned} \tag{2.33}$$

or

$$B_{ij} = \frac{1}{2}\big(\mathrm{Re}[M_{ji} + M_{ij}] - i\mathrm{Im}[M_{ji} - M_{ij}]\big) - A_{ij}\cos\alpha. \tag{2.34}$$

Note that A and B are indeed Hermitian matrices. Since we have two choices of A_{ij} for each pair of i, j as well as each choice of α and $|A_{11}|$, there are 2^6 choices of A

for each α and $|A_{11}|$ as we have three diagonal and three off-diagonal independent components in A. Moreover, since we have four choices of α for each $|A_{11}|$, there are total $2^6 \cdot 4 = 256$ different choices of A, B, and α for each choice of $|A_{11}|$. We use this method to construct lepton mass matrices in the TeV-scale MLRSM.

2.4 Conditions for the TeV-scale minimal left-right symmetric model

In the MLRSM, M_ℓ and M_D are determined from common Yukawa couplings and VEV's: f, $\widetilde{f}$, κ_1, and $\kappa_2 e^{i\alpha}$. Hence, it would be natural if the largest component of M_D is $\mathcal{O}(1)$ GeV, since the largest component of M_ℓ should be comparable to $m_\tau \sim \mathcal{O}(1)$ GeV. However, this implies that the smallest heavy neutrino mass should be larger than $\mathcal{O}(10^{10})$ GeV, since M_ν is determined from the seesaw formula of equation 2.12 and the present upper bound of the light neutrino mass is $m_\nu \lesssim \mathcal{O}(0.1)$ eV [17].

For the TeV-scale MLRSM, i.e. 0.1 TeV $\lesssim m_N \lesssim$ 100 TeV, we need $|M_{Dij}| \lesssim 10^{-3}$ GeV. Since $M_D = (f\kappa_1 + \widetilde{f}\kappa_2 e^{-i\alpha})/\sqrt{2}$ in the MLRSM, its largest component could be as small as 10^{-3} GeV when the corresponding components of $f\kappa_1$ and $\widetilde{f}\kappa_2 e^{-i\alpha}$ almost cancel each other, which is however unnatural. One solution to avoid such cancellation is that either $f\kappa_2$ or $\widetilde{f}\kappa_1$ is dominant in M_ℓ while $\widetilde{f}\kappa_2$ and $f\kappa_1$ are both small and comparable to each other in M_D. Note that we need hierarchies in both Yukawa couplings and VEV's to satisfy this condition. Even though it is good enough if only a few components of either $f\kappa_2$ or $\widetilde{f}\kappa_1$ that correspond to m_τ and m_μ are dominant in M_ℓ, we assume that all the components of either $f\kappa_2$ or $\widetilde{f}\kappa_1$ are dominant over the others for simplicity.

Now we write $A \equiv f\kappa_2/\sqrt{2}$ and $B \equiv \widetilde{f}\kappa_1/\sqrt{2}$, and thus $M_\ell = Ae^{i\alpha} + B$, as before. When $|A_{ij}| \ll |B_{ij}|$, M_ℓ must be close to a Hermitian matrix, which is equivalent to $V_L^{\ell\dagger}V_R^\ell \approx 1$. When $|A_{ij}| \gg |B_{ij}|$, we have $M_\ell \approx Ae^{i\alpha}$, which implies that $M_\ell e^{-i\alpha}$ is approximately Hermitian, i.e. $V_L^{\ell\dagger}V_R^\ell \approx e^{i\alpha}$. Note that we need the condition on mixing matrices in addition to the conditions on the Yukawa couplings and VEV's since constructing M_ℓ from mixing matrices is one of the first steps to construct all the mass matrices.

In this paper, we only consider the first case, i.e. $|A_{ij}| \ll |B_{ij}|$. For simplicity, we could assume $A = 0$, for which we need either $f = 0$ or $\kappa_2 = 0$. In these cases, the mass matrices are rather simple: $M_\ell = \widetilde{f}\kappa_1/\sqrt{2}$, $M_D = \widetilde{f}\kappa_2 e^{-i\alpha}/\sqrt{2}$ if $f = 0$, and $M_\ell = \widetilde{f}\kappa_1/\sqrt{2}$, $M_D = f\kappa_1/\sqrt{2}$ if $\kappa_2 = 0$. However, $f = 0$ is the limiting case of an extreme hierarchy between two Yukawa coupling matrices f and $\widetilde{f}$, which is rather unnatural. Furthermore, we must have $M_\ell \propto M_D \propto \widetilde{f}$, and thus M_D is diagonal in the mass basis of charged leptons, which means that we have to resort to only restrictive structures of mass matrices. On the other hand, with the condition $\kappa_2 = 0$, the W_L-W_R mixing parameter $\xi \approx -\kappa_1\kappa_2/v_R^2$ vanishes, and we have to lose the rich phenomenology dependent upon ξ, especially the EDM's of charged leptons. Therefore, we do not introduce these extreme conditions.

In summary, for the TeV-scale MLRSM without fine-tuning in M_D, we can assume the conditions either that (i) $f_{ij} \ll \widetilde{f}_{ij}$ and $\kappa_1 \gg \kappa_2$, when M_ℓ is approximately Hermitian, i.e. $V_L^\ell \approx V_R^\ell$, or that (ii) $f_{ij} \gg \widetilde{f}_{ij}$ and $\kappa_1 \ll \kappa_2$, when $M_\ell e^{-i\alpha}$ is approximately Hermitian, i.e. $V_L^\ell \approx V_R^\ell e^{-i\alpha}$. We study the first case here.

2.5 Numerical procedure

In this paper, we only consider the normal hierarchy in light neutrino masses. The procedure to calculate all the model parameters that determine the phenomenology of the MLRSM in type-I dominance is as follows:

1. Randomly generate the lightest light neutrino mass m_{ν_1}, and calculate $m_{\nu_2} = \sqrt{m_{\nu_1}^2 + \Delta m_{21}^2}$ and $m_{\nu_3} = \sqrt{m_{\nu_1}^2 + \Delta m_{31}^2}$.

2. Calculate M_ν^c from $M_\nu^c = U_{\text{PMNS}} M_\nu^{\text{diag}} U_{\text{PMNS}}^\mathsf{T}$ where M_ν^c and M_ν^{diag} are the light neutrino mass matrices in the charged lepton and light neutrino mass bases, respectively. The mixing matrix U_{PMNS} is the Pontecorvo-Maki-Nakagawa-Sakata (PMNS) matrix whose CP phases are also randomly generated.

3. Randomly generate V_L^ℓ, V_R^ℓ, and calculate $M_\ell = V_L^\ell M_\ell^c V_R^{\ell\dagger}$ where M_ℓ and M_ℓ^c are charged lepton mass matrices in the symmetry and charged lepton mass bases, repectively.

4. Find $A \equiv f\kappa_2/\sqrt{2}$, $B \equiv \widetilde{f}\kappa_1/\sqrt{2}$ from $M_\ell = Ae^{i\alpha} + B$ using the method discussed in section 2.3. Randomly generate κ_2, and calculate f, $\widetilde{f}$ from A, B.

5. Calculate $M_D = (f\kappa_1 + \widetilde{f}\kappa_2 e^{-i\alpha})/\sqrt{2}$ from f, $\widetilde{f}$, α, κ_2, $\kappa_1 = \sqrt{v_{\text{EW}}^2 - \kappa_2^2}$, and find $M_D^c = V_L^{\ell\dagger} M_D V_R^\ell$ where M_D^c is the Dirac neutrino mass matrix in the charged lepton mass basis.

6. Calculate M_R^c from the type-I seesaw formula $M_\nu^c = -M_D^c M_R^{c-1} M_D^{c\mathsf{T}}$ where M_R^c is the RH neutrino mass matrix in the charged lepton mass basis.

7. Construct the 6×6 neutrino mass matrix $M^c_{\nu N}$ from M^c_D and M^c_R, and find the 6×6 mixing matrix $V_{\nu N}$ that diagonalizes $M^c_{\nu N}$.

Here, the 6×6 neutrino mass matrix $M^c_{\nu N}$ in the charged lepton mass basis is written as

$$M^c_{\nu N} = \begin{pmatrix} 0 & M^c_D \\ M^{c\mathsf{T}}_D & M^c_R \end{pmatrix}, \tag{2.35}$$

and this matrix is diagonalized by the 6×6 unitary matrix $V_{\nu N}$:

$$M^{\text{diag}}_{\nu N} = V^{\mathsf{T}}_{\nu N} M^c_{\nu N} V_{\nu N} \tag{2.36}$$

where $M^{\text{diag}}_{\nu N}$ is the diagonal matrix with positive entries. Following the convention of reference [12], we write

$$V^*_{\nu N} = \begin{pmatrix} U & S \\ T & V \end{pmatrix} \tag{2.37}$$

where U, S, T, and V are 3×3 mixing matrices. Note that $U = U_{\text{PMNS}}$. The straightforward numerical diagonalization might not work appropriately because of the hierarchy in the components of $M^c_{\nu N}$. Instead, $V_{\nu N}$ is calculated in two steps:

$$V_{\nu N} = V_{\nu N1} V_{\nu N2} \tag{2.38}$$

where

$$V_{\nu N1} = \begin{pmatrix} 1 & -M^c_D M^{c-1}_R \\ -M^{c-1}_R M^{c\mathsf{T}}_D & -1 \end{pmatrix}, \qquad V_{\nu N2} = \begin{pmatrix} U^* & 0 \\ 0 & -V^* \end{pmatrix}. \tag{2.39}$$

Here, $V_{\nu N1}$ transforms $M_{\nu N}$ into the block-diagonal matrix

$$M^{\text{BD}}_{\nu N} = \begin{pmatrix} M^c_\nu & 0 \\ 0 & M^c_R + M^{c-1}_R M^{c\mathsf{T}}_D M^c_D + M^{c\mathsf{T}}_D M^c_D M^{c-1}_R \end{pmatrix}, \tag{2.40}$$

and $V_{\nu N2}$ is the matrix that diagonalizes $M_{\nu N}^{\mathrm{BD}}$. In addition, we use the standard parametrization of the PMNS matrix:

$$U_{\mathrm{PMNS}} = \begin{pmatrix} 1 & 0 & 0 \\ 0 & \cos\theta_{23} & \sin\theta_{23} \\ 0 & -\sin\theta_{23} & \cos\theta_{23} \end{pmatrix} \begin{pmatrix} \cos\theta_{13} & 0 & \sin\theta_{13}e^{-i\delta_D} \\ 0 & 1 & 0 \\ -\sin\theta_{13}e^{i\delta_D} & 0 & \cos\theta_{13} \end{pmatrix} \begin{pmatrix} \cos\theta_{12} & \sin\theta_{12} & 0 \\ -\sin\theta_{12} & \cos\theta_{12} & 0 \\ 0 & 0 & 1 \end{pmatrix}$$
$$\times \begin{pmatrix} 1 & 0 & 0 \\ 0 & e^{-i\delta_{M1}} & 0 \\ 0 & 0 & e^{-i\delta_{M2}} \end{pmatrix} \tag{2.41}$$

where δ_D and δ_{Mi} are Dirac and Majorana CP phases, respectively. On the other hand, we parametrize V_L^ℓ and V_R^ℓ as

$$V = V_1 V_2 V_3 \tag{2.42}$$

where

$$V_1 = \begin{pmatrix} 1 & 0 & 0 \\ 0 & e^{-i\delta_2} & 0 \\ 0 & 0 & e^{-i\delta_3} \end{pmatrix}, \tag{2.43}$$

$$V_2 = \begin{pmatrix} 1 & 0 & 0 \\ 0 & \cos\theta_{23} & \sin\theta_{23} \\ 0 & -\sin\theta_{23} & \cos\theta_{23} \end{pmatrix} \begin{pmatrix} \cos\theta_{13} & 0 & \sin\theta_{13}e^{-i\delta_1} \\ 0 & 1 & 0 \\ -\sin\theta_{13}e^{i\delta_1} & 0 & \cos\theta_{13} \end{pmatrix} \begin{pmatrix} \cos\theta_{12} & \sin\theta_{12} & 0 \\ -\sin\theta_{12} & \cos\theta_{12} & 0 \\ 0 & 0 & 1 \end{pmatrix}, \tag{2.44}$$

$$V_3 = \begin{pmatrix} e^{-i\delta_4} & 0 & 0 \\ 0 & e^{-i\delta_5} & 0 \\ 0 & 0 & e^{-i\delta_6} \end{pmatrix}. \tag{2.45}$$

Note that it is always possible to absorb V^ℓ_{R3} into V^ℓ_{L3} since $M_\ell = V^\ell_L M^c_\ell V^{\ell\dagger}_R$ where M^c_ℓ is a diagonal matrix. We can therefore write

$$V^\ell_L = V^\ell_{L1} V^\ell_{L2} V^\ell_{L3}, \qquad V^\ell_R = V^\ell_{R1} V^\ell_{R2}. \tag{2.46}$$

In addition, the Hermitian matrix A $(\equiv f\kappa_2/\sqrt{2})$ is parametrized as

$$A = \begin{pmatrix} A_{11} & |A_{12}|e^{i\theta_{A_{12}}} & |A_{13}|e^{i\theta_{A_{13}}} \\ |A_{12}|e^{-i\theta_{A_{12}}} & A_{22} & |A_{23}|e^{i\theta_{A_{23}}} \\ |A_{13}|e^{-i\theta_{A_{13}}} & |A_{23}|e^{-i\theta_{A_{23}}} & A_{33} \end{pmatrix} \tag{2.47}$$

where A_{ii} are real numbers. The list of model parameters and the ranges where they are randomly generated are summarized in table 2.2. Several appropriate constraints are imposed on some model parameters, and they are presented in table 2.3.

2.6 Numerical results

The present and future experimental bounds on CLFV, $0\nu\beta\beta$, and EDM's of charged leptons are summarized in table 2.4. The upper bound of light neutrino masses from the Planck observation is also considered. The experimental bounds on the dimensionless parameters associated with the various processes of $0\nu\beta\beta$ are given in table 2.5. The numerical results are presented in figures 2.1−2.7. The plots on the various branching ratios and conversion rates of CLFV in the MLRSM for 2 TeV $< m_{W_R} <$ 30 TeV are given in figure 2.1. The results on the dimensionless parameters of $0\nu\beta\beta$ for the same range of m_{W_R} are presented in figure 2.2. The plots on the EDM's of charged leptons are presented in figure 2.3. The effect of experimental constraints on the masses of the RH gauge boson, neutrinos, and scalar fields are shown in figures 2.4−2.7. The benchmark model parameters and their predicitons are given in appendix B.

The most notable result is that the regions of parameter space that allow small light neutrino masses are largely constrained by the experimental bounds from CLFV as well as the constraints from the light neutrino mass and mixing angles. Since the type-I seesaw formula implies $\det(M_\nu) \approx \det(M_D)^2/\det(M_R)$, we need a hierarchy in the eigenvalues of M_D or M_R when light neutrino masses have a hierarchy. However, M_D is determined from Yukawa couplings and VEV's, and it generally does not have the appropriate hierarchy in its eigenvalues to give hierachical light neutrino masses for most of the available parameter space. In other words, we generally need a hierarchy in the eigenvalues of M_R, i.e. in the heavy neutrino masses as well, in order to obtain hierachical light neutrino masses. Since we are considering a range of m_N, i.e. 0.1 TeV $\lesssim m_N \lesssim$ 100 TeV, the cases of large hierarchies in light neutrino masses are supposed to get constrained accordingly. Furthermore, since the regions of parameter space with large m_N are largely affected by the experimental constraints from CLFV, small light neutrino masses are disfavored by all those experimental constraints. These results are all clearly presented in several plots in figures 2.4, 2.6, and 2.7. For example, the 99 % contour in figure 2.7a shows that $m_{\nu_1} \sim 0.1$ eV for $m_{W_R} = 5$ TeV and $m_{\nu_1} \gtrsim 6 \cdot 10^{-3}$ eV for $m_{W_R} = 10$ TeV. Note that this does not necessarily mean that there exists a strict lower bound of the light neutrino mass for given m_{W_R}, since the results of this paper are based on the naturalness argument such as no fine-tuning in M_D. Note also that we can observe similar patterns in neutrino mass correlations in any type-I seesaw

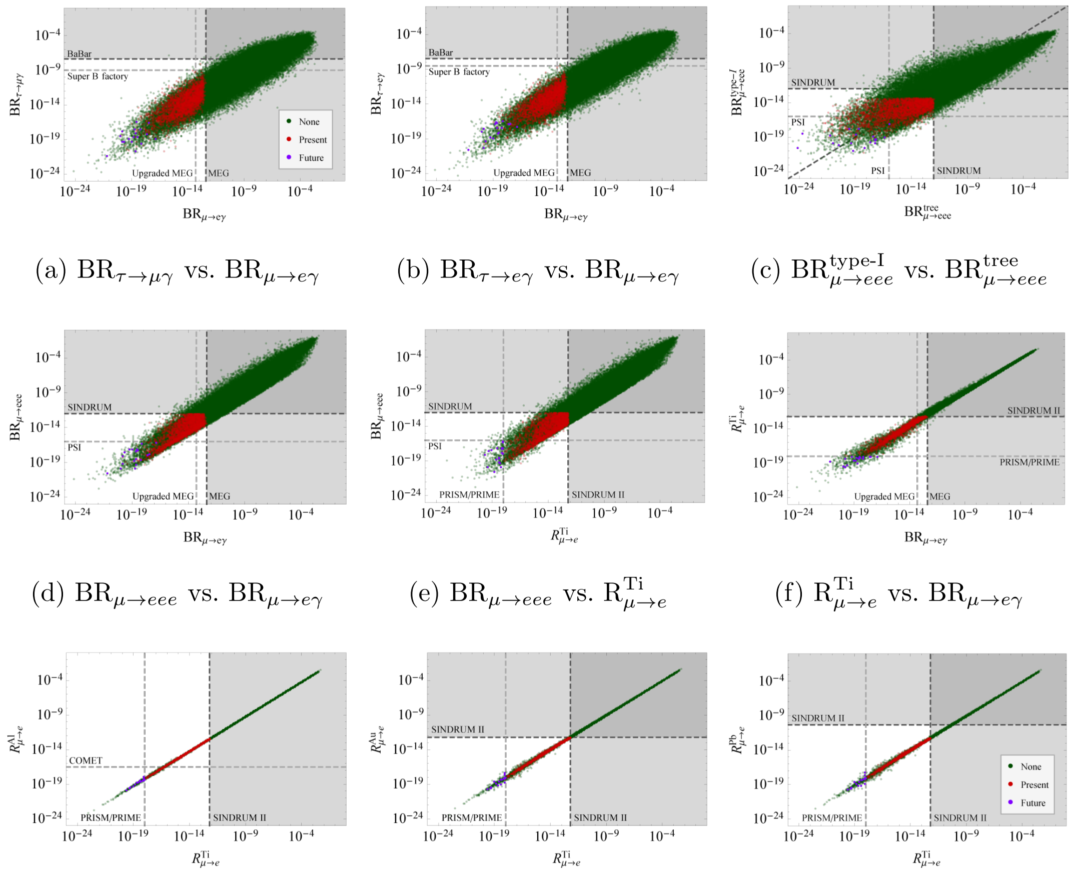

(a) $\mathrm{BR}_{\tau\to\mu\gamma}$ vs. $\mathrm{BR}_{\mu\to e\gamma}$ (b) $\mathrm{BR}_{\tau\to e\gamma}$ vs. $\mathrm{BR}_{\mu\to e\gamma}$ (c) $\mathrm{BR}^{\text{type-I}}_{\mu\to eee}$ vs. $\mathrm{BR}^{\text{tree}}_{\mu\to eee}$

(d) $\mathrm{BR}_{\mu\to eee}$ vs. $\mathrm{BR}_{\mu\to e\gamma}$ (e) $\mathrm{BR}_{\mu\to eee}$ vs. $\mathrm{R}^{\mathrm{Ti}}_{\mu\to e}$ (f) $\mathrm{R}^{\mathrm{Ti}}_{\mu\to e}$ vs. $\mathrm{BR}_{\mu\to e\gamma}$

(g) $\mathrm{R}^{\mathrm{Al}}_{\mu\to e}$ vs. $\mathrm{R}^{\mathrm{Ti}}_{\mu\to e}$ (h) $\mathrm{R}^{\mathrm{Au}}_{\mu\to e}$ vs. $\mathrm{R}^{\mathrm{Ti}}_{\mu\to e}$ (i) $\mathrm{R}^{\mathrm{Pb}}_{\mu\to e}$ vs. $\mathrm{R}^{\mathrm{Ti}}_{\mu\to e}$

Figure 2.1: CLFV in the MLRSM for 2 TeV $< m_{W_R} <$ 30 TeV. The green dots are data points that satisfy only the experimental constraints from the light lepton masses and PMNS matrix. The red dots are data points that also satisfy present bounds from the CLFV, $0\nu\beta\beta$, EDM's of charged leptons, and Planck observation. The purple dots are those that satisfy the strongest bounds from future experiments. The shaded regions are regions of parameter space excluded by present experimental bounds. Figures 2.1a and 2.1b show that there exist only small chances that $\tau\to\mu\gamma$ or $\tau\to e\gamma$ could be detected in near-future experiments. In figure 2.1c, the tree-level and 1-loop contributions to $\mu\to eee$ are compared, and it shows that we should consider both when calculating $\mathrm{BR}_{\mu\to eee}$. Figures 2.1d−2.1f show the linear correlations among various CLFV effects. Note that the strongest future bounds on CLFV come from PRISM/PRIME and PSI, as clearly shown in figure 2.1e. Figures

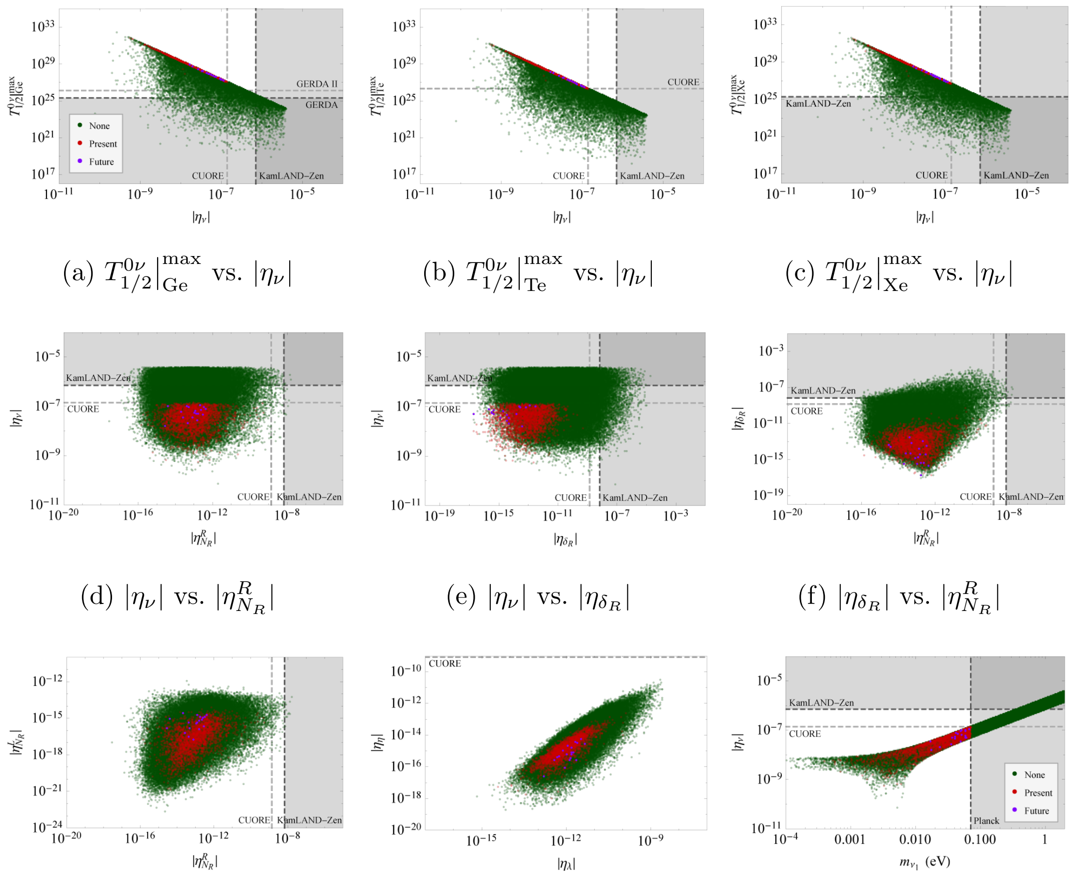

(a) $T^{0\nu}_{1/2}\big|^{\max}_{\mathrm{Ge}}$ vs. $|\eta_\nu|$

(b) $T^{0\nu}_{1/2}\big|^{\max}_{\mathrm{Te}}$ vs. $|\eta_\nu|$

(c) $T^{0\nu}_{1/2}\big|^{\max}_{\mathrm{Xe}}$ vs. $|\eta_\nu|$

(d) $|\eta_\nu|$ vs. $|\eta^R_{N_R}|$

(e) $|\eta_\nu|$ vs. $|\eta_{\delta_R}|$

(f) $|\eta_{\delta_R}|$ vs. $|\eta^R_{N_R}|$

(g) $|\eta^L_{N_R}|$ vs. $|\eta^R_{N_R}|$

(h) $|\eta_\eta|$ vs. $|\eta_\lambda|$

(i) $|\eta_\nu|$ vs. m_{ν_1}

Figure 2.2: Parameters of $0\nu\beta\beta$ in the MLRSM for 2 TeV $< m_{W_R} <$ 30 TeV. Figures 2.2a–2.2c show that only cases where η_ν dominantly determines $T^{0\nu}_{1/2}\big|^{\max}$ are allowed with a few exceptions by the present and future experimental bounds. Even though the contributions of $\eta^R_{N_R}$ and η_{δ_R} could be comparable to that of η_ν in principle, such cases have been actually almost excluded by the constraints from CLFV, as shown in figures 2.2d–2.2f. The contributions from η_η or η_λ are too small compared with experimental bounds, as shown in figure 2.2h. Figure 2.2i shows that the present upper bound of the light Majorana neutrino mass from Planck is already below the bounds from KamLAND-Zen and CUORE, which means that $0\nu\beta\beta$ processes are difficult to be detected in near-future experiments since the light neutrino exchange diagrams are dominant for most of the parameter space due to the CLFV constraints.

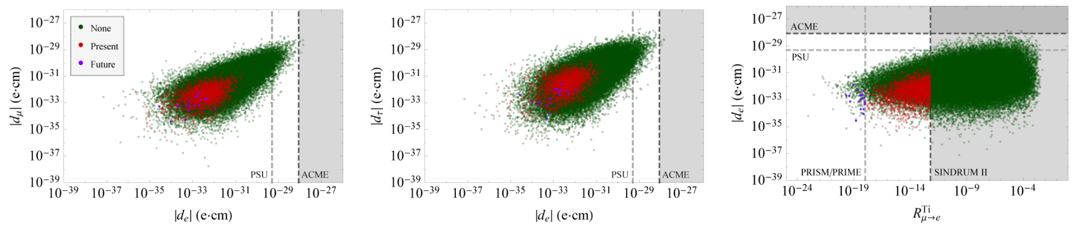

(a) $|d_\mu|$ vs. $|d_e|$ (b) $|d_\tau|$ vs. $|d_e|$ (c) $|d_e|$ vs. $\mathrm{R}^{\mathrm{Ti}}_{\mu\to e}$

Figure 2.3: EDM's of charged leptons in the MLRSM for 2 TeV $< m_{W_R} <$ 30 TeV. The predicted values are found to be too small compared with the present and future bounds, since large EDM's require small m_{W_R} whose regions of parameter space have been largely constrained as shown in figure 2.4a. Even though the correlations between EDM's and CLFV are rather weak, as shown in figure 2.3c, the larger EDM's generally require the larger CLFV effects since m_{W_R} affects both CLFV and EDM's.

models, even in the simple extension of the SM only with gauge singlet neutrinos. The difference in the MLRSM, or in a more general class of the left-right symmetric model, is that we can have large CLFV effects and thus the experimental bounds on CLFV are constraining the light neutrino masses. Moreover, since the largest possible hierarchy in heavy neutrino masses is directly associated with m_{W_R} and the regions of parameter space with smaller m_{W_R} are more constrained by CLFV bounds, we can expect that the discovery of light W_R as well as any improved experimental bounds on CLFV would largely constrain the regions of parameter space of the normal hierarchy.

Another interesting result is that the mass of the lightest heavy neutrino m_{N_1}

has been also notably constrained by the present experimental constraints, which is, of course, associated with the result on light neutrino masses just mentioned. This is shown in figures 2.5a, 2.5b, 2.6a, and 2.7b. For example, the 99 % density contour of figure 2.7b shows that $m_{N_1} \lesssim 200$ GeV for $m_{W_R} = 5$ TeV and $m_{N_1} \lesssim 2$ TeV for $m_{W_R} = 10$ TeV. Due to the mass insertion in the Dirac propagators of heavy neutrinos in some CLFV processes, large heavy neutrino masses generally induce large CLFV effects. Figure 2.4b explicitly shows how the CLFV bound is constraining m_{N_1}. The heaviest heavy neutrino mass is also affected by the experimental bounds, although its effect is rather small, as shown in figures 2.5c, 2.6b, and 2.7c.

While the CLFV effects of muons could be large enough for the associated processes to be detected in near-future experiments, the branching ratios of tau decays are either too small or just around the sensitivities of future experiments, as shown figure 2.1. The experimental bounds of CLFV are also constraining small masses of charged scalar fields as well as the RH gauge boson, as shown in figure 2.7. As a result, the $0\nu\beta\beta$ processes through the heavy neutrinos as well as RH gauge boson (denoted by $\eta^R_{N_R}$) and also processes through δ_R^{++} as well as the RH gauge boson (denoted by η_{δ_R}) are both suppressed. Hence, for most data points that satisfy the present experimental constraints, the dominant contribution to $0\nu\beta\beta$ comes from the process of the light neutrino exchange (denoted by η_ν), as shown in figures 2.2a−2.2c. However, since the upper bound of the light neutrino mass by Planck is already below the bounds of future experiments as shown in figure 2.2i, i.e. the light neutrino exchange channel has been largely constrained by the Planck observation, the possibility to detect $0\nu\beta\beta$ processes in near-future experiments is small. As for the EDM's of electrons, there seems to be also only small chances that they could be detected in near-future experiments as shown in figure 2.3, since the largest possible EDM's of electrons are well below the future sensitivities of the planned experiement. In addition, the EDM's of muons and taus are too small compared with the present upper bounds. Note that the EDM's of charged leptons has been also constrained by the experimental bounds from CLFV, since large EDM's generally require small m_{W_R} and large m_N and such regions of parameter space are largely affected by those experimental constraints. Note also that, even with the relatively small values of the RH scale, i.e. $v_R < 65$ TeV corresponding to $m_{W_R} < 30$ TeV, the observables of CLFV, $0\nu\beta\beta$, and EDM's cover very wide ranges, e.g. roughly $10^{-20} \lesssim \mathrm{BR}_{\mu\to e\gamma} \lesssim 10^{-3}$ and $10^{-35}\ e\cdot\mathrm{cm} \lesssim |d_e| \lesssim 10^{-29}\ e\cdot\mathrm{cm}$. Hence, neither a success nor a failure in detecting one of these effects rules out even the TeV-scale MLRSM, unless any other experimental results are simultaneously considered.

2.7 Conclusion

The procedure to construct lepton mass matrices has been presented in the MLRSM of type-I dominance with the parity symmetry, and the conditions for the TeV-scale MLRSM without fine-tuning have also been discussed, i.e. either (i) $\kappa_1 \gg \kappa_2$ and $f_{ij} \ll \widetilde{f}_{ij}$, which implies $V_L^\ell \approx V_R^\ell$, or (ii) $\kappa_1 \ll \kappa_2$ and $f_{ij} \gg \widetilde{f}_{ij}$, which implies $V_L^\ell \approx V_R^\ell e^{-i\alpha}$. Based on these results, the phenomenology of the TeV-scale MLRSM has been numerically investigated when the masses of light neutrinos are in the normal hierarchy, and the numerical results on how the present and future experimental bounds from the CLFV, $0\nu\beta\beta$, EDM's of charged leptons, and Planck observation constrain the parameter space of the MLRSM have been presented.

According to the numerical results, the regions of parameter space of small light neutrino masses have been constrained by the experimental bounds on CLFV effects, although it does not necessarily mean there exists a strict lower bound of light neutrino masses. The lightest heavy neutrino mass is also found to have been notably constrained by the present experimental bounds especially for small m_{W_R}. In addition, it has been shown that all the $0\nu\beta\beta$ processes and the EDM's of charged leptons have been suppressed by the experimental constraints from CLFV, and we have at best only small chances to detect any of these effects in near-future experiments.

Note that the results here are based on several nontrivial assumptions such as (i) type-I seesaw dominance, (ii) the parity symmetry, and (iii) the normal hierarchy in light neutrino masses. Furthermore, it should be emphasized that this paper is considering the TeV-scale phenomenology of the MLRSM without fine-tuning of model parameters. If fine-tuning is allowed, significantly different predictions could be made.

Physical scalar fields	Mass-squared
$h^0 = \sqrt{2}\mathrm{Re}[\phi_1^{0*} + \epsilon_2 e^{-i\alpha}\phi_2^0]$	$\frac{1}{2}(4\lambda_1 - \alpha_1^2/\rho_1)\kappa_1^2 + \frac{1}{2}\alpha_3 v_R^2 \epsilon_2^2$
$H_1^0 = \sqrt{2}\mathrm{Re}[-\epsilon_2 e^{i\alpha}\phi_1^{0*} + \phi_2^0]$	$\frac{1}{2}\alpha_3 v_R^2$
$H_2^0 = \sqrt{2}\mathrm{Re}[\delta_R^0]$	$2\rho_1 v_R^2$
$H_3^0 = \sqrt{2}\mathrm{Re}[\delta_L^0]$	$\frac{1}{2}(\rho_3 - 2\rho_1)v_R^2$
$A_1^0 = \sqrt{2}\mathrm{Im}[-\epsilon_2 e^{i\alpha}\phi_1^{0*} + \phi_2^0]$	$\frac{1}{2}\alpha_3 v_R^2$
$A_2^0 = \sqrt{2}\mathrm{Im}[\delta_L^0]$	$\frac{1}{2}(\rho_3 - 2\rho_1)v_R^2$
$H_1^+ = \delta_L^+$	$\frac{1}{2}(\rho_3 - 2\rho_1)v_R^2 + \frac{1}{4}\alpha_3\kappa_1^2$
$H_2^+ = \phi_2^+ + \epsilon_2 e^{i\alpha}\phi_1^+ + \frac{1}{\sqrt{2}}\epsilon_1\delta_R^+$	$\frac{1}{2}\alpha_3\big(v_R^2 + \frac{1}{2}\kappa_1^2\big)$
δ_R^{++}	$2\rho_2 v_R^2 + \frac{1}{2}\alpha_3\kappa_1^2$
δ_L^{++}	$\frac{1}{2}(\rho_3 - 2\rho_1)v_R^2 + \frac{1}{2}\alpha_3\kappa_1^2$

Table 2.1: Physical scalar fields and their masses in the MLRSM when $v_L = 0$ and $v_R \gg \kappa_1 \gg \kappa_2$. Here, $\epsilon_1 \equiv \kappa_1/v_R$ and $\epsilon_2 \equiv \kappa_2/\kappa_1$. The SM Higgs field is identified as h^0. Note that $m_{H_1^+} \approx m_{\delta_L^{++}}$ for $v_R \gg v_{\mathrm{EW}}$. The mixing between δ_L^{++} and δ_R^{++} is assumed to be small, although it could be large in principle for relatively small values of $\rho_3 - 2\rho_1$ and v_R [15]. It is, however, a good assumption even for such cases if we introduce an additional assumption $\beta_1, \beta_3 \lesssim \mathcal{O}(10^{-1})$.

Parameter	Range
$\log_{10}(m_{\nu_1}/\text{eV})$	$-4 - \log_{10} 2$
m_{W_R}	$2 - 35$ TeV
$\log_{10}(\kappa_2/\text{GeV})$	$-4 - 1$
δ_D, δ_{M1}, δ_{M2}, θ_{L12}, θ_{L13}, θ_{L23}, δ_{L1}, δ_{L2}, δ_{L3}	$-\pi - \pi$ rad
δ_{L4}	$(-1 - 1)\cdot 10^{-3}$ rad
$\log_{10}(\lvert A_{11}\rvert/\text{GeV})$	$\log_{10}\left\lvert \text{Im}[M_{\ell 11}]\right\rvert - \log_{10}\left(5\sqrt{2\pi}v_{\text{EW}}\right)$
$\log_{10}\alpha_3$, $\log_{10}\rho_2$	$\log_{10}(1000\ \text{GeV}^2/v_R^2) - \log_{10}(5\sqrt{4\pi})$
$\log_{10}(\rho_3 - 2\rho_1)$	$\log_{10}(1000\ \text{GeV}^2/v_R^2) - \log_{10}(15\sqrt{4\pi})$

Table 2.2: List of parameters and the ranges where those parameters are randomly generated. It is also assumed that $\delta_{L5} = \delta_{L6} = 0$, $\theta_{Rij} = \theta_{Lij}$, and $\delta_{Ri} = \delta_{Li}$ $(i, j = 1, 2, 3)$. Here, A is defined as $A \equiv f\kappa_2/\sqrt{2}$, and $M_\ell = V_L^\ell M_\ell^c V_R^{\ell\dagger}$ is the charged lepton mass matrix in the symmetry basis. The electroweak VEV is $v_{\text{EW}} = \sqrt{\kappa_1^2 + \kappa_2^2} = 246$ GeV, and $v_R = m_{W_R}\sqrt{2}/g$ $(g = 0.65)$ is the VEV of the $\text{SU}(2)_R$ triplet. Since Yukawa coupling matrices f, $\widetilde{f}$ are constructed from given M_ℓ by the method presented in section 2.3, we explicitly consider only the condition $\kappa_1 \gg \kappa_2$ for the TeV-scale MLRSM. Any Yukawa couplings that do not satisfy $f_{ij} \ll \widetilde{f}_{ij}$ can be excluded by filtering M_R with large entries, which is one of the constraints given in table 2.3. The ranges and values of δ_{L4}, δ_{L5}, δ_{L6}, θ_{Rij}, and δ_{Ri} are chosen to guarantee $V_R^\ell \approx V_L^\ell$ for TeV-scale m_N. In principle, we only need $\delta_{L4} \approx 0$, $\delta_{L5} \approx 0$, $\delta_{L6} \approx 0$, $\theta_{Rij} \approx \theta_{Lij}$, and $\delta_{Ri} \approx \delta_{Li}$ for $V_R^\ell \approx V_L^\ell$. However, for the parameters other than δ_{L4}, it turned out that only extremely small deviations ($\lesssim 10^{-6}$) from the values

	Present bound	Future sensitivity
$\mathrm{BR}_{\mu\to e\gamma}$	$< 4.2 \cdot 10^{-13}$ (MEG) [19]	$< 5.0 \cdot 10^{-14}$ (Upgraded MEG) [20]
$\mathrm{BR}_{\tau\to\mu\gamma}$	$< 4.4 \cdot 10^{-8}$ (BaBar) [21]	$< 1.0 \cdot 10^{-9}$ (Super B factory) [22]
$\mathrm{BR}_{\tau\to e\gamma}$	$< 3.3 \cdot 10^{-8}$ (BaBar) [21]	$< 3.0 \cdot 10^{-9}$ (Super B factory) [22]
$\mathrm{BR}_{\mu\to eee}$	$< 1.0 \cdot 10^{-12}$ (SINDRUM) [23]	$< 1.0 \cdot 10^{-16}$ (PSI) [24]
$\mathrm{R}^{\mathrm{Al}}_{\mu\to e}$	.	$< 3.0 \cdot 10^{-17}$ (COMET) [25]
$\mathrm{R}^{\mathrm{Ti}}_{\mu\to e}$	$< 6.1 \cdot 10^{-13}$ (SINDRUM II) [26]	$< 1.0 \cdot 10^{-18}$ (PRISM/PRIME) [27]
$\mathrm{R}^{\mathrm{Au}}_{\mu\to e}$	$< 6.0 \cdot 10^{-13}$ (SINDRUM II) [25]	.
$\mathrm{R}^{\mathrm{Pb}}_{\mu\to e}$	$< 4.6 \cdot 10^{-11}$ (SINDRUM II) [28]	.
$T^{0\nu}_{1/2}\big\vert_{\mathrm{Ge}}$	$> 2.1 \cdot 10^{25}$ yrs. (GERDA) [29]	$> 1.35 \cdot 10^{26}$ yrs. (GERDA II) [29]
$T^{0\nu}_{1/2}\big\vert_{\mathrm{Te}}$	.	$> 2.1 \cdot 10^{26}$ yrs. (CUORE) [29]
$T^{0\nu}_{1/2}\big\vert_{\mathrm{Xe}}$	$> 1.9 \cdot 10^{25}$ yrs. (KamLAND-Zen) [29]	.
$\vert d_e\vert$	$< 8.7 \cdot 10^{-29}$ e·cm (ACME) [53]	$< 5.0 \cdot 10^{-30}$ e·cm (PSU) [54]
$\vert d_\mu\vert$	$< 1.9 \cdot 10^{-19}$ e·cm (Muon $(g-2)$) [55]	.
$\vert d_\tau\vert$	$\lesssim 5.0 \cdot 10^{-17}$ e·cm (Belle) [56]	.
$\sum_i^3 m_{\nu_i}$	< 0.23 eV (Planck) [17]	.

Table 2.4: Experimental bounds on CLFV, $0\nu\beta\beta$, EDM's of charged leptons, and light neutrino masses. The actual present bounds on d_τ reported by Belle Collaboration are $-2.2 \cdot 10^{-17}e$·cm $<$ Re$[d_\tau]$ $< 4.5 \cdot 10^{-17}e$·cm and $-2.5 \cdot 10^{-17}e$·cm $<$ Im$[d_\tau]$ $< 0.8 \cdot 10^{-17}e$·cm. For the normal hierarchy, the constraint from the Planck observation corresponds to the upper bound of the lightest neutrino mass $m_{\nu_1} < 0.071$ eV.

	Present bound (KamLAND-Zen)	Future sensitivity (CUORE)
$\|\eta_\nu\|$	$< 7.1 \cdot 10^{-7}$	$< 1.4 \cdot 10^{-7}$
$\|\eta^L_{N_R}\|$	$< 6.8 \cdot 10^{-9}$	$< 1.4 \cdot 10^{-9}$
$\|\eta^R_{N_R}\|$	$< 6.8 \cdot 10^{-9}$	$< 1.4 \cdot 10^{-9}$
$\|\eta_{\delta_R}\|$	$< 6.8 \cdot 10^{-9}$	$< 1.4 \cdot 10^{-9}$
$\|\eta_\lambda\|$	$< 5.7 \cdot 10^{-7}$	$< 1.2 \cdot 10^{-7}$
$\|\eta_\eta\|$	$< 3.0 \cdot 10^{-9}$	$< 8.2 \cdot 10^{-10}$

Table 2.5: Experimental bounds on the dimensionless parameters associated with the various processes of $0\nu\beta\beta$. The present bounds come from KamLAND-Zen, and the strongest future bounds are from CUORE [29]. To obtain each bound, the associated decay channel is assumed to be dominant over the others. Even though there exist regions of parameter space where contributions from η_ν, $\eta^R_{N_R}$, and η_{δ_R} are comparable to each other, it does not invalidate the assumption at least for the data points of interest around the present and future bounds, since larger values of $|\eta^R_{N_R}|$ and $|\eta_{\delta_R}|$ are rarely allowed by the constraints from CLFV, as shown in figures 2.2d$-$2.2f.

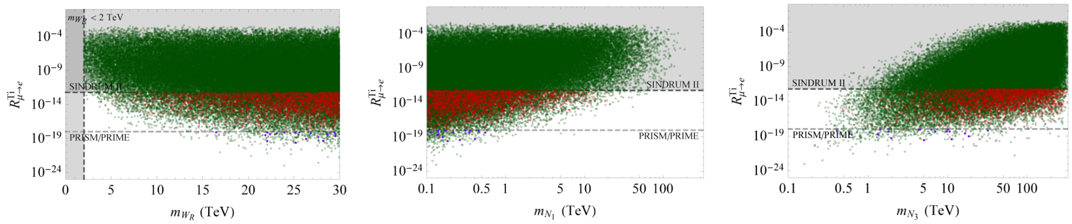

(a) $\mathrm{R}^{\mathrm{Ti}}_{\mu\to e}$ vs. m_{W_R} (b) $\mathrm{R}^{\mathrm{Ti}}_{\mu\to e}$ vs. m_{N_1} (c) $\mathrm{R}^{\mathrm{Ti}}_{\mu\to e}$ vs. m_{N_3}

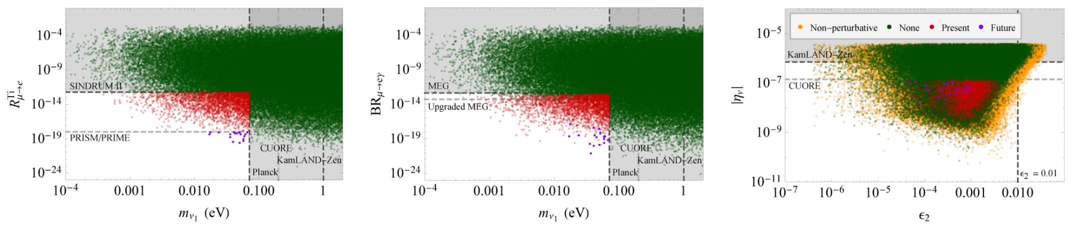

(d) $\mathrm{R}^{\mathrm{Ti}}_{\mu\to e}$ vs. m_{ν_1} (e) $\mathrm{BR}_{\mu\to e\gamma}$ vs. m_{ν_1} (f) $|\eta_\nu|$ vs. ϵ_2 ($\equiv \kappa_2/\kappa_1$)

Figure 2.4: Figures 2.4a−2.4e show the effect of CLFV constraints on the masses of neutrinos and the RH gauge boson. Here, $\mathrm{R}^{\mathrm{Ti}}_{\mu\to e}$ is chosen since it most clearly divides the colors of data points through its experimental bounds. The smaller values of the lightest light neutrino mass m_{ν_1} produce the larger CLFV effects, as in figures 2.4d and 2.4e, since they require the larger values of the heaviest heavy neutrino mass m_{N_3} in most of the parameter space, as shown in figure 2.6f. As a result, the regions of parameter space of small light neutrino masses get constrained by the experimental bounds on CLFV. In figure 2.4f, additional data points (yellow dots) are also presented in order to show the effects of the perturvativity constraints, and all the data points generated in the ranges of parameters given in table 2.2 are shown in this plot. For those yellow points, at least one of the coupling constants are larger than $\sqrt{4\pi}$ while the experimental constraints in the light neutrino sector are still satisfied. This figure shows that $\epsilon_2 \equiv \kappa_2/\kappa_1 \lesssim 0.01$ is satisfied for all the data points due to the perturvativity constraints as well as the condition $\kappa_2 < 10$ GeV, and thus the Higgs mass constraints can be easily satisfied, as mentioned in table 2.3.

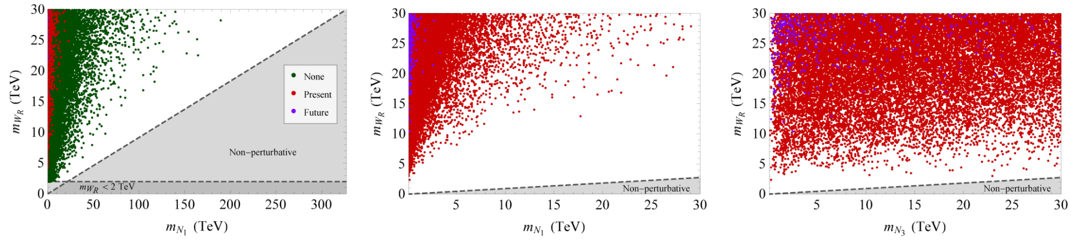

(a) m_{W_R} vs. m_{N_1} (b) m_{W_R} vs. m_{N_1} (c) m_{W_R} vs. m_{N_3}

Figure 2.5: Masses of heavy neutrinos in the TeV-scale MLRSM for 2 TeV $< m_{W_R} <$ 30 TeV. For figure 2.5a, the same data set as in the previous plots are used to show the effect of the consraints from CLFV, $0\nu\beta\beta$, EDM's, and Planck on the parameter space. The non-perturbative regions are where at least one coupling constant is larger than $\sqrt{4\pi}$. Note that green dots in figure 2.5a do not completely fill the available parameter space because of the constraints on masses and angles in the light lepton sector. For figures 2.5b and 2.5c, much more amount of data points was used to show how the present and future bounds constrain the parameter space. Figures 2.5a and 2.5b show that the lightest heavy neutrino mass m_{N_1} has been notably constrained by the experimental bounds, especially for smaller m_{W_R}. Figure 2.5c is the plot on the heaviest heavy neutrino mass m_{N_3}, and it shows that only a small region of parameter space with small m_{W_R} seems to have been excluded. Even though these plots in the linear scale are better in presenting the effect of experimental constraints on largest possible masses of heavy neutrinos, they do not correctly show the density distributions since the matrix A ($\equiv f\kappa_2/\sqrt{2}$) is generated in the logarithmic scale. Plots of m_N in the logarithmic scale are presented in figure 2.7. For figures 2.5b and 2.5c, the data sets for figures 2.7b and 2.7c are used, respectively.

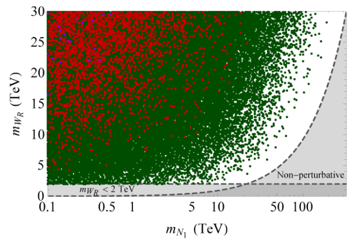

(a) m_{W_R} vs. m_{N_1}

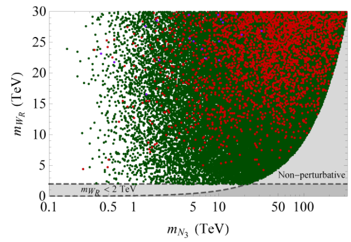

(b) m_{W_R} vs. m_{N_3}

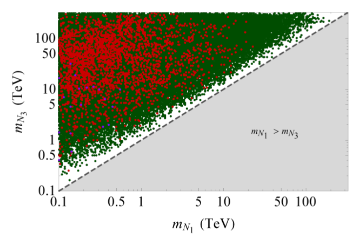

(c) m_{N_3} vs. m_{N_1}

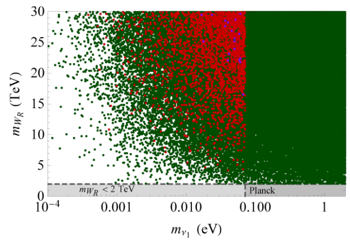

(d) m_{W_R} vs. m_{ν_1}

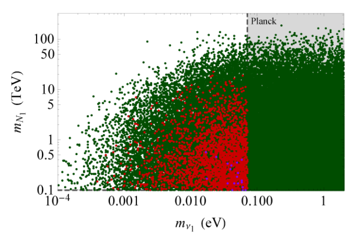

(e) m_{N_1} vs. m_{ν_1}

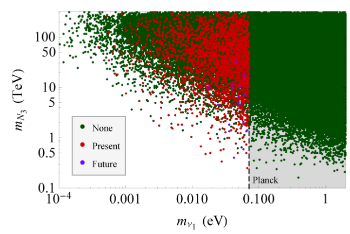

(f) m_{N_3} vs. m_{ν_1}

Figure 2.6: Figures 2.6a−2.6d show the effect of experimental bounds on the masses of neutrinos and the RH gauge boson. Figures 2.6a and 2.6b show that the regions with smaller m_{W_R} and larger m_N are more affected by the present bounds on CLFV, $0\nu\beta\beta$, and EDM's. Figures 2.6e and 2.6f show that, for smaller m_{ν_1}, i.e. for the light neutrino masses with a larger hierarchy, the heavy neutrino masses also generally need to have a larger hierarchy accordingly since M_D itself does not have the structure that would give hierarchical light neutrino masses. Due to this effect, only larger m_{W_R} is generally allowed for smaller m_{ν_1}, as shown in figure 2.7a, since large m_{N_3} requires large v_R.

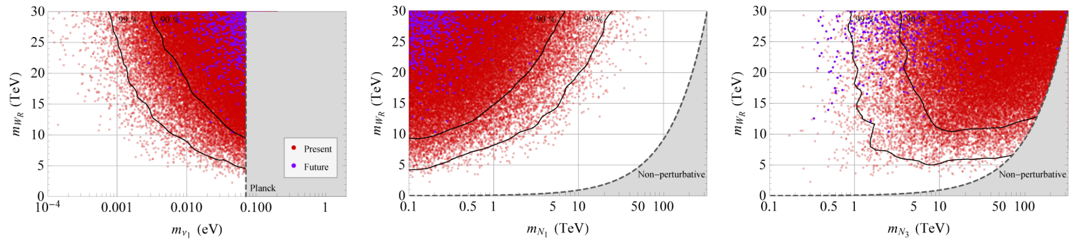

(a) m_{W_R} vs. m_{ν_1} (b) m_{W_R} vs. m_{N_1} (c) m_{W_R} vs. m_{N_3}

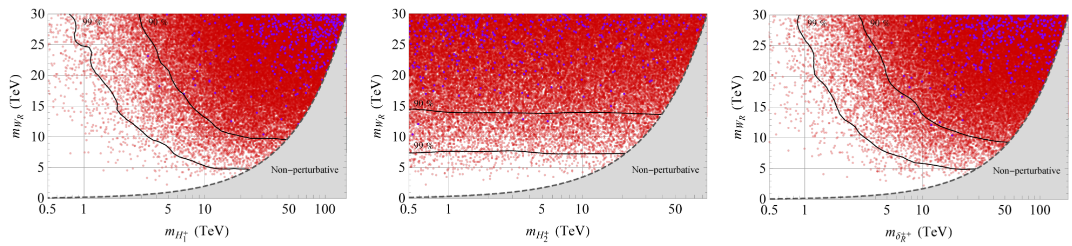

(d) m_{W_R} vs. $m_{H_1^+}$ $(\approx m_{\delta_L^{++}})$ (e) m_{W_R} vs. $m_{H_2^+}$ (f) m_{W_R} vs. $m_{\delta_R^{++}}$

Figure 2.7: Masses of neutrinos and charged scalar fields in the MLRSM for $m_{W_R} <$ 30 TeV. The contours of 90 % and 99 % densities are also presented for illustration purposes. According to the 99 % contour in figure 2.7a, $m_{\nu_1} \sim 0.1$ eV for $m_{W_R} = 5$ TeV and $m_{\nu_1} \gtrsim 6 \cdot 10^{-3}$ eV for $m_{W_R} = 10$ TeV. In addition, the 99 % contour in figure 2.7b shows that $m_{N_1} \lesssim 200$ GeV for $m_{W_R} < 5$ TeV and $m_{N_1} \lesssim 2$ TeV for $m_{W_R} < 10$ TeV. While the masses of H_1^+, δ_L^{++}, and δ_R^{++} have been also constrained by the experimental bounds, the mass of H_2^+ which appears only in the Z_1-exchange diagrams of CLFV processes has been barely constrained, as shown in figure 2.7e. Hence, the constraint of $m_{H_2^+} \gtrsim 10$ TeV from the absence of flavour changing neutral current in the quark sector is not considered in this paper. The total number of data points is 51971 = 51561 (red) + 410 (purple).

Chapter 3: Natural TeV-scale left-right symmetric model

3.1 Introduction

Our goal here is to explore whether the two key aspects of the seesaw physics, i.e. (i) the Majorana character of heavy and light neutrino masses, and (ii) the heavy-light neutrino mixing, can be tested at the LHC as well as in complementary experiments at low energies, e.g. in planned high sensitivity searches for CLFV, $0\nu\beta\beta$, etc. A necessary requirement for this synergic exploration to have any chance of success is that the seesaw scale be in the TeV range as well as the heavy-light mixing being relatively large. With this in mind, we discuss a class of the LRSM where both the above ingredients of type-I seesaw, i.e. TeV seesaw scale and observable heavy-light neutrino mixing emerge in a natural manner.

A simple candidate seesaw model is based on the left-right symmetric theory of weak interactions where the key ingredients of seesaw, i.e. the RH neutrino and its Majorana mass, appear naturally. The RH neutrino field ν_R arises as the necessary parity gauge partner of the left-handed (LH) neutrino field ν_L and is also required by anomaly cancellation, whereas the seesaw scale is identified as the one at which the RH counterpart of the SM $SU(2)_L$ gauge symmetry, namely the $SU(2)_R$ symmetry, is broken. The RH neutrinos are therefore a necessary part of the model and do not have to be added just to implement the seesaw mechanism. An important point is that the RH neutrinos acquire a Majorana mass as soon as the $\mathrm{SU}(2)_R$ symmetry is broken at a scale v_R. This is quite analogous to the way the charged fermions get mass as soon as the SM gauge symmetry $\mathrm{SU}(2)_L$ is broken at the electroweak scale v. The Higgs field that gives mass to the RH neutrinos becomes the analog of the 125 GeV Higgs boson discovered at the LHC. Clearly, the seesaw scale is not added in an adhoc manner but rather becomes intimately connected to the $\mathrm{SU}(2)_R \otimes \mathrm{U}(1)_{B-L}$ symmetry breaking scale.

In generic TeV-scale seesaw models without any special structures for M_D and M_N, in order to get small neutrino masses, we must fine-tune the magnitude of the elements of M_D to be very small (of order MeV for $M_N \sim$ TeV), as is evident from the seesaw formula in equation 1.10. As a result, the heavy-light neutrino mixing $\xi \sim M_D M_N^{-1} \simeq (M_\nu M_N^{-1})^{1/2} \lesssim 10^{-6}$. This suppresses all heavy-light mixing effects to an unobservable level which keeps this key aspect of seesaw shielded from being tested experimentally. To overcome this shortcoming, some special textures for M_D and M_N have been studied in the literature [30–39] for which even with TeV-scale seesaw, the mixing parameter ξ can be significantly enhanced whereas the neutrino masses still remain small, thereby enriching the seesaw phenomenology. Here, we present an LRSM embedding of one such special texture using an appropriate family symmetry. This is a highly non-trivial result since in the LRSM the charged lepton mass matrix and the Dirac neutrino mass matrix are related, especially when there are additional discrete symmetries to guarantee a specific form of the Dirac mass matrix M_D.

When we have the mass matrices of

$$M_D = \begin{pmatrix} m_1 & 0 & 0 \\ m_2 & 0 & 0 \\ m_3 & 0 & 0 \end{pmatrix}, \quad M_R = \begin{pmatrix} 0 & M_1 & 0 \\ M_1 & 0 & 0 \\ 0 & 0 & M_2 \end{pmatrix}, \tag{3.1}$$

then the type-I seesaw formula gives

$$M_\nu = -M_D M_R^{-1} M_D^{\mathsf{T}} = 0. \tag{3.2}$$

By introducting small values in the zero entries, we can generate small light neutrino masses. We want the mass matrices in the symmetry basis to be

$$M_\ell = \begin{pmatrix} \delta a_{11} & a_{12} & a_{13} \\ \delta a_{21} & a_{22} & a_{23} \\ \delta a_{31} & a_{32} & a_{33} \end{pmatrix}, \quad M_D = \begin{pmatrix} m_{11} & \delta m_{12} & \delta m_{13} \\ m_{21} & \delta m_{22} & \delta m_{23} \\ m_{31} & \delta m_{32} & \delta m_{33} \end{pmatrix}, \quad M_R = \begin{pmatrix} 0 & M_1 & 0 \\ M_1 & 0 & 0 \\ 0 & 0 & M_2 \end{pmatrix} \tag{3.3}$$

where $|\delta a_{ij}| \ll |a_{kl}|$ and $|\delta m_{ij}| \ll |m_{kl}| \ll |M_n|$ ($i, j, k, l = 1, 2, 3$ and $n = 1, 2$). If the symmetry basis is close to the charged lepton mass basis, then we can expect the followings:

1. Explanation of the small mass of an electron.

2. Large CLFV and EDM of an electron.

As for the second point, note that both CLFV and EDM's of charged leptons have a contribution of the form $\sum_{i=1}^{3} S_{\alpha i} V_{\alpha i} m_{N_i}$. Since $S \approx (M_D^c M_R^{c-1})^* V$, we can write

$$\sum_{i=1}^{3} S_{\alpha i} V_{\alpha i} m_{N_i} \approx \sum_{i,j=1}^{3} (M_D^c M_R^{c-1})^*_{\alpha j} V_{ji} V_{\alpha i} m_{N_i} = \sum_{j=1}^{3} (M_D^c M_R^{c-1})^*_{\alpha j} M_{Rj\alpha}^{c*} = M_{D\alpha\alpha}^{c*}. \tag{3.4}$$

Since M^c_{D11} is large in this model, we can expect the large CLFV and EDM of an electron.

3.2 Outline of the model

When we have multiple bi-doublet and RH triplet scalar fields, the Lagrangian terms with Yukawa couplings are given by

$$\mathcal{L}_Y^\ell = -\overline{L'_{Li}}(f^\ell_{aij}\Phi_a + \widetilde{f}^\ell_{aij}\widetilde{\Phi}_a)L'_{Rj} - h_{Laij}\overline{L'^c_{Li}}i\sigma_2\Delta_{La}L'_{Lj} - h_{Raij}\overline{L'^c_{Ri}}i\sigma_2\Delta_{Ra}L'_{Rj} + \text{H.c.}. \tag{3.5}$$

Now we introduce a discrete symmetry $Z_4 \otimes Z_4 \otimes Z_4$, and define the transformation rule of the fermions and scalar fields as in table 3.1. The Yukawa interaction terms

Field	$Z_4 \otimes Z_4 \otimes Z_4$
L_{La}	$(1,1,1)$
L_{R1}	$(-i,1,1)$
L_{R2}	$(1,-i,1)$
L_{R3}	$(1,1,-i)$
Φ_1	$(-i,1,1)$
Φ_2	$(1,i,1)$
Φ_3	$(1,1,i)$
Δ_{R1}	$(i,i,1)$
Δ_{R2}	$(1,1,-1)$

Table 3.1: Transformation property of leptons and scalar fields under $Z_4 \otimes Z_4 \otimes Z_4$.

under this symmetry are written as

$$\mathcal{L}_Y^\ell = -f_{i1}\overline{L'_{Li}}\widetilde{\Phi}_1 L'_{R1} - f_{i2}\overline{L'_{Li}}\Phi_2 L'_{R2} - f_{i3}\overline{L'_{Li}}\Phi_3 L'_{R3}$$
$$- h_{12}\overline{L'^c_{R1}} i\sigma_2 \Delta_{R1} L'_{R2} - h_{12}\overline{L'^c_{R2}} i\sigma_2 \Delta_{R1} L'_{R1} - h_{33}\overline{L'^c_{R3}} i\sigma_2 \Delta_{R2} L'_{R3} + \text{H.c.}. \tag{3.6}$$

The scalar potential is given by

$$\begin{aligned}
V = & -\mu_{1a}^2 \mathrm{tr}\big[\Phi_a^\dagger \Phi_a\big] - \mu_{2a}^2 \mathrm{tr}\big[\Delta_{Ra}^\dagger \Delta_{Ra}\big] \\
& + \lambda_{1ab}\mathrm{tr}\big[\Phi_a^\dagger \Phi_a\big]\mathrm{tr}\big[\Phi_b^\dagger \Phi_b\big] + \Big(\lambda_{2a} e^{i\delta_a}\mathrm{tr}\big[\widetilde{\Phi}_a^\dagger \Phi_a\big]^2 + \text{H.c.}\Big) \\
& + \lambda_{3ab}\mathrm{tr}\big[\widetilde{\Phi}_a^\dagger \Phi_b\big]\mathrm{tr}\big[\Phi_a^\dagger \widetilde{\Phi}_b\big] + \lambda_{4ab}\mathrm{tr}\big[\Phi_a^\dagger \Phi_b\big]\mathrm{tr}\big[\widetilde{\Phi}_a^\dagger \widetilde{\Phi}_b\big] \\
& + \alpha_{1ab}\mathrm{tr}\big[\Phi_a^\dagger \Phi_a\big]\mathrm{tr}\big[\Delta_{Rb}^\dagger \Delta_{Rb}\big] + \alpha_{2ab}\mathrm{tr}\big[\Phi_a^\dagger \Phi_a \Delta_{Rb}\Delta_{Rb}^\dagger\big] \\
& + \alpha_{3ab}\mathrm{tr}\big[\Delta_{Ra}^\dagger \Delta_{Ra}\big]\mathrm{tr}\big[\Delta_{Rb}^\dagger \Delta_{Rb}\big] + \alpha'_3\mathrm{tr}\big[\Delta_{R1}^\dagger \Delta_{R2}\big]\mathrm{tr}\big[\Delta_{R2}^\dagger \Delta_{R1}\big] \\
& + \alpha_{4ab}\mathrm{tr}\big[\Delta_{Ra}^\dagger \Delta_{Rb}^\dagger\big]\mathrm{tr}\big[\Delta_{Ra}\Delta_{Rb}\big].
\end{aligned} \tag{3.7}$$

Note that the potential terms $\mathrm{tr}\big[\widetilde{\Phi}_a^\dagger \Phi_b\big]$ are not allowed due to the discrete symmetry. Without loss of generality, the VEV's of scalar fields are written as

$$\langle\Phi_a\rangle = \begin{pmatrix} \kappa_a e^{i\alpha_a} & 0 \\ 0 & \kappa'_a e^{i\alpha'_a}/\sqrt{2} \end{pmatrix}, \quad \langle\Delta_{R1}\rangle = \begin{pmatrix} 0 & 0 \\ v_{R1}/\sqrt{2} & 0 \end{pmatrix}, \quad \langle\Delta_R\rangle = \begin{pmatrix} 0 & 0 \\ v_{R2} e^{i\theta_R}/\sqrt{2} & 0 \end{pmatrix}, \tag{3.8}$$

where we can choose $\alpha_1 = 0$ by gauge transformation. Some of the minimazation conditions of the scalar potential are written as

$$\frac{\partial\langle V\rangle}{\partial\kappa_1} = \kappa_1\left[\sum_{a=1}^{3}(\lambda'_{a1}\kappa'^2_a + \lambda_{a1}\kappa^2_a) + \sum_{a=1}^{2}\alpha_{a1}v^2_{Ra} + 2\mu^2_1\right] + \lambda''_{12}\kappa'_1\kappa'_2\kappa_2 + \lambda''_{13}\kappa'_1\kappa'_3\kappa_3 = 0, \tag{3.9}$$

$$\frac{\partial\langle V\rangle}{\partial\kappa'_1} = \kappa'_1\left[\sum_{a=1}^{3}(\lambda'_{a1}\kappa^2_a + \lambda_{a1}\kappa'^2_a) + \sum_{a=1}^{2}\alpha'_{a1}v^2_{Ra} + 2\mu^2_1\right] + \lambda''_{12}\kappa_1\kappa_2\kappa'_2 + \lambda''_{13}\kappa_1\kappa_3\kappa'_3 = 0 \tag{3.10}$$

where the coefficients are appropriately defined from the coefficients of the potential and the phases of VEV's. We can write similar equations for κ_2, κ'_2, κ_3, and κ'_3. Now we assume that v_{Ra} are determined from the other minimization conditions. Further assuming $\kappa_a \ll \kappa'_a$ and there exists no large hierarchy among the same type of coupling constants, we can obtain from the equations of type 3.10.

$$\sum_{a=1}^{3}\lambda_{ab}\kappa'^2_a + \sum_{a=1}^{2}\alpha'_{ab}v^2_{Ra} + 2\mu^2_b \approx 0 \tag{3.11}$$

where $b = 1, 2, 3$. These are coupled linear equations, from which κ'_a is easily determined. Now, equation 3.9 can be written as

$$\kappa_1\left[\sum_{a=1}^{3}\lambda'_{a1}\kappa'^2_a + \sum_{a=1}^{2}\alpha_{a1}v^2_{Ra} + 2\mu^2_1\right] + \lambda''_{12}\kappa'_1\kappa'_2\kappa_2 + \lambda''_{13}\kappa'_1\kappa'_3\kappa_3 \approx 0, \tag{3.12}$$

and we can write similar equations from the derivatives with respective to κ_2 and κ_3. They are also coupled linear equations whose solution is clearly $\kappa_1 = \kappa_2 = \kappa_3 = 0$. Note that this derivation of VEV's is possible due to the absence of the term $\mathrm{tr}\left[\widetilde{\Phi}^\dagger_a\Phi_b\right]$ which is prohibited by the discrete symmetry, although its absence is not a sufficient condition for $\kappa_1 = \kappa_2 = \kappa_3 = 0$. Therefore, when there exists the potential terms $\mathrm{tr}\left[\widetilde{\Phi}^\dagger_a\Phi_b\right]$ with very small coefficients, we can have very small nonzero κ_a.

Now we introduce that potential as a soft symmetry-breaking term

$$V_{\mathrm{SB}} = -\sum_{a,b=1}^{3} \mu^2_{\mathrm{SB}ab} \mathrm{tr}\big[\widetilde{\Phi}^\dagger_a \Phi_b\big] + \mathrm{H.c.} \tag{3.13}$$

which would change the minimization conditions above into

$$\begin{aligned}\frac{\partial\langle V\rangle}{\partial\kappa_1} &= \kappa_1 \sum_a (\lambda'_{a1}\kappa'^2_a + \lambda_{a1}\kappa^2_a + \alpha_{a1}v^2_{Ra} + 2\mu^2_1) + \lambda''_{12}\kappa'_1\kappa'_2\kappa_2 + \lambda''_{13}\kappa'_1\kappa'_3\kappa_3 + \sum_a \mu'^2_{\mathrm{SB}a1}\kappa'_a \\ &\approx \kappa_1 \sum_a (\lambda'_{a1}\kappa'^2_a + \alpha_{a1}v^2_{Ra} + 2\mu^2_1) + \lambda''_{12}\kappa'_1\kappa'_2\kappa_2 + \lambda''_{13}\kappa'_1\kappa'_3\kappa_3 + \sum_a \mu'^2_{\mathrm{SB}a1}\kappa'_a \approx 0,\end{aligned} \tag{3.14}$$

$$\begin{aligned}\frac{\partial\langle V\rangle}{\partial\kappa'_1} &= \kappa'_1 \sum_a (\lambda'_{a1}\kappa^2_a + \lambda_{a1}\kappa'^2_a + \alpha'_{a1}v^2_{Ra} + 2\mu^2_1) + \lambda''_{12}\kappa_1\kappa_2\kappa'_2 + \lambda''_{13}\kappa_1\kappa_3\kappa'_3 + \sum_a \mu'^2_{\mathrm{SB}a1}\kappa_a \\ &\approx \kappa'_1 \sum_a (\lambda_{a1}\kappa'^2_a + \alpha'_{a1}v^2_{Ra} + 2\mu^2_1) + \lambda''_{12}\kappa_1\kappa_2\kappa'_2 + \lambda''_{13}\kappa_1\kappa_3\kappa'_3 \approx 0.\end{aligned} \tag{3.15}$$

The second equation and its companions from κ'_2 and κ'_3 would give (approximately) the same expressions of κ'_a, and the first equation and its companions from κ_2 and κ_3 are now coupled linear equations with solutions $\kappa_a = \delta\kappa_a$.

With those VEV's, we can write the lepton mass matrices in the symmetry basis as

$$M_\ell = \frac{1}{\sqrt{2}} \begin{pmatrix} f_{11}\delta\kappa_1 & f_{12}\kappa_2' e^{i\alpha_2'} & f_{13}\kappa_3' e^{i\alpha_3'} \\ f_{21}\delta\kappa_1 & f_{22}\kappa_2' e^{i\alpha_2'} & f_{23}\kappa_3' e^{i\alpha_3'} \\ f_{31}\delta\kappa_1 & f_{32}\kappa_2' e^{i\alpha_2'} & f_{33}\kappa_3' e^{i\alpha_3'} \end{pmatrix}, \tag{3.16}$$

$$\begin{aligned} M_D &= \frac{1}{\sqrt{2}} \begin{pmatrix} f_{11}\kappa_1' e^{-i\alpha_1'} & f_{12}\delta\kappa_2 e^{i\alpha_2} & f_{13}\delta\kappa_3 e^{i\alpha_3} \\ f_{21}\kappa_1' e^{-i\alpha_1'} & f_{22}\delta\kappa_2 e^{i\alpha_2} & f_{23}\delta\kappa_3 e^{i\alpha_3} \\ f_{31}\kappa_1' e^{-i\alpha_1'} & f_{32}\delta\kappa_2 e^{i\alpha_2} & f_{33}\delta\kappa_3 e^{i\alpha_3} \end{pmatrix} \\ &= M_\ell D \quad \text{where} \quad D \equiv \begin{pmatrix} \frac{\kappa_1'}{\delta\kappa_1} e^{-i\alpha_1'} & 0 & 0 \\ 0 & \frac{\delta\kappa_2}{\kappa_2'} e^{-i(\alpha_2'-\alpha_2)} & 0 \\ 0 & 0 & \frac{\delta\kappa_3}{\kappa_3'} e^{-i(\alpha_3'-\alpha_3)} \end{pmatrix}, \end{aligned} \tag{3.17}$$

$$M_R = \sqrt{2} \begin{pmatrix} 0 & h_{12}v_{R1} & 0 \\ h_{21}v_{R1} & 0 & 0 \\ 0 & 0 & h_{33}v_{R2} \end{pmatrix} \tag{3.18}$$

where we have redefined the phase of L_{R3} to absorb θ_R into α_3 and α_3', i.e. $\alpha_3 - \theta_R/2 \to \alpha_3$ and $\alpha_3' - \theta_R/2 \to \alpha_3'$.

The motivation for the discrete symmetry is now clear:

1. No scalar potential terms of the form $\mathrm{tr}\big[\widetilde{\Phi}_a \Phi_b^\dagger\big]$.

2. No fine-tuning in M_D for the TeV-scale phenomenology.

3. Explanation of the small mass of an electron.

4. Large branching ratios of various muon decay processes and a large EDM of

an electron.

The mass term for charged weak gauge bosons is

$$\mathcal{L}_g^{\rm mass} = (W_L^{+\mu}\ W_R^{+\mu}) \begin{pmatrix} \frac{1}{4}g_L^2\sum_{a=0}^3(\delta\kappa_a^2+\kappa_a'^2) & -\frac{1}{2}g_Lg_R\sum_{a=0}^3\delta\kappa_a\kappa_a' e^{i(\alpha_a'-\alpha_a)} \\ -\frac{1}{2}g_Lg_R\sum_{a=0}^3\delta\kappa_a\kappa_a' e^{-i(\alpha_a'-\alpha_a)} & \frac{1}{4}g_R^2\sum_a^3(\delta\kappa_a^2+\kappa_a'^2)+2\sum_{a=1}^2 v_{Ra}^2 \end{pmatrix} \begin{pmatrix} W_{L\mu}^- \\ W_{R\mu}^- \end{pmatrix}. \tag{3.19}$$

Their masses can still be written as

$$m_{W_1}^2 \approx \frac{1}{4}g_L^2 v_{\rm EW}^2, \qquad m_{W_2}^2 \approx \frac{1}{2}g_R^2 v_R^2 \tag{3.20}$$

where $v_{\rm EW} = \sqrt{\sum_{a=0}^3(\delta\kappa_a^2+\kappa_a'^2)} = 246$ GeV and $v_R \equiv \sqrt{v_{R1}^2+v_{R2}^2}$, and the W_L-W_R mixing parameter is given by

$$\xi e^{i\alpha} \approx -\frac{g_L\sum_{a=0}^3\delta\kappa_a\kappa_a' e^{i(\alpha_a'-\alpha_a)}}{g_R v_R^2} \tag{3.21}$$

where α is defined as the complex phase of the mixing parameter in this model, not the phase of the electroweak VEV as in the MLRSM.

3.3 Numerical procedure

In the symmetry basis, we assume that M_R has the form

$$M_R = \begin{pmatrix} 0 & M_1 & 0 \\ M_1 & M_3 & 0 \\ 0 & 0 & M_2 \end{pmatrix}, \tag{3.22}$$

where M_3 is not necessarily small yet. In the same basis, we have $M_D = M_\ell D$, and thus $M_\nu = -M_D M_R^{-1} M_D^\mathsf{T} = -M_\ell^a M_R^{a-1} M_\ell^{a\mathsf{T}} \equiv M_\nu^a$ where $M_\ell^a \equiv M_\ell$ and

$M_R^a \equiv D^{-1} M_R D^{-1}$. Note that M_R^a has the same structure as M_R since D is diagonal. While M_ℓ^a and M_ν^a (i.e. M_ℓ and M_ν) can be easily constructed by $M_\ell^a = V_L^\ell M_\ell^c V_R^{\ell\dagger}$ and $M_\nu^a = V_L^\ell M_\nu^c V_L^{\ell\mathsf{T}}$ for arbitrary unitary matrices V_L^ℓ and V_R^ℓ, the matrix M_R^a calculated from $M_R^a = -M_\ell^{a\mathsf{T}} M_\nu^{a-1} M_\ell^a$ does not have the structure we want for those arbitary mixing matrices in general.

In order to have M_R^a with the desired structure, we generate arbitrary $V_L^{\ell b}$ and $V_R^{\ell b}$ (instead of V_L^ℓ and V_R^ℓ), and calculate $M_\ell^b \equiv V_L^{\ell b} M_\ell^c V_R^{\ell b\dagger}$, $M_\nu^b \equiv V_L^{\ell b} M_\nu^c V_L^{\ell b\mathsf{T}}$, and $M_R^b \equiv -M_\ell^{b\mathsf{T}} (M_\nu^b)^{-1} M_\ell^b$. Note that there always exists a unitary matrix V_R that transforms M_R^b into $M_R^a = V_R^{\mathsf{T}} M_R^b V_R$ where M_R^a is in the form of 3.22. Defining $M_\ell^a \equiv M_\ell^b V_R$ and $M_\nu^a \equiv M_\nu^b$, we obtain $M_R^a = -M_\ell^{a\mathsf{T}} M_\nu^{a-1} M_\ell^a$. Further defining $M_\ell \equiv M_\ell^a$ $(= M_\ell^b V_R)$, $M_R \equiv D M_R^a D$ $(= D V_R^{\mathsf{T}} M_R^b V_R D)$, $M_D \equiv M_\ell^a D$ $(= M_\ell^b V_R D)$, and $M_\nu \equiv M_\nu^a$ $(= M_\nu^b)$, we can finally obtain $M_R = -M_D^{\mathsf{T}} M_\nu^{-1} M_D$ where $M_D = M_\ell D$ and M_R is in the form of 3.22. For M_R^a and D given by

$$M_R^a = \begin{pmatrix} 0 & M_1^a & 0 \\ M_1^a & M_3^a & 0 \\ 0 & 0 & M_2^a \end{pmatrix}, \qquad D = \begin{pmatrix} d_1 & 0 & 0 \\ 0 & d_2 & 0 \\ 0 & 0 & d_3 \end{pmatrix}, \tag{3.23}$$

we have

$$M_R = D M_R^a D = \begin{pmatrix} 0 & M_1^a d_1 d_2 & 0 \\ M_1^a d_1 d_2 & M_3^a d_2^2 & 0 \\ 0 & 0 & M_2^a d_3^2 \end{pmatrix}. \tag{3.24}$$

Hence, by choosing small $|d_2|$ and large $|d_1|$, we can have M_R with $|M_1|, |M_2| \gg |M_3| \approx 0$, and also $M_D = M_\ell D$ with the first column large and the second column small, as desired. If $|M_3|$ is small enough, we can set it to zero to have the structure allowed by the exact discrete symmetry while all the experimental constraints are still satisfied within their uncertainties.

In order for this model to explain the small electron mass, the mixing matrix $V_R^\ell = V_R^\dagger V_R^{\ell b}$ should not largely mix the first column of M_ℓ with the others. Note that the stronger condition $|V_{Rij}^\ell| \approx \delta_{ij}$ is the general prediction of the model. By construction, we have

$$M_R^a = V_R^\mathsf{T} M_R^b V_R = -V_R^{\ell *} M_\ell^{c\mathsf{T}} (M_\nu^c)^{-1} M_\ell^c V_R^{\ell\dagger}, \tag{3.25}$$

i.e. V_R^ℓ is the mixing matrix that transforms $M_\ell^{c\mathsf{T}}(M_\nu^c)^{-1}M_\ell^c$ into the form of 3.22. Since $M \equiv M_\ell^{c\mathsf{T}}(M_\nu^c)^{-1}M_\ell^c$ has the structure of $M_{33} \gg M_{i3}$ $(i = 1, 2)$ and $M_{22}, M_{12} \gg M_{11}$ due to the mass hierarchy in charged leptons as well as the large mixing in light neutrinos, we always have $|V_{Rij}^\ell| \approx \delta_{ij}$.

In summary, the numerical procedure to generate the model parameters is as follows:

1. Randomly generate m_{ν_1}, and calculate $m_{\nu_2} = \sqrt{m_{\nu_1}^2 + \Delta m_{21}^2}$ and $m_{\nu_3} = \sqrt{m_{\nu_1}^2 + \Delta m_{31}^2}$.

2. Calculate M_ν^c from $M_\nu^c = U_{\text{PMNS}} M_\nu^d U_{\text{PMNS}}^\mathsf{T}$ where the CP phases of U_{PMNS} are also randomly generated.

3. Randomly generate $V_L^{\ell b}$, $V_R^{\ell b}$, and calculate $M_\ell^b = V_L^{\ell b} M_\ell^c V_R^{\ell b\dagger}$, $M_\nu^b = V_L^{\ell b} M_\nu^c V_L^{\ell b\mathsf{T}}$, and $M_R^b = M_\ell^{b\mathsf{T}} (M_\nu^b)^{-1} M_\ell^b$.

4. Find V_R which transforms M_R^b into a matrix M_R^a in the form of 3.22 by $M_R^a = V_R^\mathsf{T} M_R^b V_R$. In that basis, we have $M_\ell^a = M_\ell^b V_R$ and $M_\nu^a = M_\nu^b$.

5. Randomly generate D, and calculate the lepton mass matrices in the symmetry basis by $M_\ell = M_\ell^a$, $M_D = M_\ell^a D$, and $M_R = D M_R^a D$.

6. Randomly generate κ_0, κ_0', κ_1', κ_2', κ_3' which satisfies $\sqrt{\kappa_0^2 + \kappa_0'^2 + \kappa_1'^2 + \kappa_2'^2 + \kappa_3'^2} = v_{\mathrm{EW}}$, and calculate $\delta\kappa_1 = \kappa_1'/D_{11}$, $\delta\kappa_2 = \kappa_2' D_{22}$, $\delta\kappa_3 = \kappa_3' D_{33}$. Calculate the Yukawa coupling matrix f in the symmetry basis from M_ℓ and the electroweak VEV's.

7. Define $V_L^\ell \equiv V_L^{\ell b}$, $V_R^\ell \equiv V_R^\dagger V_R^{\ell b}$, and calculate $M_D^c = V_L^{\ell\dagger} M_D V_R^\ell$ and $M_R^c = V_R^{\ell\intercal} M_R V_R^\ell$.

8. Construct the 6×6 neutrino mass matrix $M_{\nu N}^c$ from M_D^c and M_R^c, and find the 6×6 mixing matrix $V_{\nu N}$ that diagonalizes $M_{\nu N}^c$.

The mixing matrices U_{PMNS}, V_L^ℓ, V_R^ℓ, and $V_{\nu N}$ are parametrized in the same way as in the MLRSM.

The ranges of model parameters where they are randomly generated are presented in table 3.2. The constraints imposed on model parameters are given in table 3.3. We assume that the contribution of charged scalar fields to CLFV and $0\nu\beta\beta$ are negligible. It is usually a good assumption for all the CLFV and $0\nu\beta\beta$ processes of our interest even when the masses of those charged scalar fileds are small, since we have $h_{11} = h_{13} = h_{23} = 0$ and $|V_{Rij}^\ell| \approx \delta_{ij}$. For example, the Feynman diagrams of muon or tau decays in the symmetry basis always involve one of h_{11}, h_{13}, h_{23}.

3.4 Numerical results

The numerical results for $m_{W_R} = 3$ TeV are presented in figure 3.1. The most notable result is that a large EDM of an electron is allowed in spite of the CLFV constraints, as expected. The prediction $|V^{\ell}_{Rij}| \approx \delta_{ij}$ has been also verified, as shown in figure 3.1f.

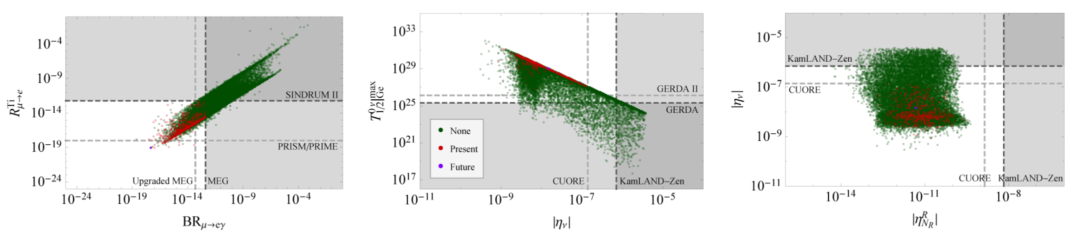

(a) $\mathrm{R}^{\mathrm{Ti}}_{\mu\to e}$ vs. $\mathrm{BR}_{\mu\to e\gamma}$ (b) $T^{\mathrm{Ge}}_{1/2}$ vs. $|\eta_\nu|$ (c) $|\eta_\nu|$ vs. $|\eta^R_{N_R}|$

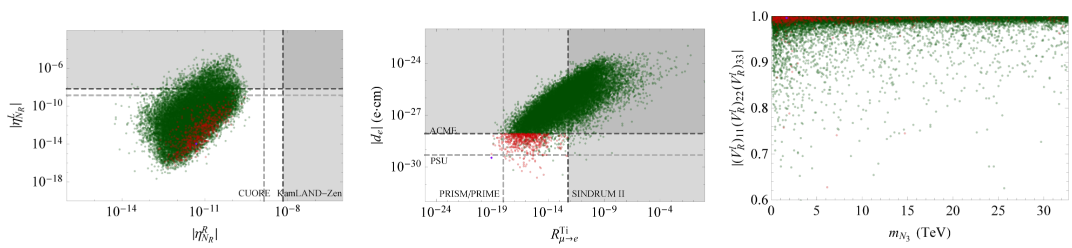

(d) $|\eta^L_{N_R}|$ vs. $|\eta^R_{N_R}|$ (e) $|d_e|$ vs. $\mathrm{R}^{\mathrm{Ti}}_{\mu\to e}$ (f) $|V^{\ell}_{R11}V^{\ell}_{R22}V^{\ell}_{R33}|$ vs. m_{N_3}

Figure 3.1: Predictions of the model for $m_{W_R} = 3$ TeV. Figures 3.1b–3.1d show that other processes such as $\eta^L_{N_R}$ can be dominant in this model. In addition, a large EDM of e is allowed as shown in figure 3.1e. Figure 3.1f shows $|V^{\ell}_{Rij}| \approx \delta_{ij}$.

3.5 Conclusion

We have presented a new TeV-scale seesaw model based on the left-right symmetric gauge group but without parity symmetry where a particular texture for the Dirac and Majorana masses guarantees that neutrino masses are naturally small while keeping the heavy-light neutrino mixing in the LHC-observable range. A discrete flavour symmetry has been shown to guarantee the stability of this texture, while being consistent with the observed lepton masses and mixing. We then explored its tests in the domain of the CLFV and EDM of an electron.

Parameter	Range
$\log_{10}(m_{\nu_1}/\mathrm{eV})$	$-4 - \log_{10} 2$
$\log_{10}(\kappa'_0/\mathrm{GeV})$	$\log_{10} 70 - \log_{10}\sqrt{v_{\mathrm{EW}}^2 - 4\cdot 10^2}$
$\log_{10}(\kappa_0/\mathrm{GeV})$	$-1 - 1$
$\log_{10}(\kappa'_1/\mathrm{GeV})$	$1 - \log_{10}\sqrt{v_{\mathrm{EW}}^2 - \kappa_0'^2 - \kappa_0^2 - 2\cdot 10^2}$
$\log_{10}(\kappa'_2/\mathrm{GeV})$	$1 - \log_{10}\sqrt{v_{\mathrm{EW}}^2 - \kappa_0'^2 - \kappa_0^2 - \kappa_1'^2 - 10^2}$
$\log_{10}(\kappa'_1/\delta\kappa_1)$	$2 - 5$
$\log_{10}(\kappa'_2/\delta\kappa_2)$	$5 - 8$
$\log_{10}(\kappa'_3/\delta\kappa_3)$	$2 - 5$
δ_D, δ_{M1}, δ_{M2}, $\alpha'_a - \alpha_a$, θ_{Lij}, δ_{Li}, θ_{Rij}, δ_{Ri}	$-\pi - \pi$ rad

Table 3.2: List of parameters and the ranges where those parameters are randomly generated. We have set $m_{W_R} = 3$ TeV and $g_R = g_L = 0.65$. Here, $\alpha'_a - \alpha_a$ is the difference of the phases of κ'_a and $\delta\kappa_a$, and we have used $v_{\mathrm{EW}}^2 = \sum_{a=1}^3(\delta\kappa_i^2 + \kappa_a'^2) \approx \sum_{a=1}^3 \kappa_a'^2$. The angles δ_D, δ_{M1}, δ_{M2} are the CP phases of the PMNS matrix, and θ_{Lij}, δ_{Li} and θ_{Rij}, δ_{Ri} are the parameters of V_L^ℓ and V_R^ℓ, respectively.

Parameter	Constraint
$\lvert f_{ij}\rvert$	$< \sqrt{4\pi}$
$\lvert M_{R11}\rvert^2 + \lvert M_{R12}\rvert^2$	$< 8\pi v_R^2$
$\lvert M^c_{R11}/M^c_{R12}\rvert$	< 0.1

Table 3.3: List of constraints imposed on the model parameters. Here, M_R and M_R^c are the Majorana mass matrices in the symmetry and charged lepton mass bases, respectively. Since $|M_{R11}|^2/|\sqrt{2}h_{11}|^2 + |M_{R12}|^2/|\sqrt{2}h_{12}|^2 = v_{R1}^2 + v_{R2}^2 = v_R^2$,

Chapter 4: TeV-scale resonant leptogenesis

4.1 Introduction

An attractive feature of the seesaw mechanism is that the same Yukawa couplings that give rise to light neutrino masses, can also resolve one of the outstanding puzzles of cosmology, namely, the origin of matter-antimatter asymmetry, via leptogenesis [40]. The key driver of leptogenesis are the out-of-equilibrium decays of the RH Majorana neutrinos via the modes $N \to L_i\phi$ and $N \to L_i^c\phi^\dagger$, where $L_i = (\nu_i, \ell_i)^\mathsf{T}$ $(i = 1, 2, 3)$ are the $\mathrm{SU}(2)_L$ lepton doublets, and ϕ are the Higgs doublets. In the presence of CP violation in the Yukawa sector, these decays can lead to a dynamical lepton asymmetry in the early Universe. This asymmetry will undergo thermodynamic evolution as the universe expands and different reactions present in the model have their impact on washing out part of the asymmetry. The remaining final lepton asymmetry is converted to the baryon asymmetry via sphaleron transitions before the electroweak phase transition. There is also a weak connection between the CP violation in neutrino oscillations and the amount of lepton asymmetry.

For TeV-scale seesaw models, the generation of adequate lepton asymmetry requires one to invoke resonant leptogenesis [41–43], where at least two of the heavy neutrinos have a small mass difference comparable to their decay widths. In this case, the heavy Majorana neutrino self-energy contributions [44] to the leptonic CP asymmetry become dominant [?, 45] and get resonantly enhanced, even up to order one [41, 42]. In the context of an embedding of seesaw into TeV-scale LRSM, there are additional complications due to the presence of RH gauge interactions that contribute to the dilution and washout of the primordial lepton asymmetry generated via resonant leptogenesis. This was explored in detail in [46] where it was pointed out that there is significant dilution of the primordial lepton asymmetry due to $\Delta L = 1$ scattering processes such as $N\ell_R \to ud^c$ mediated by W_R. This leads to an extra suppression of the final lepton symmetry, in addition to the usual inverse decay $L\phi \to N$ and $\Delta L = 0, 2$ scattering processes $L\phi \leftrightarrow L\phi$ $(L^c\phi^\dagger)$ present in generic SM seesaw scenarios. This additional dilution factor κ (also sometimes called efficiency) in this case is of order $\frac{Y_\nu^2 m_{W_R}^4}{g_R^4 m_N^4}$, which for $m_N \sim$ TeV and $m_{W_R} \sim 3$–4 TeV can be easily $\leq 10^{-7}$ or so for $Y \simeq 10^{-5.5}$. Combined with entropy dilution effect and the dilution from inverse decays, this implies that even for the maximal CP asymmetry $\varepsilon \sim \mathcal{O}(1)$, the observed baryon to photon ratio can be obtained only if $m_{W_R} \geq 18$ TeV. This result is very important because, as argued in [46], this can provide a way to falsify leptogenesis if a W_R with mass below this limit is observed in colliders.

We investigate whether there are *any* allowed parameter space in the TeV-scale LRSM where leptogenesis can work with a weakened lower bound on m_{W_R}, without conflicting with observed neutrino data and charged lepton masses. We work in a version of the model that is parity asymmetric at the TeV scale, which is anyway necessary if we want type-I seesaw to be the only contribution to neutrino masses.

According to our classification above, the work of [46] falls into the class I models. We explore whether the lower bound can be weakened in the other classes of models discussed above. It could very well be that if other observations push the Yukawa parameters to the range of class I models, the bound of [46] cannot be avoided, thereby providing a way to disprove leptogenesis at the LHC. However, to see how widely applicable the bound of [46] is, we consider in this paper an example of a model which belongs to class II, i.e. neutrino fits are done by cancellation leading to a specific texture for Dirac masses.

We implement the class II strategy for small neutrino masses in the minimal LRSM with a single bi-doublet field in the lepton sector where all leptonic Yukawa couplings are significantly larger than the canonical value of $\mathcal{O}(10^{-5.5})$ and the W_R mass is in the few TeV range. As noted above, to get small neutrino masses via type-I seesaw, we invoke cancellation between two Yukawa couplings to generate extra suppression and a particular resulting texture for the Dirac masses. We find that due to enhanced Yukawa couplings, the dilution of lepton asymmetry due to the W_R mediated scatterings as well as due to 3-body decays of RH neutrinos such as $N \to \ell_R u d^c$ become considerably less than the CP-violating 2-body decay modes $N \to L\phi, L^c\phi^\dagger$, and as a result, the lower limit on W_R mass can be brought within the LHC reach for a range of Yukawa couplings for which the washout effect due to inverse decay is in control. New aspects in our work that goes beyond that of [46] are the following: (i) we give a realistic fit for all lepton masses and mixing with larger Yukawa couplings ($\sim 10^{-2}$ or so); (ii) reference [46] assumes that the CP asymmetry $\varepsilon \sim 1$ whereas we calculate the primordial CP asymmetry ε in our model using the

Yukawa couplings demanded by our specific neutrino fit. As a result, our ε is still of order 10^{-1} (see text for precise numbers); (iii) finally, we take the flavour effects into account in our washout and lepton asymmetry calculation. It is a consequence of (i) and (iii), which leads us to lower the W_R mass bound from leptogenesis.

When $T_c < T < T_R$, we write the scalar bi-doublet as

$$\Phi = (\phi, \phi') \tag{4.1}$$

where ϕ and ϕ' are $\mathrm{SU}(2)_L$ doublets. Then, we can write

$$\widetilde{\Phi} \equiv \sigma_2 \Phi^* \sigma_2 = \left(\widetilde{\phi}', \widetilde{\phi}\right) \tag{4.2}$$

where $\widetilde{\phi} \equiv i\sigma_2\phi^*$ and $\widetilde{\phi}' \equiv -i\sigma_2\phi'^*$. For simplicity, we assume that ϕ' acquires a mass larger than m_N through v_R while ϕ remains massless. Then, ϕ is identified as the Higgs doublet of the SM. The Yukawa interaction Lagrangian of the lepton sector in the RH neutrino mass basis when $T_c < T < T_R$ is written as

$$\mathcal{L}_Y^\ell = -\overline{L_{Li}}(f_{ij}\Phi + \widetilde{f}_{ij}\widetilde{\Phi})L_{Rj} - h_{Rij}\overline{L^c_{Ri}}i\sigma_2\Delta_R L_{Rj} + \text{H.c.} \tag{4.3}$$

$$\begin{aligned}
&= -f_{ij}\overline{L_{Li}}\phi N_{Rj} - f_{ij}\overline{L_{Li}}\phi'\ell_{Rj} - \widetilde{f}_{ij}\overline{L_{Li}}\widetilde{\phi}' N_{Rj} - \widetilde{f}_{ij}\overline{L_{Li}}\widetilde{\phi}\ell_{Rj} \\
&\quad - f^*_{ji}\overline{N_{Rj}}\phi^\dagger L_{Li} - f^*_{ji}\overline{\ell_{Rj}}\phi'^\dagger L_{Li} - \widetilde{f}^*_{ji}\overline{N_{Rj}}\widetilde{\phi}'^\dagger L_{Li} - \widetilde{f}^*_{ji}\overline{\ell_{Rj}}\widetilde{\phi}^\dagger L_{Li} \\
&\quad - \frac{1}{\sqrt{2}}h_{Rij}v_R\overline{N^c_{Ri}}N_{Rj} - h_{Rij}\delta^0_R\overline{N^c_{Ri}}N_{Rj} + \sqrt{2}h_{Rij}\delta^+_R\overline{\ell^c_{Ri}}N_{Rj} + h_{Rij}\delta^{++}_R\overline{\ell^c_{Ri}}\ell_{Rj} \\
&\quad - \frac{1}{\sqrt{2}}h^*_{Rji}v_R\overline{N_{Rj}}N^c_{Ri} - h^*_{Rji}\delta^{0*}_R\overline{N_{Rj}}N^c_{Ri} + \sqrt{2}h^*_{Rji}\delta^-_R\overline{N_{Rj}}\ell^c_{Ri} + h^*_{Rji}\delta^{--}_R\overline{\ell_{Rj}}\ell^c_{Ri},
\end{aligned} \tag{4.4}$$

from which we can identify interactions that contribute to the lepton asymmetry.

4.2 One-loop resummed effective Yukawa couplings and decay rates

For simplicity, we write

$$L_i \equiv L_{Li}, \quad \ell_i \equiv \ell_{Ri}, \quad Q \equiv Q_L, \quad u \equiv u_R, \quad d \equiv d_R \tag{4.5}$$

where i is the lepton flavour index, and u, d can be any pair in the three flavours. We also use Greek and Roman indices for RH neutrino and LH lepton doublet flavours, respectively. The partial decay rates $\Gamma(N_\alpha \to L_i\phi)$ and $\Gamma(N_\alpha \to L_i^c\phi^\dagger)$ at $T = 0$ are given by

$$\Gamma(N_\alpha \to L_i\phi) = m_{N_\alpha} A^i_{\alpha\alpha}(\widehat{\mathbf{f}}), \qquad \Gamma(N_\alpha \to L_i^c\phi^\dagger) = m_{N_\alpha} A^i_{\alpha\alpha}(\widehat{\mathbf{f}}^c) \tag{4.6}$$

where $A^i_{\alpha\beta}$ is the absorptive transition amplitude defined by

$$A^i_{\alpha\beta}(\widehat{\mathbf{f}}) = \frac{1}{16\pi}\widehat{\mathbf{f}}_{i\alpha}\widehat{\mathbf{f}}^*_{i\beta}. \tag{4.7}$$

Here, $\widehat{\mathbf{f}}_{i\alpha}$ is the one-loop resummed effective Yukawa couplings given by [50]

$$\begin{aligned}\widehat{\mathbf{f}}_{i\alpha} = f_{i\alpha} - i\sum_{\beta,\gamma}|\epsilon_{\alpha\beta\gamma}|f_{i\beta} \\ \times \frac{m_\alpha(m_\alpha A_{\alpha\beta} + m_\beta A_{\beta\alpha}) - iR_{\alpha\gamma}\big[m_\alpha A_{\gamma\beta}(m_\alpha A_{\alpha\gamma} + m_\gamma A_{\gamma\alpha}) + m_\beta A_{\beta\gamma}(m_\alpha A_{\gamma\alpha} + m_\gamma A_{\alpha\gamma})\big]}{m_\alpha^2 - m_\beta^2 + 2im_\alpha^2 A_{\beta\beta} + 2i\mathrm{Im}[R_{\alpha\gamma}]\big(m_\alpha^2|A_{\beta\gamma}|^2 + m_\beta m_\gamma \mathrm{Re}[A^2_{\beta\gamma}]\big)}\end{aligned} \tag{4.8}$$

where $\epsilon_{\alpha\beta\gamma}$ is the Levi-Civita anti-symmetric tensor and

$$m_\alpha \equiv m_{N_\alpha}, \qquad A_{\alpha\beta} \equiv \sum_{i=1}^{3} A^i_{\alpha\beta}(\widehat{\mathbf{f}}), \qquad R_{\alpha\beta} = \frac{m_\alpha^2}{m_\alpha^2 - m_\beta^2 + 2im_\alpha^2 A_{\beta\beta}}. \tag{4.9}$$

The CP-conjugate effective Yukawa couplings $\widehat{\mathbf{f}}^c_{i\alpha}$ are obtained by replacing $h_{i\alpha}$ with $h^*_{i\alpha}$. The total two-body decay rate at $T = 0$ is written as

$$\Gamma^{N_\alpha}_{L\phi} = \sum_{i=1}^{3}\big[\Gamma(N_\alpha \to L_i\phi) + \Gamma(N_\alpha \to L_i^c\phi^\dagger)\big] = \frac{m_{N_\alpha}}{16\pi}\Big[\big(\widehat{\mathbf{f}}^\dagger\widehat{\mathbf{f}}\big)_{\alpha\alpha} + \big(\widehat{\mathbf{f}}^{c\dagger}\widehat{\mathbf{f}}^c\big)_{\alpha\alpha}\Big] \tag{4.10}$$

and the total three-body decay rate at $T = 0$ as

$$\Gamma^{N_\alpha}_{\ell_\alpha u d^c} = \Gamma(N_\alpha \to \ell_\alpha u d^c) + \Gamma(N_\alpha \to \ell^c_\alpha u^c d). \tag{4.11}$$

Here,

$$\Gamma(N_\alpha \to \ell_\alpha u d^c) = \Gamma(N_\alpha \to \ell^c_\alpha u^c d) = \frac{3 g_R^4}{2^9 \pi^3 m^3_{N_\alpha}} \int_0^{m^2_{N_\alpha}} ds \frac{m^6_{N_\alpha} - 3 m^2_{N_\alpha} s^2 + 2 s^3}{(s - m^2_{W_R})^2 + m^2_{W_R} \Gamma^2_{W_R}} \tag{4.12}$$

where $\Gamma_{W_R} \approx (g_R^2/4\pi) m_{W_R}$ is the total decay rate of W_R at $T = 0$ when $m_{N_\alpha} < W_R$, and all three quark flavours and colors have been considered. Note that we can have only one lepton flavour ℓ_α for each N_α.

4.3 Boltzmann equations and the lepton asymmetry

The generic Boltzmann equation is written as [48]

$$\frac{dn_a}{dt} + 3 H n_a = - \sum_{aX \leftrightarrow Y} \left[\frac{n_a n_X}{n_a^{\mathrm{eq}} n_X^{\mathrm{eq}}} \gamma(aX \to Y) - \frac{n_Y}{n_Y^{\mathrm{eq}}} \gamma(Y \to aX) \right] \tag{4.13}$$

where γ is the thermally averaged collision term. We define the CP-conserving collision terms for various decay and scattering processes by

$$\gamma^{aX}_Y \equiv \gamma(aX \to Y) + \gamma(\overline{a}\overline{X} \to \overline{Y}) \tag{4.14}$$

where $\overline{a}\overline{X} \to \overline{Y}$ is the CP-conjugate process of $aX \to Y$. Note that the CPT invariance implies

$$\gamma^{aX}_Y = \gamma^Y_{aX}. \tag{4.15}$$

We introduce the dimensionless time variable defined by

$$z \equiv \frac{m_{N_1}}{T}. \tag{4.16}$$

Then, the thermally averaged decay rates of N_α are wirtten as

$$\gamma^{N_\alpha}_{L_i\phi} \approx n^{\rm eq}_{N_1}\frac{K_1(z)}{K_2(z)}\Gamma^{N_\alpha}_{L_i\phi} = \frac{m^3_{N_1}}{\pi^2 z}K_1(z)\Gamma^{N_\alpha}_{L_i\phi}, \tag{4.17}$$

$$\gamma^{N_\alpha}_{\ell_\alpha ud^c} \approx n^{\rm eq}_{N_1}\frac{K_1(z)}{K_2(z)}\Gamma^{N_\alpha}_{\ell_\alpha ud^c} = \frac{m^3_{N_1}}{\pi^2 z}K_1(z)\Gamma^{N_\alpha}_{\ell_\alpha ud^c} \tag{4.18}$$

where $K_1(z)/K_2(z)$ is the thermally averaged time dilation factor. Defining the leptonic CP-asymmetry by

$$\delta^i_{N_\alpha} = \frac{\Gamma(N_\alpha \to L_i\phi) - \Gamma(N_\alpha \to L^c_i\phi^\dagger)}{\sum_{j=1}^3\left[\Gamma(N_\alpha \to L_j\phi) + \Gamma(N_\alpha \to L^c_j\phi^\dagger)\right]}, \tag{4.19}$$

we can write the CP-violating decay term as

$$\delta\gamma^{N_\alpha}_{L_i\phi} \equiv \gamma(N_\alpha \to L_i\phi) - \gamma(N_\alpha \to L^c_i\phi^\dagger) = \delta^i_{N_\alpha}\gamma^{N_\alpha}_{L\phi} \tag{4.20}$$

where

$$\gamma^{N_\alpha}_{L\phi} \equiv \sum_{i=1}^3 \gamma^{N_\alpha}_{L_i\phi}. \tag{4.21}$$

For $2 \to 2$ scattering processes, the thermally averaged collision term can be written as

$$\begin{aligned}\gamma^{XY}_{AB} &= \frac{T}{64\pi^4}\int_{s_{\min}}^\infty ds\ \sqrt{s}\ \hat\sigma^{XY}_{AB}(s)\ K_1\left(\frac{\sqrt{s}}{T}\right) \\ &= \frac{m^4_{N_1}}{64\pi^4 z}\int_{x_{\min}}^\infty dx\sqrt{x}K_1(z\sqrt{x})\hat\sigma^{XY}_{AB}(x)\end{aligned} \tag{4.22}$$

where $\hat\sigma^{XY}_{AB}$ is CP-conserving reduced cross section defined by

$$\hat\sigma^{XY}_{AB} \equiv \hat\sigma(XY \to AB) + \hat\sigma(AB \to XY). \tag{4.23}$$

The CP-conserving reduced cross sections for the dominant scattering processes are derived in appendix D, and they are given by

$$\hat{\sigma}_{\ell_\alpha d^c}^{N_\alpha u^c}(s) = \frac{9g_R^4}{4\pi s}\int_{m_N^2-s}^{0} dt\ \frac{(s+t)(s+t-m_N^2)}{(t-m_{W_R}^2)^2} \tag{4.24}$$

$$\hat{\sigma}_{\ell_\alpha d^c}^{N_\alpha u^c}(s) = \frac{9g_R^4}{4\pi s}\int_{m_N^2-s}^{0} dt\ \frac{(s+t)(s+t-m_N^2)}{(t-m_{W_R}^2)^2} \tag{4.25}$$

$$\hat{\sigma}_{\ell_\alpha u}^{N_\alpha d}(s) = \frac{9g_R^4}{4\pi}\frac{(m_N^2-s)^2}{m_{W_R}^2(s+m_{W_R}^2-m_N^2)}. \tag{4.26}$$

Following the steps in appendix D, we can write the Boltzmann equations for the RH neutrino density and the LH lepton doublet density as

$$\frac{dn_{N_\alpha}}{dt} + 3Hn_{N_\alpha} = \left(1-\frac{n_{N_\alpha}}{n_{N_\alpha}^{\rm eq}}\right)\left(\gamma_{L\phi}^{N_\alpha} + \gamma_{\ell_\alpha u d^c}^{N_\alpha} + \gamma_\alpha^{S_R}\right) - \sum_{j=1}^{3}\frac{n_{\Delta L_j}}{2n_{\ell_j}^{\rm eq}}\delta\gamma_{L_j\phi}^{N_\alpha}, \tag{4.27}$$

$$\frac{dn_{\Delta L_i}}{dt} + 3Hn_{\Delta L_i} = \sum_{\alpha=1}^{3}\left(\frac{n_{N_\alpha}}{n_{N_\alpha}^{\rm eq}}-1\right)\delta\gamma_{L_i\phi}^{N_\alpha} - \frac{n_{\Delta L_i}}{2n_{\ell_i}^{\rm eq}}\sum_{\alpha=1}^{3}\gamma_{L_i\phi}^{N_\alpha} \tag{4.28}$$

where

$$\gamma_\alpha^{S_R} \equiv \gamma_{u^c d}^{N_\alpha \ell_\alpha} + \gamma_{\ell_\alpha d^c}^{N_\alpha u^c} + \gamma_{\ell_\alpha u}^{N_\alpha d}. \tag{4.29}$$

We can simplify the Boltzmann equations using the dimensionless time variable z introduced above and also using normalized densities of RH neutrinos and lepton asymmetry. First, we write the Hubble parameter at $z=1$ as

$$H_N \equiv H(z=1) \approx \sqrt{\frac{8\pi^3 g_*}{90}}\frac{m_{N_1}^2}{M_{\rm Pl}} = z^2 H \tag{4.30}$$

where g_* is the SM degree of freedom. The photon number density is given by

$$n_\gamma = \frac{2m_{N_1}^3\zeta(3)}{\pi^2 z^3}. \tag{4.31}$$

where $\zeta(x) = \sum_{n=1}^{\infty} n^{-x}$ is the Riemann zeta function. Now we introduce the normalized densities of RH neutrinos and lepton asymmetry defined by

$$\eta_{N_\alpha} \equiv \frac{n_{N_\alpha}}{n_\gamma}, \qquad \eta_{\Delta_{L_i}} \equiv \frac{n_{\Delta L_i}}{n_\gamma}, \tag{4.32}$$

and the normalized RH neutrino density in equilibrium is

$$\eta^{\text{eq}}_{N_\alpha} = \frac{n^{\text{eq}}_{N_\alpha}}{n_\gamma} \approx \frac{n^{\text{eq}}_{N_1}}{n_\gamma} = \frac{1}{2\zeta(3)} z^2 K_2(z). \tag{4.33}$$

As shown in appendix D, we can simplify the left-hand sides of the Boltzmann equations 4.27 and 4.28 using the normalized densities, and they are written as

$$\frac{H_N n_\gamma}{z}\frac{d\eta_{N_\alpha}}{dz} = -\left(\frac{\eta_{N_\alpha}}{\eta^{\text{eq}}_{N_\alpha}} - 1\right)\left(\gamma^{N_\alpha}_{L\phi} + \gamma^{N_\alpha}_{\ell_\alpha u d^c} + \gamma^{S_R}_\alpha\right) - \frac{2}{3}\sum_{j=1}^{3} \eta_{\Delta L_j} \delta^j_{N_\alpha} \gamma^{N_\alpha}_{L\phi}, \tag{4.34}$$

$$\frac{H_N n_\gamma}{z}\frac{d\eta_{\Delta L_i}}{dz} = \sum_{\alpha=1}^{3} \delta^i_{N_\alpha}\left(\frac{\eta_{N_\alpha}}{\eta^{\text{eq}}_{N_\alpha}} - 1\right)\gamma^{N_\alpha}_{L\phi} - \frac{2}{3}\eta_{\Delta L_i}\sum_{\alpha=1}^{3}\gamma^{N_\alpha}_{L_i\phi} \tag{4.35}$$

where we have used $n^{\text{eq}}_{\ell_i} = 3/4$. When the lepton asymmetry satisfies $|\delta^i_{N_\alpha}| \ll 1$, we can safely neglect the second term in equation 4.34 to obtain

$$\frac{H_N n_\gamma}{z}\frac{d\eta_{N_\alpha}}{dz} = -\left(\frac{\eta_{N_\alpha}}{\eta^{\text{eq}}_{N_\alpha}} - 1\right)\left(\gamma^{N_\alpha}_{L\phi} + \gamma^{N_\alpha}_{\ell_\alpha u d^c} + \gamma^{S_R}_\alpha\right), \tag{4.36}$$

$$\frac{H_N n_\gamma}{z}\frac{d\eta_{\Delta L_i}}{dz} = \sum_{\alpha=1}^{3} \delta^i_{N_\alpha}\left(\frac{\eta_{N_\alpha}}{\eta^{\text{eq}}_{N_\alpha}} - 1\right)\gamma^{N_\alpha}_{L\phi} - \frac{2}{3}\eta_{\Delta L_i}\sum_{\alpha=1}^{3}\gamma^{N_\alpha}_{L_i\phi}. \tag{4.37}$$

From equation 4.36, we can find the expression

$$\frac{\eta_{N_\alpha}}{\eta^{\text{eq}}_{N_\alpha}} - 1 = -\frac{H_N n_\gamma}{z}\frac{d\eta_{N_\alpha}}{dz}\frac{1}{\gamma^{N_\alpha}_{L\phi} + \gamma^{N_\alpha}_{\ell_\alpha u d^c} + \gamma^{S_R}_\alpha}, \tag{4.38}$$

which we can substitute into equation 4.37 to obtain

$$\frac{d\eta_{\Delta L_i}}{dz} = -\sum_{\alpha=1}^{3} \delta^i_{N_\alpha}\frac{d\eta_{N_\alpha}}{dz}\frac{\widetilde{D}_\alpha}{D_\alpha + S_\alpha} - \frac{2}{3}\eta_{\Delta L_i} W_i \tag{4.39}$$

where

$$\widetilde{D}_\alpha \equiv \frac{z}{H_N n_\gamma}\gamma_{L\phi}^{N_\alpha}, \quad D_\alpha \equiv \frac{z}{H_N n_\gamma}(\gamma_{L\phi}^{N_\alpha} + \gamma_{\ell_\alpha u d^c}^{N_\alpha}), \quad S_\alpha \equiv \frac{z}{H_N n_\gamma}\gamma_\alpha^{S_R}, \quad W_i = \frac{z}{H_N n_\gamma}\sum_{\alpha=1}^{3}\gamma_{L_i\phi}^{N_\alpha}. \tag{4.40}$$

The differential equation 4.39 can be solved by the integrating factor method, as shown in appendix E. Assuming the initial lepton asymmetry is negligible, we obtain the expression

$$\eta_{\Delta L_i}(z) = -\sum_{\alpha=1}^{3}\delta_{N_\alpha}^i \kappa_{N_\alpha}^i(z) \tag{4.41}$$

where $\kappa_{N_\alpha}^i$ is the efficiency factor defined by

$$\kappa_{N_\alpha}^i(z) \equiv \int_{z_0}^{z} dz' \frac{d\eta_{N_\alpha}}{dz'}\frac{\widetilde{D}_\alpha}{D_\alpha + S_\alpha}\left[-\frac{2}{3}\int_{z'}^{z} dz'' W_i(z'')\right]. \tag{4.42}$$

Due to the strong washout of RH neutrino densities in the TeV-scale leptogenesis, we have $|\eta_{N_\alpha}/\eta_{N_\alpha}^{\mathrm{eq}} - 1| \ll 1$. We may therefore approximately assume $\eta_{N_\alpha} \approx \eta_{N_\alpha}^{\mathrm{eq}}$, and thus

$$\frac{d\eta_{N_\alpha}}{dz} \approx \frac{d\eta_{N_\alpha}^{\mathrm{eq}}}{dz} \approx \frac{d\eta_{N_1}^{\mathrm{eq}}}{dz} = -\frac{1}{2\zeta(3)}z^2 K_1(z) \tag{4.43}$$

where z_0 is the initial time with the initial lepton asymmetry. If the lepton washout term satisfies $W_i(z_c) \lesssim 1$, the lepton asymmetry freezes out at $z_B < z_c$ where z_B can be found by the steepest descent method [51]. On the other hand, if $W_i(z_c) \gg 1$ as in the TeV-scale leptogenesis, we can find an approximate expression of the lepton asymmetry from equations 4.41 and 4.42, as shown in appendix D [52]. The approximate form of the asymmetry in the LH lepton doublet is now given by

$$\eta_{\Delta L_i}(z) \approx \frac{3z^2 K_1(z)}{4W_i(z)}\sum_{\alpha=1}^{3}\delta_{N_\alpha}^i \frac{\widetilde{D}_\alpha}{D_\alpha + S_\alpha}, \tag{4.44}$$

and the total asymmetry is

$$\eta_{\Delta L}(z) \equiv \sum_{i=1}^{3} \eta_{\Delta L_i}(z). \tag{4.45}$$

4.4 Numerical procedure

For the successful leptogenesis, we should be able to find the model parameters that would give $|\eta_{\Delta L}(z_c)| = (2.47 \pm 0.03) \cdot 10^{-8}$ which is the value consistent with the observed baryon asymmetry. The following is the numerical procedure:

1. Randomly generate the lightest light neutrino mass m_{ν_1}, and calculate $m_{\nu_2} = \sqrt{m_{\nu_1}^2 + \Delta m_{21}^2}$ and $m_{\nu_3} = \sqrt{m_{\nu_1}^2 + \Delta m_{31}^2}$.

2. Calculate M_ν^c from $M_\nu^c = U_{\text{PMNS}} M_\nu^d U_{\text{PMNS}}^\intercal$ where M_ν^c and M_ν^d are the light neutrino mass matrices in the charged lepton and light neutrino mass bases, respectively. The mixing matrix U_{PMNS} is the PMNS matrix whose CP phases are also randomly generated.

3. Randomly generate m_{N_2}, $m_{N_2} - m_{N_1}$, and $m_{N_3} - m_{N_2}$ which determine M_R in the RH neutrino mass basis.

4. Randomly generate a complex orthogonal matrix O, and calculate $M_D = -iU_{\text{PMNS}}\sqrt{M_\nu^d}O\sqrt{M_R^d}$ [47] where M_D is the Dirac mass matrix in the RH neutrino mass basis.

5. Randomly generate V_R^ℓ, and calculate $M_\ell = M_\ell^c V_R^{\ell\dagger}$ where M_ℓ is the charged lepton mass basis in the RH neutrino mass basis.

6. Randomly generate κ_2, α, and calculate $\kappa_1 = \sqrt{v_{\rm EW}^2 - \kappa_2^2}$. Find the Yukawa coupling matrices in RH neutrino mass basis from

$$f = \sqrt{2}\frac{\kappa_1 M_D - \kappa_2 e^{-i\alpha} M_\ell}{\kappa_1^2 - \kappa_2^2}, \qquad \widetilde{f} = \sqrt{2}\frac{\kappa_1 M_\ell - \kappa_2 e^{i\alpha} M_D}{\kappa_1^2 - \kappa_2^2}, \tag{4.46}$$

   where f is the Yukawa couplings associated with the decay and scattering processes of our interest under the assumption we have introduced.

7. Calculate one-loop resummed effective Yukawa couplings $\widehat{\mathbf{f}}$, $\widehat{\mathbf{f}}^c$ from f, m_{N_α}, and calculate the CP asymmetry and collision terms.

8. Calculate $\eta_{\Delta L_i}(z_c)$, the normalized asymmetry in the LH lepton doublet at z_c, from the CP asymmetry and collision terms we have obtained.

9. Calculate $M_D^c = M_D V_R^\ell$ and $M_R^c = V_R^{\ell\mathsf{T}} M_R V_R^\ell$ where M_D^c and M_R^c are the Dirac and RH neutrino mass matrices in the charged lepton mass basis, respectively.

10. Construct the 6×6 neutrino mass matrix $M_{\nu N}^c$ from M_D^c and M_R^c, and find the 6×6 mixing matrix $V_{\nu N}$ that diagonalizes $M_{\nu N}^c$.

The mixing matrices $U_{\rm PMNS}$, V_L^ℓ, V_R^ℓ, and $V_{\nu N}$ are parametrized in the same way as in the MLRSM. The complex orthogonal matrix can be parametrized as $O = e^S$ where S is a skew-symmetric complex matrix, i.e. $S^\mathsf{T} = -S$.

4.5 Numerical results

The lower bound of m_{W_R} compatible with leptogenesis is found to be 6.9 TeV, which is beyond the upper limit observable at the LHC. The numerical results are presented in figure 4.1. If we discover W_R much lighter than this value, the idea of leptogenesis can be falsified.

4.6 Conclusion

We have analyzed the leptogenesis constraints on the mass of the right-handed gauge boson in TeV scale Left-Right Symmetric Models. While the existing bound of $m_{W_R} > 18$ TeV applies for generic LRSM scenarios with small Yukawa couplings, we have found a significantly weaker bound of $m_{W_R} > 6.9$ TeV in a new class of LRSM scenarios with relatively larger Yukawa couplings, which is consistent with charged lepton and neutrino mass data. The key factors responsible for our result is the inclusion of flavour effects in the lepton asymmetry calculation. This lower bound, $m_{W_R} > 6.9$ TeV is for the case $g_L = g_R$ and will be proportionately weaker for the case $g_R < g_L$.

$$\eta_{\Delta L} = -2.56625 \times 10^{-8}$$

$$\delta^{1}_{N_\alpha} = \begin{pmatrix} -0.0098659 & -0.0164987 & -0.0129664 \\ -0.0273944 & -0.046093 & -0.0396994 \\ -0.677135 & -0.793726 & -0.686942 \end{pmatrix}$$

$$M^c_e = \begin{pmatrix} 0.000510999 & 0 & 0 \\ 0 & 0.105658 & 0 \\ 0 & 0 & 1.77682 \end{pmatrix}$$

$$M^c_D = \begin{pmatrix} -0.000635111 + 0.000740116\, i & 0.000572994 - 0.00255843\, i & 0.00399996 - 0.000938214\, i \\ -0.00215076 - 0.000149496\, i & 0.00508133 - 0.00251575\, i & 0.00699261 + 0.00533485\, i \\ -0.00129373 - 0.00113779\, i & 0.00444275 + 0.000813458\, i & 0.00193709 + 0.00671706\, i \end{pmatrix}$$

$$M^c_N = \begin{pmatrix} -574.638 - 130.881\, i & 190.491 - 91.8402\, i & -26.5036 + 128.904\, i \\ 190.491 - 91.8402\, i & 357.293 - 338.94\, i & 344.719 + 57.3294\, i \\ -26.5036 + 128.904\, i & 344.719 + 57.3294\, i & -170.303 - 490.855\, i \end{pmatrix}$$

$$M^c_\nu = \begin{pmatrix} 2.35638 \times 10^{-12} - 3.69644 \times 10^{-12}\, i & -3.70912 \times 10^{-12} - 6.89858 \times 10^{-12}\, i & -2.75962 \times 10^{-12} - 1.4165 \times 10^{-12}\, i \\ -3.70912 \times 10^{-12} - 6.89858 \times 10^{-12}\, i & -1.15321 \times 10^{-11} - 2.04493 \times 10^{-11}\, i & -1.56218 \times 10^{-11} - 1.64126 \times 10^{-11}\, i \\ -2.75962 \times 10^{-12} - 1.4165 \times 10^{-12}\, i & -1.56218 \times 10^{-11} - 1.64126 \times 10^{-11}\, i & -1.55944 \times 10^{-11} - 2.56137 \times 10^{-11}\, i \end{pmatrix}$$

$$V^e_L = \begin{pmatrix} 1 & 0 & 0 \\ 0 & 1 & 0 \\ 0 & 0 & 1 \end{pmatrix}$$

$$V^e_R = \begin{pmatrix} -0.0294241 + 0.\, i & -0.622585 + 0.\, i & -0.581052 + 0.523354\, i \\ 0.222044 - 0.560449\, i & 0.550676 - 0.27554\, i & -0.171041 + 0.477673\, i \\ 0.0278173 + 0.79684\, i & 0.297245 - 0.380614\, i & 0.00611647 + 0.361959\, i \end{pmatrix}$$

$$V_N = \begin{pmatrix} 0.0370865 + 0.0140632\, i & -0.214522 - 0.670525\, i & -0.0595627 + 0.70658\, i \\ 0.642664 + 0.011654\, i & -0.480788 - 0.216845\, i & -0.367472 - 0.416691\, i \\ 0.574962 + 0.50467\, i & 0.188928 + 0.436467\, i & 0.0252783 + 0.433463\, i \end{pmatrix}$$

$$V_\nu = \begin{pmatrix} 0.82424 + 0.\, i & -0.417488 - 0.353112\, i & 0.0717677 + 0.128427\, i \\ -0.494707 - 0.0035396\, i & -0.436112 - 0.365788\, i & 0.29512 + 0.586653\, i \\ 0.275435 - 0.00398674\, i & 0.467104 + 0.398541\, i & 0.332402 + 0.660763\, i \end{pmatrix}$$

$$V_{PMNS} = V^*_\nu = \begin{pmatrix} 0.82424 + 0.\, i & -0.417488 + 0.353112\, i & 0.0717677 - 0.128427\, i \\ -0.494707 + 0.0035396\, i & -0.436112 + 0.365788\, i & 0.29512 - 0.586653\, i \\ 0.275435 + 0.00398674\, i & 0.467104 - 0.398541\, i & 0.332402 - 0.660763\, i \end{pmatrix}$$

$$= \begin{pmatrix} 0.82424 & 0.546795 & 0.14698 + 0.00639777\, i \\ -0.494707 + 0.0035396\, i & 0.5692 + 0.00234814\, i & 0.656702 \\ 0.275435 + 0.00398674\, i & -0.614015 + 0.00264478\, i & 0.739661 \end{pmatrix} \begin{pmatrix} 1 & 0 & 0 \\ 0 & -0.763519 + 0.645785\, i & 0 \\ 0 & 0 & 0.449397 - 0.893332\, i \end{pmatrix}$$

$$\kappa_1 = 245.853$$

$$\kappa_2 = 8.50597 \exp[0 \pi i]$$

$$m_{W_R} = 6900.$$

$$m_{\nu_1} = 3.62394 \times 10^{-12}$$

$$m_{\nu_2} = 9.38791 \times 10^{-12}$$

$$m_{\nu_3} = 5.037 \times 10^{-11}$$

$$m_{N_1} = 639.827$$

$$m_{N_2} = 639.827$$

$$m_{N_3} = 639.827$$

$$f = \begin{pmatrix} -0.0000181571 + 1.31424 \times 10^{-7}\, i & -3.86773 \times 10^{-6} - 0.0000184449\, i & 8.06605 \times 10^{-6} - 8.38068 \times 10^{-6}\, i \\ -0.000012068 - 0.000029883\, i & 0.0000140342 - 0.000037341\, i & 0.000018292 - 5.72388 \times 10^{-6}\, i \\ 0.000203769 + 0.000154248\, i & 0.0000919429 + 0.000161169\, i & 0.0000122986 + 0.000141232\, i \end{pmatrix}$$

$$\tilde{f} = \begin{pmatrix} 5.41707 \times 10^{-7} - 4.54699 \times 10^{-9}\, i & 7.86491 \times 10^{-7} + 2.28554 \times 10^{-6}\, i & -1.97301 \times 10^{-7} - 2.05228 \times 10^{-6}\, i \\ -0.000377975 + 1.03389 \times 10^{-6}\, i & 0.000334202 + 0.000168759\, i & 0.000180025 + 0.000231526\, i \\ -0.00594585 - 0.00535442\, i & -0.00175135 - 0.00488776\, i & 0.0000620894 - 0.00370438\, i \end{pmatrix}$$

$$h = \begin{pmatrix} 0.0301368 - 2.75093 \times 10^{-18}\, i & 0. - 1.73472 \times 10^{-18}\, i & -1.73472 \times 10^{-18} + 0.\, i \\ 1.73472 \times 10^{-18} + 2.60209 \times 10^{-18}\, i & 0.0301368 - 4.33681 \times 10^{-18}\, i & -1.73472 \times 10^{-18} - 1.30104 \times 10^{-18}\, i \\ -1.73472 \times 10^{-18} + 2.60209 \times 10^{-18}\, i & -2.60209 \times 10^{-18} - 8.67362 \times 10^{-19}\, i & 0.0301368 - 3.52366 \times 10^{-19}\, i \end{pmatrix}$$

$$\tilde{h}_L = \begin{pmatrix} 0.0927286 - 8.46441 \times 10^{-18}\, i & 0. - 5.33761 \times 10^{-18}\, i & -5.33761 \times 10^{-18} + 0.\, i \\ 5.33761 \times 10^{-18} + 8.00642 \times 10^{-18}\, i & 0.0927286 - 1.3344 \times 10^{-17}\, i & -5.33761 \times 10^{-18} - 4.00321 \times 10^{-18}\, i \\ -5.33761 \times 10^{-18} + 8.00642 \times 10^{-18}\, i & -8.00642 \times 10^{-18} - 2.66881 \times 10^{-18}\, i & 0.0927286 - 1.0842 \times 10^{-18}\, i \end{pmatrix}$$

$$\tilde{h}_R = \begin{pmatrix} -0.0832808 - 0.0189682\, i & 0.0276075 - 0.0133102\, i & -0.0038411 + 0.0186818\, i \\ 0.0276075 - 0.0133102\, i & 0.0517817 - 0.0491218\, i & 0.0499593 + 0.00830861\, i \\ -0.0038411 + 0.0186818\, i & 0.0499593 + 0.00830861\, i & -0.0246817 - 0.0711384\, i \end{pmatrix}$$

$$S = \begin{pmatrix} 0 & 14.9546 + 6.58761\, i & 6.53022 - 4.55682\, i \\ -14.9546 - 6.58761\, i & 0 & 15.8559 + 2.05712\, i \\ -6.53022 + 4.55682\, i & -15.8559 - 2.05712\, i & 0 \end{pmatrix}$$

$$O = \begin{pmatrix} -23.2185 - 11.8264\, i & 7.05841 - 26.4874\, i & 16.7591 - 5.22894\, i \\ -29.8507 + 42.8762\, i & -49.765 - 21.8951\, i & -5.7836 - 32.8985\, i \\ 36.2855 + 27.705\, i & -21.2896 + 42.3987\, i & -28.4491 + 3.60783\, i \end{pmatrix}$$

Figure 4.1: Values of parameters and mass matrices that give the lower bound of $m_{W_R} = 6.9$ TeV. The lepton asymmetry is slightly larger than $2.47 \cdot 10^{-8}$, and thus slightly smaller value of m_{W_R} is allowed.

Chapter 5: Conclusion

We have investigated the TeV-scale phenomenology of the LRSM. We have provided a new method to construct lepton mass matrices in the MLRSM of type-I dominance with the parity symmetry. Using this method, we have investigated the TeV-scale phenomenology of the MLRSM in the normal hierarchy of light neutrino masses, and explored the model predictions for the CLFV, $0\nu\beta\beta$, EDM's of charged leptons. We have also presented a natual TeV-scale seesaw model which does not require fine-tuning of model parameters for the TeV-scale phenomenology. A discrete flavour symmetry is shown to guarantee a specific texture of lepton mass matrices. In addition, we have studied the leptogenesis with TeV-scale W_R and m_N, and presented a lower bound of m_{W_R} which allows leptogenesis.

Appendix A: Derivation of various expressions in the minimal left-right symmetric model

A.1 Gauge group and fields

The gauge group of the left-right symmetric model (LRSM) is given by

$$\mathrm{SU}(2)_L \otimes \mathrm{SU}(2)_R \otimes \mathrm{U}(1)_{B-L}. \tag{A.1}$$

The representations of the leptons are

$$L'_{Li} = \begin{pmatrix} \nu'_{Li} \\ \ell'_{Li} \end{pmatrix} \sim (\mathbf{2}, \mathbf{1}, -1), \qquad L'_{Ri} = \begin{pmatrix} \nu'_{Ri} \\ \ell'_{Ri} \end{pmatrix} \sim (\mathbf{1}, \mathbf{2}, -1), \tag{A.2}$$

and for quarks, we have

$$Q'_{Li} = \begin{pmatrix} u'_{Li} \\ d'_{Li} \end{pmatrix} \sim (\mathbf{2}, \mathbf{1}, 1/3), \qquad Q'_{Ri} = \begin{pmatrix} u'_{Ri} \\ d'_{Ri} \end{pmatrix} \sim (\mathbf{1}, \mathbf{2}, 1/3) \tag{A.3}$$

where i is the generation index. In addition, the scalar bi-doublet field is given by

$$\Phi = \begin{pmatrix} \phi_1^0 & \phi_2^+ \\ \phi_1^- & \phi_2^0 \end{pmatrix} \sim (\mathbf{2}, \mathbf{2}, 0), \tag{A.4}$$

and the scalar triplet field is

$$\Delta_L = \begin{pmatrix} \delta_L^+/\sqrt{2} & \delta_L^{++} \\ \delta_L^0 & -\delta_L^+/\sqrt{2} \end{pmatrix} \sim (\mathbf{3}, \mathbf{1}, 2), \qquad \Delta_R = \begin{pmatrix} \delta_R^+/\sqrt{2} & \delta_R^{++} \\ \delta_R^0 & -\delta_R^+/\sqrt{2} \end{pmatrix} \sim (\mathbf{1}, \mathbf{3}, 2). \tag{A.5}$$

A.2 Current and generators

The SU(2)$_L\otimes$ SU(2)$_R$ generators are

$$\begin{aligned} T_{L+} &= \int d^3x(\nu_L'^\dagger e_L' + u_L'^\dagger d_L'), \qquad T_{L-} = (T_{L+})^\dagger, \qquad T_{L3} = \frac{1}{2}\int d^3x(\nu_L'^\dagger \nu_L' - e_L'^\dagger e_L' + u_L'^\dagger u_L' - d_L'^\dagger d_L'), \\ T_{R+} &= \int d^3x(\nu_R'^\dagger e_R' + u_R'^\dagger d_R'), \qquad T_{R-} = (T_{R+})^\dagger, \qquad T_{R3} = \frac{1}{2}\int d^3x(\nu_R'^\dagger \nu_R' - e_R'^\dagger e_R' + u_R'^\dagger u_R' - d_R'^\dagger d_R'). \end{aligned} \tag{A.6}$$

The electric charge generator is given by

$$Q = \int d^3x \left(-e'^\dagger e' + \frac{2}{3}u'^\dagger u' - \frac{1}{3}d'^\dagger d' \right). \tag{A.7}$$

Now we can find the U(1)$_{B-L}$ generator given by

$$\begin{aligned} Q - T_{L3} - T_{R3} &= \int d^3x \left[-\frac{1}{2}(\nu_L'^\dagger \nu_L' + \nu_R'^\dagger \nu_R' + e_L'^\dagger e_L' + e_R'^\dagger e_R') + \frac{1}{6}(u_L'^\dagger u_L' + u_R'^\dagger u_R' + d_L'^\dagger d_L' + d_R'^\dagger d_R') \right] \\ &= \frac{B-L}{2}. \end{aligned} \tag{A.8}$$

Since we have $Y = 2(Q - T_{L3})$, the generators satisfy

$$\frac{Y}{2} = T_{R3} + \frac{B-L}{2}. \tag{A.9}$$

A.3 Yukawa interaction Lagrangian

The Yukawa interaction Lagrangian is written as

$$\mathcal{L}_Y^\ell = -\overline{L'_{Li}}(f_{ij}\Phi + \widetilde{f}_{ij}\widetilde{\Phi})L'_{Rj} - h_{Lij}\overline{L'^c_{Li}}i\sigma_2\Delta_L L'_{Lj} - h_{Rij}\overline{L'^c_{Ri}}i\sigma_2\Delta_R L'_{Rj} + \text{H.c.} \tag{A.10}$$

$$\begin{aligned} = &-f_{ij}\phi_2^0\overline{\ell'_{Li}}\ell'_{Rj} - f_{ij}\phi_1^0\overline{\nu'_{Li}}\nu'_{Rj} - f_{ij}\phi_1^-\overline{\ell'_{Li}}\nu'_{Rj} - f_{ij}\phi_2^+\overline{\nu'_{Li}}\ell'_{Rj} \\ &- \widetilde{f}_{ij}\phi_1^{0*}\overline{\ell'_{Li}}\ell'_{Rj} - \widetilde{f}_{ij}\phi_2^{0*}\overline{\nu'_{Li}}\nu'_{Rj} + \widetilde{f}_{ij}\phi_2^-\overline{\ell'_{Li}}\nu'_{Rj} + \widetilde{f}_{ij}\phi_1^+\overline{\nu'_{Li}}\ell'_{Rj} \\ &- h_{Lij}\delta_L^0\overline{\nu'^c_{Li}}\nu_{Lj} + \frac{1}{\sqrt{2}}h_{Lij}\delta_L^+\overline{\ell'^c_{Li}}\nu'_{Lj} + \frac{1}{\sqrt{2}}h_{Lij}\delta_L^+\overline{\nu'^c_{Li}}\ell'_{Lj} + h_{Lij}\delta_L^{++}\overline{\ell'^c_{Li}}\ell'_{Lj} \\ &- h_{Rij}\delta_R^0\overline{\nu'^c_{Ri}}\nu'_{Rj} + \frac{1}{\sqrt{2}}h_{Rij}\delta_R^+\overline{\ell'^c_{Ri}}\nu'_{Rj} + \frac{1}{\sqrt{2}}h_{Rij}\delta_R^+\overline{\nu'^c_{Ri}}\ell'_{Rj} + h_{Rij}\delta_R^{++}\overline{\ell'^c_{Ri}}\ell'_{Rj} \\ &+ \text{H.c.} \end{aligned} \tag{A.11}$$

where

$$\widetilde{\Phi} \equiv \sigma_2\Phi^*\sigma_2 = \begin{pmatrix} \phi_2^{0*} & -\phi_1^+ \\ -\phi_2^- & \phi_1^{0*} \end{pmatrix}. \tag{A.12}$$

We have also defined $\psi^c \equiv \mathsf{C}\psi^*$ and $\overline{\psi^c} = -\psi^\mathsf{T}\mathsf{C}$ where $\mathsf{C} = i\gamma^2\gamma^0$ is the charge conjugation operator in the Dirac-Pauli representation.

A.4 Spontaneous symmetry breaking and fermion masses

Without loss of generality, the scalar fields after the spontaneous symmetry breaking are written as

$$\langle\Phi\rangle = \begin{pmatrix} \kappa_1/\sqrt{2} & 0 \\ 0 & \kappa_2 e^{i\alpha}/\sqrt{2} \end{pmatrix}, \qquad \langle\Delta_L\rangle = \begin{pmatrix} 0 & 0 \\ v_L e^{i\theta_L}/\sqrt{2} & 0 \end{pmatrix}, \qquad \langle\Delta_R\rangle = \begin{pmatrix} 0 & 0 \\ v_R/\sqrt{2} & 0 \end{pmatrix}. \tag{A.13}$$

After spontaneous symmetry breaking, the Yukawa coupling terms are written as

$$\langle \mathcal{L}_Y^\ell \rangle = -\frac{1}{\sqrt{2}} f_{ij}\kappa_2 e^{i\alpha}\overline{\ell'_{Li}}\ell'_{Rj} - \frac{1}{\sqrt{2}} f_{ij}\kappa_1 \overline{\nu'_{Li}}\nu'_{Rj} - \frac{1}{\sqrt{2}}\widetilde{f}_{ij}\kappa_1\overline{\ell'_{Li}}\ell'_{Rj} - \frac{1}{\sqrt{2}}\widetilde{f}_{ij}\kappa_2 e^{-i\alpha}\overline{\nu'_{Li}}\nu'_{Rj}$$
$$- \frac{1}{\sqrt{2}} h_{Lij} v_L e^{i\theta_L}\overline{\nu'^c_{Li}}\nu'_{Lj} - \frac{1}{\sqrt{2}} h_{Rij} v_R \overline{\nu'^c_{Ri}}\nu'_{Rj} + \text{H.c.}. \tag{A.14}$$

The mass terms for leptons are written as

$$\mathcal{L}_\ell^{\text{mass}} = -\frac{1}{\sqrt{2}}(f_{ij}\kappa_2 e^{i\alpha} + \widetilde{f}_{ij}\kappa_1)\overline{\ell'_{Li}}\ell'_{Rj} + \text{H.c.}. \tag{A.15}$$

We therefore have

$$M_\ell = \frac{1}{\sqrt{2}}(f\kappa_2 e^{i\alpha} + \widetilde{f}\kappa_1). \tag{A.16}$$

The neutrino mass terms are given by

$$\mathcal{L}_\nu^{\text{mass}} = -\frac{1}{\sqrt{2}}(f_{ij}\kappa_1 + \widetilde{f}_{ij}\kappa_2 e^{-i\alpha})\overline{\nu'_{Li}}\nu'_{Rj} - \frac{1}{\sqrt{2}} h_{Lij} v_L e^{i\theta_L}\overline{\nu'^c_{Li}}\nu'_{Lj} - \frac{1}{\sqrt{2}} h_{Rij} v_R \overline{\nu'^c_{Ri}}\nu'_{Rj} + \text{H.c.}. \tag{A.17}$$

We have the identity

$$\overline{\nu'_L}\nu'_R = (\overline{\nu'_L}\nu'_R)^\mathsf{T} = -\nu'^\mathsf{T}_R\gamma_0^\mathsf{T}\nu'^*_L = -\nu'^\mathsf{T}_R \mathsf{C}^\dagger\mathsf{C}\gamma_0^\mathsf{T}\nu'^*_L = (\mathsf{C}\nu'^*_R)^\dagger\gamma_0\mathsf{C}\nu'^*_L = \overline{\nu'^c_R}\nu'^c_L \tag{A.18}$$

where we have used $\mathsf{C}^{-1}\gamma_\mu\mathsf{C} = -\gamma_\mu^\mathsf{T}$. Similarly,

$$\overline{\nu'^c_{Li}}\nu'_{Lj} = \overline{\nu'^c_{Lj}}\nu'_{Li}, \qquad \overline{\nu'^c_{Ri}}\nu'_{Rj} = \overline{\nu'^c_{Rj}}\nu'_{Ri}. \tag{A.19}$$

Hence, we can write

$$\mathcal{L}_\nu^{\text{mass}} = -\frac{1}{2}(\overline{\nu'_L}\ \overline{\nu'^c_R})\begin{pmatrix} M_L & M_D \\ M_D^\mathsf{T} & M_R \end{pmatrix}\begin{pmatrix} \nu'^c_L \\ \nu'_R \end{pmatrix} + \text{H.c.} \tag{A.20}$$

where

$$M_D = \frac{1}{\sqrt{2}}(f\kappa_1 + \widetilde{f}\kappa_2 e^{-i\alpha}), \qquad M_L = \sqrt{2}h_L^* v_L e^{-i\theta_L}, \qquad M_R = \sqrt{2}h_R v_R. \tag{A.21}$$

A.5 Gauge bosons

The covariant derivative is given by

$$D_\mu = \partial_\mu - ig_L \boldsymbol{T}_L \cdot \boldsymbol{W}_{L\mu} - ig_R \boldsymbol{T}_R \cdot \boldsymbol{W}_{R\mu} - ig' \frac{B-L}{2} B_\mu. \tag{A.22}$$

Now we define

$$W_\mu^+ \equiv \frac{1}{\sqrt{2}}(W_\mu^1 - iW_\mu^2), \quad W_\mu^- \equiv \frac{1}{\sqrt{2}}(W_\mu^1 + iW_\mu^2). \tag{A.23}$$

Kinetic terms

The kinetic terms for SU(2) gauge bosons are

$$\begin{aligned}
-\frac{1}{4}F_a^{\mu\nu}F^a_{\mu\nu} &= -\frac{1}{4}(\partial^\mu W_a^\nu - \partial^\nu W_a^\mu - gf^{abc}W_b^\mu W_c^\nu)(\partial_\mu W_\nu^a - \partial_\nu W_\mu^a - gf^{abc}W_\mu^b W_\nu^c) \\
&= -\frac{1}{4}(\partial^\mu W_a^\nu - \partial^\nu W_a^\mu)(\partial_\mu W_\nu^a - \partial_\nu W_\mu^a) + \frac{1}{2}gf^{abc}W_b^\mu W_c^\nu(\partial_\mu W_\nu^a - \partial_\nu W_\mu^a) \\
&\quad - \frac{1}{4}g^2 f^{abc}f^{ade}W_b^\mu W_c^\nu W_\mu^d W_\nu^e.
\end{aligned} \tag{A.24}$$

Lepton sector

For the LH leptons and neutrinos, we have

$$\begin{aligned}
\overline{L'_{Li}}i\gamma^\mu D_\mu L'_{Li} &= (\overline{\nu'_{Li}}\ \overline{\ell'_{Li}})i\gamma^\mu\partial_\mu \begin{pmatrix} \nu'_{Li} \\ \ell'_{Li} \end{pmatrix} + \frac{1}{2}(\overline{\nu'_{Li}}\ \overline{\ell'_{Li}})\gamma^\mu \begin{pmatrix} g_L W_{L\mu}^3 - g'B_\mu & \sqrt{2}g_L W_{L\mu}^+ \\ \sqrt{2}g_L W_{L\mu}^- & -g_L W_{L\mu}^3 - g'B_\mu \end{pmatrix} \begin{pmatrix} \nu'_{Li} \\ \ell'_{Li} \end{pmatrix} \\
&= \overline{\nu'_{Li}}i\gamma^\mu\partial_\mu\nu'_{Li} + \overline{\ell'_{Li}}i\gamma^\mu\partial_\mu\ell'_{Li} + \frac{1}{2}\overline{\nu'_{Li}}\gamma^\mu\nu'_{Li}(g_L W_{L\mu}^3 - g'B_\mu) \\
&\quad - \frac{1}{2}\overline{\ell'_{Li}}\gamma^\mu\ell'_{Li}(g_L W_{L\mu}^3 + g'B_\mu) + \frac{1}{\sqrt{2}}g_L\overline{\nu'_{Li}}\gamma^\mu\ell'_{Li}W_{L\mu}^+ + \frac{1}{\sqrt{2}}g_L\overline{\ell'_{Li}}\gamma^\mu\nu'_{Li}W_{L\mu}^-
\end{aligned} \tag{A.25}$$

Similarly, the kinetic terms for the RH leptons and neutrinos are written as

$$\overline{L'_{Ri}} i\gamma^\mu D_\mu L'_{Ri} = \overline{\nu'_{Ri}} i\gamma^\mu \partial_\mu \nu'_{Ri} + \overline{\ell'_{Ri}} i\gamma^\mu \partial_\mu \ell'_{Ri} + \frac{1}{2}\overline{\nu'_{Ri}}\gamma^\mu \nu'_{Ri}(g_R W^3_{R\mu} - g' B_\mu) \\ - \frac{1}{2}\overline{\ell'_{Ri}}\gamma^\mu \ell'_{Ri}(g_R W^3_{R\mu} + g' B_\mu) + \frac{1}{\sqrt{2}} g_R \overline{\nu'_{Ri}}\gamma^\mu \ell'_{Ri} W^+_{R\mu} + \frac{1}{\sqrt{2}} g_R \overline{\ell'_{Ri}}\gamma^\mu \nu'_{Ri} W^-_{R\mu}. \tag{A.26}$$

Quark sector

For quarks, we have

$$\overline{Q_{Li}} i\gamma^\mu D_\mu Q_{Li} = \overline{u_{Li}} i\gamma^\mu \partial_\mu u_{Li} + \overline{d_{Li}} i\gamma^\mu \partial_\mu d_{Li} + \frac{1}{2}\overline{u_{Li}}\gamma^\mu u_{Li}\left(g_L W^3_{L\mu} + \frac{1}{3} g' B_\mu\right) \\ - \frac{1}{2}\overline{d_{Li}}\gamma^\mu d_{Li}\left(g_L W^3_{L\mu} - \frac{1}{3} g' B_\mu\right) + \frac{1}{\sqrt{2}} g_L \overline{u_{Li}}\gamma^\mu d_{Li} W^+_{L\mu} + \frac{1}{\sqrt{2}} g_L \overline{d_{Li}}\gamma^\mu u_{Li} W^-_{L\mu} \tag{A.27}$$

and

$$\overline{Q_{Ri}} i\gamma^\mu D_\mu Q_{Ri} = \overline{u_{Ri}} i\gamma^\mu \partial_\mu u_{Ri} + \overline{d_{Ri}} i\gamma^\mu \partial_\mu d_{Ri} + \frac{1}{2}\overline{u_{Ri}}\gamma^\mu u_{Ri}\left(g_L W^3_{R\mu} + \frac{1}{3} g' B_\mu\right) \\ - \frac{1}{2}\overline{d_{Ri}}\gamma^\mu d_{Ri}\left(g_L W^3_{R\mu} - \frac{1}{3} g' B_\mu\right) + \frac{1}{\sqrt{2}} g_R \overline{u_{Ri}}\gamma^\mu d_{Ri} W^+_{R\mu} + \frac{1}{\sqrt{2}} g_R \overline{d_{Ri}}\gamma^\mu u_{Ri} W^-_{R\mu}. \tag{A.28}$$

Scalar field sector

For scalar fields, we have

$$\mathcal{L}_s = \mathrm{tr}[(D^\mu \Phi)^\dagger (D_\mu \Phi)] + \mathrm{tr}[(D^\mu \Delta_L)^\dagger (D_\mu \Delta_L)] + \mathrm{tr}[(D^\mu \Delta_R)^\dagger (D_\mu \Delta_R)]. \tag{A.29}$$

Now we explicitly calculate the masses of gauge bosons.

Contribution from $\langle\Phi\rangle$

We have

$$
\begin{aligned}
\mathcal{L}_\Phi &= \mathrm{tr}[(D^\mu\Phi)^\dagger(D_\mu\Phi)] \\
&= \mathrm{tr}\left[\left(\partial^\mu\Phi^\dagger + ig_L\Phi^\dagger\frac{\sigma_L^a}{2}W_L^{a\mu} - ig_R\frac{\sigma_R^a}{2}W_R^{a\mu}\Phi^\dagger\right)\left(\partial_\mu\Phi - ig_L\frac{\sigma_L^b}{2}W_{L\mu}^b\Phi + ig_R\Phi\frac{\sigma_R^b}{2}W_{R\mu}^b\right)\right] \\
&= \mathrm{tr}\Big[\partial^\mu\Phi^\dagger\partial_\mu\Phi - \frac{i}{2}g_L\partial^\mu\Phi^\dagger\sigma_L^a W_{L\mu}^a\Phi + \frac{i}{2}g_R\partial^\mu\Phi^\dagger\Phi\sigma_R^a W_{R\mu}^a + \frac{i}{2}g_L\Phi^\dagger\sigma_L^a W_L^{a\mu}\partial_\mu\Phi - \frac{i}{2}g_R\sigma_R^a W_R^{a\mu}\Phi^\dagger\partial_\mu\Phi \\
&\quad + \frac{1}{4}\big(g_L^2\Phi^\dagger\sigma_L^a\sigma_L^b\Phi W_L^{a\mu}W_{L\mu}^b - g_Lg_R\Phi^\dagger\sigma_L^a\Phi\sigma_R^b W_L^{a\mu}W_{R\mu}^b \\
&\qquad - g_Lg_R\sigma_R^a\Phi^\dagger\sigma_L^b\Phi W_R^{a\mu}W_{L\mu}^b + g_R^2\sigma_R^a\Phi^\dagger\Phi\sigma_R^b W_R^{a\mu}W_{R\mu}^b\big)\Big]\,.
\end{aligned}
\tag{A.30}
$$

After Φ acquires the VEV, we can write

$$
\mathrm{tr}\left[\langle\Phi^\dagger\rangle\sigma_L^a\sigma_L^b\langle\Phi\rangle W_L^{a\mu}W_{L\mu}^b\right] = \frac{1}{2}(\kappa_1^2+\kappa_2^2)W_L^{3\mu}W_{L\mu}^3 + (\kappa_1^2+\kappa_2^2)W_L^{+\mu}W_{L\mu}^-, \tag{A.31}
$$

$$
\mathrm{tr}\left[\langle\Phi^\dagger\rangle\sigma_L^a\langle\Phi\rangle\sigma_R^b W_L^{a\mu}W_{R\mu}^b\right] = \frac{1}{2}(\kappa_1^2+\kappa_2^2)W_L^{3\mu}W_{R\mu}^3 + \kappa_1\kappa_2 e^{i\alpha}W_L^{+\mu}W_{R\mu}^- + \kappa_1\kappa_2 e^{-i\alpha}W_L^{-\mu}W_{R\mu}^+, \tag{A.32}
$$

$$
\begin{aligned}
\mathrm{tr}\left[\langle\Phi\rangle\sigma_R^a\langle\Phi^\dagger\rangle\sigma_L^b W_L^{a\mu}W_{R\mu}^b\right] &= \mathrm{tr}\left[\langle\Phi^\dagger\rangle\sigma_L^a\langle\Phi\rangle\sigma_R^b W_L^{a\mu}W_{R\mu}^b\right]^\dagger \\
&= \frac{1}{2}(\kappa_1^2+\kappa'^2)W_L^{3\mu}W_{R\mu}^3 + \kappa_1\kappa_2 e^{i\alpha}W_L^{+\mu}W_{R\mu}^- + \kappa\kappa_2 e^{-i\alpha}W_L^{-\mu}W_{R\mu}^+,
\end{aligned}
\tag{A.33}
$$

$$
\begin{aligned}
\mathrm{tr}\left[\langle\Phi\rangle\sigma_R^b\sigma_R^a\langle\Phi^\dagger\rangle W_R^{a\mu}W_{R\mu}^b\right] &= \mathrm{tr}\left[\langle\Phi^\dagger\rangle\sigma_R^a\sigma_R^b\langle\Phi\rangle W_R^{a\mu}W_{R\mu}^b\right]^\dagger \\
&= \frac{1}{2}(\kappa_1^2+\kappa_2^2)W_R^{3\mu}W_{R\mu}^3 + (\kappa_1^2+\kappa_2^2)W_R^{+\mu}W_{R\mu}^-.
\end{aligned}
\tag{A.34}
$$

We therefore have

$$
\begin{aligned}
\langle\mathcal{L}_\Phi\rangle = \frac{1}{8}(\kappa_1^2+\kappa_2^2)&\left(g_L^2W_L^{3\mu}W_{L\mu}^3 - 2g_Lg_RW_L^{3\mu}W_{R\mu}^3 + g_R^2W_R^{3\mu}W_{R\mu}^3\right) \\
&+ \frac{1}{4}g_L^2(\kappa_1^2+\kappa_2^2)W_L^{+\mu}W_{L\mu}^- - \frac{1}{2}g_Lg_R\kappa_1\kappa_2e^{i\alpha}W_L^{+\mu}W_{R\mu}^- \\
&- \frac{1}{2}g_Lg_R\kappa_1\kappa_2e^{-i\alpha}W_L^{-\mu}W_{R\mu}^+ + \frac{1}{4}g_R^2(\kappa_1^2+\kappa_2^2)W_R^{+\mu}W_{R\mu}^- + \cdots\,.
\end{aligned}
\tag{A.35}
$$

Contribution from $\langle\Delta\rangle$

We can write the scalar triplet Δ as

$$\Delta = \frac{1}{\sqrt{2}}\sigma^a\delta^a \tag{A.36}$$

where

$$\delta^0 = \frac{1}{\sqrt{2}}(\delta^1 + i\delta^2), \quad \delta^+ = \delta^3, \quad \delta^{++} = \frac{1}{\sqrt{2}}(\delta^1 - i\delta^2). \tag{A.37}$$

The gauge invariant kinetic term for Δ is given by

$$\begin{aligned}
\mathcal{L}_\Delta &= \mathrm{tr}[(D^\mu\Delta)^\dagger(D_\mu\Delta)] = \frac{1}{2}\mathrm{tr}[\{D^\mu(\sigma^a\delta^a)\}^\dagger\{D_\mu(\sigma^b\delta^b)\}] \\
&= \frac{1}{2}\mathrm{tr}[\sigma^a\sigma^b](\partial^\mu\delta^{a*} + ig\delta^{c*}\boldsymbol{T}^{ca}\cdot\boldsymbol{W}^\mu + ig'B^\mu\delta^{a*})(\partial_\mu\delta^b - ig\boldsymbol{T}^{bd}\cdot\boldsymbol{W}_\mu\delta^d - ig'B_\mu\delta^b) \\
&= \partial^\mu\delta^{a*}\partial_\mu\delta^a - ig\partial^\mu\delta^{a*}(T^i)^{ad}\delta^d W^i_\mu - ig'\partial^\mu\delta^{a*}\delta^a B_\mu \\
&\quad + ig\delta^{c*}(T^i)^{ca}\partial_\mu\delta^a W^{i\mu} + g^2\delta^{c*}(T^i)^{ca}(T^j)^{ad}\delta^d W^{i\mu}W^j_\mu + gg'\delta^{c*}(T^i)^{ca}\delta^a W^{i\mu}B_\mu \\
&\quad + ig'\delta^{a*}\partial_\mu\delta^a B^\mu + gg'\delta^{a*}(T^j)^{ad}\delta^d W^j_\mu B^\mu + g'^2\delta^{a*}\delta^a B^\mu B_\mu \\
&= \partial^\mu\delta^{a*}\partial_\mu\delta^a - ig\partial^\mu\delta^{a*}(T^i)^{ad}\delta^d W^i_\mu + ig\delta^{c*}(T^i)^{ca}\partial_\mu\delta^a W^{i\mu} + g^2\delta^{c*}(T^i)^{ca}(T^j)^{ad}\delta^d W^{i\mu}W^j_\mu \\
&\quad + 2gg'\delta^{c*}(T^i)^{ca}\delta^a W^{i\mu}B_\mu - ig'\partial^\mu\delta^{a*}\delta^a B_\mu + ig'\delta^{a*}\partial_\mu\delta^a B^\mu + g'^2\delta^{a*}\delta^a B^\mu B_\mu
\end{aligned} \tag{A.38}$$

where T^i is the generator of the SU(2) adjoint representation. Since $(T^c)^{ab} = -i\epsilon^{abc}$, we have

$$\begin{aligned}
\delta^{c*}(T^i)^{ca}(T^j)^{ad}\delta^d &= \delta^{c*}\epsilon^{aci}\epsilon^{adj}\delta^d = \delta^{c*}(\delta^{cd}\delta^{ij} - \delta^{cj}\delta^{id})\delta^d = \delta^{c*}\delta^c\delta^{ij} - \delta^{j*}\delta^i, \\
\delta^{c*}(T^i)^{ca}\delta^a &= -i\delta^{c*}\epsilon^{cai}\delta^a.
\end{aligned} \tag{A.39}$$

Therefore, the kinetic terms can be written as

$$\mathcal{L}_\Delta = \partial^\mu \delta^{a*}\partial_\mu \delta^a - g\epsilon^{abc}\partial^\mu\delta^{a*}\delta^b W^c_\mu + g\epsilon^{abc}\delta^{a*}\partial_\mu\delta^b W^{c\mu} + g^2\delta^{a*}\delta^a W^{b\mu}W^b_\mu - g^2\delta^{a*}\delta^b W^{a\mu}W^b_\mu$$
$$- 2igg'\epsilon^{abc}\delta^{a*}\delta^b W^{c\mu}B_\mu - ig'\partial^\mu\delta^{a*}\delta^a B_\mu + ig'\delta^{a*}\partial_\mu\delta^a B^\mu + g'^2\delta^{a*}\delta^a B^\mu B_\mu. \tag{A.40}$$

We also have

$$\begin{aligned}
\delta^{a*}\delta^a &= \delta^{0*}\delta^0 + \delta^-\delta^+ + \delta^{--}\delta^{++},\\
\delta^{a*}W^a_\mu &= \delta^{--}W^+_\mu + \delta^{0*}W^-_\mu + \delta^- W^3_\mu,\\
\delta^a W^a_\mu &= \delta^{++}W^-_\mu + \delta^0 W^+_\mu + \delta^+ W^3_\mu,\\
\epsilon^{abc}\delta^{a*}\delta^b W^c_\mu &= (\delta^{1*}\delta^2 - \delta^{2*}\delta^1)W^3_\mu + (\delta^{2*}\delta^3 - \delta^{3*}\delta^2)W^1_\mu + (\delta^{3*}\delta^1 - \delta^{1*}\delta^3)W^2_\mu\\
&= i(\delta^{++}\delta^{--}W^3_\mu - \delta^{0*}\delta^0 W^3_\mu + \delta^0\delta^- W^+_\mu - \delta^{--}\delta^+ W^+_\mu + \delta^{0*}\delta^+ W^-_\mu - \delta^{++}\delta^- W^-_\mu).
\end{aligned} \tag{A.41}$$

After Δ acquires the VEV, the Lagrangian terms relevant to the masses of gauge bosons can be written as

$$\begin{aligned}
\langle\mathcal{L}_\Delta\rangle &= \frac{1}{2}g^2v^2(2W^{+\mu}W^-_\mu + W^{3\mu}W^3_\mu) - \frac{1}{2}g^2v^2W^{+\mu}W^-_\mu - gg'v^2W^{3\mu}B_\mu + \frac{1}{2}g'^2v^2B^\mu B_\mu + \cdots\\
&= \frac{1}{2}g^2v^2W^{+\mu}W^-_\mu + \frac{1}{2}g^2v^2W^{3\mu}W^3_\mu - gg'v^2W^{3\mu}B_\mu + \frac{1}{2}g'^2v^2B^\mu B_\mu + \cdots .
\end{aligned} \tag{A.42}$$

Total contributions

Hence, we have

$$
\begin{aligned}
\langle \mathcal{L}_s \rangle &= \langle \mathcal{L}_\Phi \rangle + \langle \mathcal{L}_{\Delta_L} \rangle + \langle \mathcal{L}_{\Delta_R} \rangle \\
&= \frac{1}{8}(\kappa_1^2 + \kappa_2^2)\left(g_L^2 W_L^{3\mu} W_{L\mu}^3 - 2 g_L g_R W_L^{3\mu} W_{R\mu}^3 + g_R^2 W_R^{3\mu} W_{R\mu}^3 \right) \\
&\quad + \frac{1}{4} g_L^2 (\kappa_1^2 + \kappa_2^2) W_L^{+\mu} W_{L\mu}^- - \frac{1}{2} g_L g_R \kappa_1 \kappa_2 e^{i\alpha} W_L^{+\mu} W_{R\mu}^- \\
&\qquad - \frac{1}{2} g_L g_R \kappa_1 \kappa_2 e^{-i\alpha} W_L^{-\mu} W_{R\mu}^+ + \frac{1}{4} g_R^2 (\kappa_1^2 + \kappa_2^2) W_R^{+\mu} W_{R\mu}^- \\
&\quad + \frac{1}{2} g_L^2 v_L^2 W_L^{+\mu} W_{L\mu}^- + \frac{1}{2} g_L^2 v_L^2 W_L^{3\mu} W_{L\mu}^3 - g_L g' v_L^2 W_L^{3\mu} B_\mu + \frac{1}{2} g'^2 v_L^2 B^\mu B_\mu \\
&\quad + \frac{1}{2} g_R^2 v_R^2 W_R^{+\mu} W_{R\mu}^- + \frac{1}{2} g_R^2 v_R^2 W_R^{3\mu} W_{R\mu}^3 - g_R g' v_R^2 W_R^{3\mu} B_\mu + \frac{1}{2} g'^2 v_R^2 B^\mu B_\mu + \cdots \\
&= \frac{1}{8} g_L^2 (\kappa_1^2 + \kappa_2^2 + 4 v_L^2) W_L^{3\mu} W_{L\mu}^3 - \frac{1}{4} g_L g_R (\kappa_1^2 + \kappa_2^2) W_L^{3\mu} W_{R\mu}^3 + \frac{1}{8} g_R^2 (\kappa_1^2 + \kappa_2^2 + 4 v_R^2) W_R^{3\mu} W_{R\mu}^3 \\
&\qquad - g_L g' v_L^2 W_L^{3\mu} B_\mu - g_R g' v_R^2 W_R^{3\mu} B_\mu + \frac{1}{2} g'^2 (v_L^2 + v_R^2) B^\mu B_\mu \\
&\quad + \frac{1}{4} g_L^2 (\kappa_1^2 + \kappa_2^2 + 2 v_L^2) W_L^{+\mu} W_{L\mu}^- - \frac{1}{2} g_L g_R \kappa_1 \kappa_2 e^{i\alpha} W_L^{+\mu} W_{R\mu}^- - \frac{1}{2} g_L g_R \kappa_1 \kappa_2 e^{-i\alpha} W_L^{-\mu} W_{R\mu}^+ \\
&\qquad + \frac{1}{2} g_R^2 (\kappa_1^2 + \kappa_2^2 + 2 v_R^2) W_R^{+\mu} W_{R\mu}^- + \cdots .
\end{aligned}
\tag{A.43}
$$

We therefore can write the mass terms for gauge bosons as

$$
\begin{aligned}
\mathcal{L}_g^{\text{mass}} &= \frac{1}{2} (W_L^{3\mu}\ W_R^{3\mu}\ B^\mu)
\begin{pmatrix}
\frac{1}{4} g_L^2 (\kappa_1^2 + \kappa_2^2 + 4 v_L^2) & -\frac{1}{4} g_L g_R (\kappa_1^2 + \kappa_2^2) & -g_L g' v_L^2 \\
-\frac{1}{4} g_L g_R (\kappa_1^2 + \kappa_2^2) & \frac{1}{4} g_R^2 (\kappa_1^2 + \kappa_2^2 + 4 v_R^2) & -g_R g' v_R^2 \\
-g_L g' v_L^2 & -g_R g' v_R^2 & g'^2 (v_L^2 + v_R^2)
\end{pmatrix}
\begin{pmatrix} W_{L\mu}^3 \\ W_{R\mu}^3 \\ B_\mu \end{pmatrix} \\
&\quad + (W_L^{+\mu}\ W_R^{+\mu})
\begin{pmatrix}
\frac{1}{4} g_L^2 (\kappa_1^2 + \kappa_2^2 + 2 v_L^2) & -\frac{1}{2} g_L g_R \kappa_1 \kappa_2 e^{i\alpha} \\
-\frac{1}{2} g_L g_R \kappa_1 \kappa_2 e^{-i\alpha} & \frac{1}{4} g_R^2 (\kappa_1^2 + \kappa_2^2 + 2 v_R^2)
\end{pmatrix}
\begin{pmatrix} W_{L\mu}^- \\ W_{R\mu}^- \end{pmatrix} + \cdots .
\end{aligned}
\tag{A.44}
$$

(i) *Charged gauge bosons*

Without loss of generality, the general form of the change of basis for charged gauge bosons can be written as

$$\begin{pmatrix} W_L^- \\ \\ W_R^- \end{pmatrix} = \begin{pmatrix} \cos\xi & \sin\xi e^{i\alpha} \\ \\ -\sin\xi e^{-i\alpha} & \cos\xi \end{pmatrix} \begin{pmatrix} W_1^- \\ \\ W_2^- \end{pmatrix} \tag{A.45}$$

where W_1^- and W_2^- are mass eigenstates. We can find

$$\cos\xi = \frac{b-a+\sqrt{(b-a)^2+4c^2}}{\sqrt{[b-a+\sqrt{(b-a)^2+4c^2}]^2+4c^2}}, \quad \sin\xi = -\frac{2c}{\sqrt{[b-a+\sqrt{(b-a)^2+4c^2}]^2+4c^2}} \tag{A.46}$$

where

$$a \equiv \frac{1}{4}g_L^2(\kappa_1^2+\kappa_2^2+2v_L^2), \qquad b \equiv \frac{1}{4}g_R^2(\kappa_1^2+\kappa_2^2+2v_R^2), \qquad c \equiv \frac{1}{2}g_L g_R \kappa_1\kappa_2. \tag{A.47}$$

Note that we have

$$\tan 2\xi = -\frac{2c}{b-a} = -\frac{4g_L g_R\kappa_1\kappa_2}{(g_R^2-g_L^2)(\kappa_1^2+\kappa_2^2)+2(g_R^2v_R^2-g_L^2v_L^2)}. \tag{A.48}$$

The masses of charged gauge bosons are found to be

$$m_{W_1}^2 = \frac{1}{2}[b+a-\sqrt{(b-a)^2+4c^2}], \qquad m_{W_2}^2 = \frac{1}{2}[b+a+\sqrt{(b-a)^2+4c^2}]. \tag{A.49}$$

With the phenomenological assumption $v_L \ll \kappa_1, \kappa_2 \ll v_R$, we have $a, c \ll b$. Then, we can approximately write $\sqrt{(b-a)^2+4c^2} \approx b-a+2c^2/b$, which gives

$$\cos\xi \approx 1-\frac{c^2}{2b^2} = 1-\frac{2g_L^2\kappa_1^2\kappa_2^2}{g_R^2(\kappa_1^2+\kappa_2^2+2v_R^2)^2} \approx 1-\frac{g_L^2\kappa_1^2\kappa_2^2}{2g_R^2v_R^4}, \tag{A.50}$$

$$\sin\xi \approx -\frac{c}{b}\left(1+\frac{a}{b}\right) = -\frac{2g_L\kappa_1\kappa_2}{g_R(\kappa^2+\kappa_2^2+2v_R^2)}\left[1+\frac{g_L^2(\kappa_1^2+\kappa_2^2+2v_L^2)}{g_R^2(\kappa_1^2+\kappa_2^2+2v_R^2)}\right] \approx -\frac{g_L\kappa_1\kappa_2}{g_R v_R^2}, \tag{A.51}$$

$$\tag{A.52}$$

and

$$\tan 2\xi \approx -\frac{2g_L\kappa_1\kappa_2}{g_R v_R^2}. \tag{A.53}$$

Note that we have $0 < -\xi \ll 1$. The charged gauge boson masses can also be written as

$$m_{W_1}^2 \approx a - \frac{c^2}{b} = \frac{1}{4}g_L^2(\kappa_1^2+\kappa_2^2+2v_L^2) - \frac{2g_L^2\kappa_1^2\kappa_2^2}{\kappa_1^2+\kappa_2^2+2v_R^2}, \tag{A.54}$$

$$m_{W_2}^2 \approx b + \frac{c^2}{b} = \frac{1}{4}g_R^2(\kappa_1^2+\kappa_2^2+2v_R^2) + \frac{2g_L^2\kappa_1^2\kappa_2^2}{\kappa_1^2+\kappa_2^2+2v_R^2}, \tag{A.55}$$

or simply as

$$m_{W_1}^2 \approx \frac{1}{4}g_L^2(\kappa_1^2+\kappa_2^2), \qquad m_{W_2}^2 \approx \frac{1}{2}g_R^2 v_R^2. \tag{A.56}$$

These approximate expressions are obtained by systematically expanding the trigonometric functions and gauge boson masses in terms of the small parameters a/b and c/b up to the second order.

(ii) *Neutral gauge bosons*

Without loss of generality, the general form of the change of basis for neutral gauge bosons can be written as

$$\begin{pmatrix} W_L^3 \\ W_R^3 \\ B \end{pmatrix} = \begin{pmatrix} 1 & 0 & 0 \\ 0 & \cos\zeta_1 & \sin\zeta_1 \\ 0 & -\sin\zeta_1 & \cos\zeta_1 \end{pmatrix} \begin{pmatrix} \cos\zeta_2 & 0 & \sin\zeta_2 \\ 0 & 1 & 0 \\ -\sin\zeta_2 & 0 & \cos\zeta_2 \end{pmatrix} \begin{pmatrix} \cos\zeta_3 & \sin\zeta_3 & 0 \\ -\sin\zeta_3 & \cos\zeta_3 & 0 \\ 0 & 0 & 1 \end{pmatrix} \begin{pmatrix} Z_1 \\ Z_2 \\ A \end{pmatrix} \tag{A.57}$$

$$= \begin{pmatrix} \cos\zeta_2\cos\zeta_3 & \cos\zeta_2\sin\zeta_3 & \sin\zeta_2 \\ -\sin\zeta_1\sin\zeta_2\cos\zeta_3 - \cos\zeta_1\sin\zeta_3 & \cos\zeta_1\cos\zeta_3 - \sin\zeta_1\sin\zeta_2\sin\zeta_3 & \sin\zeta_1\cos\zeta_2 \\ -\cos\zeta_1\sin\zeta_2\cos\zeta_3 + \sin\zeta_1\sin\zeta_3 & -\sin\zeta_1\cos\zeta_3 - \cos\zeta_1\sin\zeta_2\sin\zeta_3 & \cos\zeta_1\cos\zeta_2 \end{pmatrix} \begin{pmatrix} Z_1 \\ Z_2 \\ A \end{pmatrix} \tag{A.58}$$

where Z_1, Z_2, and A are the mass eigenstates, and the mixing angles are given by

$$\cos\zeta_1 = \frac{g_R}{\sqrt{g_R^2+g'^2}}, \qquad \sin\zeta_1 = \frac{g'}{\sqrt{g_R^2+g'^2}}, \tag{A.59}$$

$$\cos\zeta_2 = \frac{g_L\sqrt{g_R^2+g'^2}}{\sqrt{g_L^2g_R^2+g_L^2g'^2+g_R^2g'^2}}, \qquad \sin\zeta_2 = \frac{g_Rg'}{\sqrt{g_L^2g_R^2+g_L^2g'^2+g_R^2g'^2}}, \tag{A.60}$$

$$\tan 2\zeta_3 = \frac{2\sqrt{g_L^2g_R^2+g_L^2g'^2+g_R^2g'^2}[4g'^2v_L^2-g_R^2(\kappa_1^2+\kappa_2^2)]}{(g_R^4-g_L^2g_R^2-g_L^2g'^2-g_R^2g'^2)(\kappa_1^2+\kappa_2^2)+4(g'^4-g_L^2g_R^2-g_L^2g'^2-g_R^2g'^2)v_L^2+4(g_R^2+g'^2)^2v_R^2}. \tag{A.61}$$

Note that we have the identity

$$\frac{g_Lg_Rg'}{\sqrt{g_L^2g_R^2+g_L^2g'^2+g_R^2g'^2}} = g'\cos\zeta_1\cos\zeta_2 = g_L\sin\zeta_2 \tag{A.62}$$

or

$$g' = \frac{g_L\tan\zeta_2}{\cos\zeta_1}. \tag{A.63}$$

The gauge field A corresponds to the photon with zero mass, and the masses of the other neutral gauge bosons are

$$\begin{aligned} m_{Z_1}^2 = {} & \frac{1}{8}(g_L^2+g_R^2)(\kappa_1^2+\kappa_2^2)+\frac{1}{2}(g_L^2+g'^2)v_L^2+\frac{1}{2}(g_R^2+g'^2)v_R^2 \\ & -\frac{1}{4(g_R^2+g'^2)}\Bigg\{(g_L^2g_R^2+g_L^2g'^2+g_R^2g'^2)[4g'^2v_L^2-g_R^2(\kappa_1^2+\kappa_2^2)]^2 \\ & +\Bigg[\frac{1}{2}(g_R^4-g_L^2g_R^2-g_L^2g'^2-g_R^2g'^2)(\kappa_1^2+\kappa_2^2) \\ & +2(g'^4-g_L^2g_R^2-g_L^2g'^2-g_R^2g'^2)v_L^2+2(g_R^2+g'^2)^2v_R^2\Bigg]^2\Bigg\}^{1/2}, \end{aligned} \tag{A.64}$$

$$\begin{aligned} m_{Z_2}^2 = {} & \frac{1}{8}(g_L^2+g_R^2)(\kappa_1^2+\kappa_2^2)+\frac{1}{2}(g_L^2+g'^2)v_L^2+\frac{1}{2}(g_R^2+g'^2)v_R^2 \\ & +\frac{1}{4(g_R^2+g'^2)}\Bigg\{(g_L^2g_R^2+g_L^2g'^2+g_R^2g'^2)[4g'^2v_L^2-g_R^2(\kappa_1^2+\kappa_2^2)]^2 \\ & +\Bigg[\frac{1}{2}(g_R^4-g_L^2g_R^2-g_L^2g'^2-g_R^2g'^2)(\kappa_1^2+\kappa_2^2) \\ & +2(g'^4-g_L^2g_R^2-g_L^2g'^2-g_R^2g'^2)v_L^2+2(g_R^2+g'^2)^2v_R^2\Bigg]^2\Bigg\}^{1/2}. \end{aligned} \tag{A.65}$$

The neutral gauge bosons that couple to the LH fermions can be written as

$$
\begin{aligned}
g_L W^3_{L\mu} - g' B_\mu &= g_L(\cos\zeta_2\cos\zeta_3 Z_1 + \cos\zeta_2\sin\zeta_3 Z_2 + \sin\zeta_2 A) \\
&\quad - g'\big[(-\cos\zeta_1\sin\zeta_2\cos\zeta_3 + \sin\zeta_1\sin\zeta_3)Z_1 \\
&\qquad + (-\sin\zeta_1\cos\zeta_3 - \cos\zeta_1\sin\zeta_2\sin\zeta_3)Z_2 + \cos\zeta_1\cos\zeta_2 A\big] \\
&= \big[g_L\cos\zeta_2\cos\zeta_3 - g'(-\cos\zeta_1\sin\zeta_2\cos\zeta_3 + \sin\zeta_1\sin\zeta_3)\big]Z_1 \\
&\quad + \big[g_L\cos\zeta_1\sin\zeta_2 - g'(-\sin\zeta_1\cos\zeta_3 - \cos\zeta_1\sin\zeta_2\sin\zeta_3)\big]Z_2 \\
&\quad + (g_L\sin\zeta_2 - g'\cos\zeta_1\cos\zeta_2)A \\
&= (g_L\cos\zeta_2\cos\zeta_3 + g'\cos\zeta_1\sin\zeta_2\cos\zeta_3 - g'\sin\zeta_1\sin\zeta_3)Z_1 \\
&\quad + (g_L\cos\zeta_2\sin\zeta_3 + g'\sin\zeta_1\cos\zeta_3 + g'\cos\zeta_1\sin\zeta_2\sin\zeta_3)Z_2 \\
&= \frac{g_L}{\cos\zeta_2}\big[(\cos\zeta_3 - \tan\zeta_1\sin\zeta_2\sin\zeta_3)Z_1 + (\tan\zeta_1\sin\zeta_2\cos\zeta_3 + \sin\zeta_3)Z_2\big] \qquad \text{(A.66)}
\end{aligned}
$$

and

$$
\begin{aligned}
g_L W^3_{L\mu} + g' B_\mu &= g_L(\cos\zeta_2\cos\zeta_3 Z_1 + \cos\zeta_2\sin\zeta_3 Z_2 + \sin\zeta_2 A) \\
&\quad + g'\big[(-\cos\zeta_1\sin\zeta_2\cos\zeta_3 + \sin\zeta_1\sin\zeta_3)Z_1 \\
&\qquad + (-\sin\zeta_1\cos\zeta_3 - \cos\zeta_1\sin\zeta_2\sin\zeta_3)Z_2 + \cos\zeta_1\cos\zeta_2 A\big] \\
&= \big[g_L\cos\zeta_2\cos\zeta_3 + g'(-\cos\zeta_1\sin\zeta_2\cos\zeta_3 + \sin\zeta_1\sin\zeta_3)\big]Z_1 \\
&\quad + \big[g_L\cos\zeta_2\sin\zeta_3 + g'(-\sin\zeta_1\cos\zeta_3 - \cos\zeta_1\sin\zeta_2\sin\zeta_3)\big]Z_2 \\
&\quad + (g_L\sin\zeta_2 + g'\cos\zeta_1\cos\zeta_2)A \\
&= (g_L\cos\zeta_2\cos\zeta_3 - g'\cos\zeta_1\sin\zeta_2\cos\zeta_3 + g'\sin\zeta_1\sin\zeta_3)Z_1 \\
&\quad + (g_L\cos\zeta_2\sin\zeta_3 - g'\sin\zeta_1\cos\zeta_3 - g'\cos\zeta_1\sin\zeta_2\sin\zeta_3)Z_2 \\
&\quad + 2g_L\sin\zeta_2 A \\
&= \frac{g_L}{\cos\zeta_2}\big[(\cos 2\zeta_2\cos\zeta_3 + \tan\zeta_1\sin\zeta_2\sin\zeta_3)Z_1 \\
&\qquad + (-\tan\zeta_1\sin\zeta_2\cos\zeta_3 + \cos 2\zeta_2\sin\zeta_3)Z_2\big] + 2g_L\sin\zeta_2 A. \qquad \text{(A.67)}
\end{aligned}
$$

For the RH sector, we have

$$
g_R W^3_{R\mu} - g' B_\mu = g_R\big[(-\sin\zeta_1\sin\zeta_2\cos\zeta_3 - \cos\zeta_1\sin\zeta_3)Z_1
$$

$$
\begin{aligned}
&\quad + (\cos\zeta_1 \cos\zeta_3 - \sin\zeta_1 \sin\zeta_2 \sin\zeta_3) Z_2 + \sin\zeta_1 \cos\zeta_2 A\big] \\
&- g'\big[(-\cos\zeta_1 \sin\zeta_2 \cos\zeta_3 + \sin\zeta_1 \sin\zeta_3) Z_1 \\
&\quad + (-\sin\zeta_1 \cos\zeta_3 - \cos\zeta_1 \sin\zeta_2 \sin\zeta_3) Z_2 + \cos\zeta_1 \cos\zeta_2 A\big] \\
= &\big[g_R(-\sin\zeta_1 \sin\zeta_2 \cos\zeta_3 - \cos\zeta_1 \sin\zeta_3) - g'(-\cos\zeta_1 \sin\zeta_2 \cos\zeta_3 + \sin\zeta_1 \sin\zeta_3)\big] Z_1 \\
&+ \big[g_R(\cos\zeta_1 \cos\zeta_3 - \sin\zeta_1 \sin\zeta_2 \sin\zeta_3) - g'(-\sin\zeta_1 \cos\zeta_3 - \cos\zeta_1 \sin\zeta_2 \sin\zeta_3)\big] Z_2 \\
&+ (g_R \sin\zeta_1 \cos\zeta_2 - g' \cos\zeta_1 \cos\zeta_2) A \\
= &(-g_R \sin\zeta_1 \sin\zeta_2 \cos\zeta_3 - g_R \cos\zeta_1 \sin\zeta_3 + g' \cos\zeta_1 \sin\zeta_2 \cos\zeta_3 - g' \sin\zeta_1 \sin\zeta_3) Z_1 \\
&+ (g_R \cos\zeta_1 \cos\zeta_3 - g_R \sin\zeta_1 \sin\zeta_2 \sin\zeta_3 + g' \sin\zeta_1 \cos\zeta_3 + g' \cos\zeta_1 \sin\zeta_2 \sin\zeta_3) Z_2 \\
= &\frac{g_R}{\cos\zeta_1}(-\sin\zeta_3 Z_1 + \cos\zeta_3 Z_2) \qquad \text{(A.68)}
\end{aligned}
$$

and

$$
\begin{aligned}
g_R W^3_{R\mu} + g' B_\mu = &\, g_R\big[(-\sin\zeta_1 \sin\zeta_2 \cos\zeta_3 - \cos\zeta_1 \sin\zeta_3) Z_1 \\
&\quad + (\cos\zeta_1 \cos\zeta_3 - \sin\zeta_1 \sin\zeta_2 \sin\zeta_3) Z_2 + (\sin\zeta_1 \cos\zeta_2) A\big] \\
&+ g'\big[(-\cos\zeta_1 \sin\zeta_2 \cos\zeta_3 + \sin\zeta_1 \sin\zeta_3) Z_1 \\
&\quad + (-\sin\zeta_1 \cos\zeta_3 - \cos\zeta_1 \sin\zeta_2 \sin\zeta_3) Z_2 + \cos\zeta_1 \cos\zeta_2 A\big] \\
= &\big[g_R(-\sin\zeta_1 \sin\zeta_2 \cos\zeta_3 - \cos\zeta_1 \sin\zeta_3) + g'(-\cos\zeta_1 \sin\zeta_2 \cos\zeta_3 + \sin\zeta_1 \sin\zeta_3)\big] Z_1 \\
&+ \big[g_R(\cos\zeta_1 \cos\zeta_3 - \sin\zeta_1 \sin\zeta_2 \sin\zeta_3) + g'(-\sin\zeta_1 \cos\zeta_3 - \cos\zeta_1 \sin\zeta_2 \sin\zeta_3)\big] Z_2 \\
&+ (g_R \sin\zeta_1 \cos\zeta_2 + g' \cos\zeta_1 \cos\zeta_2) A \\
= &(-g_R \sin\zeta_1 \sin\zeta_2 \cos\zeta_3 - g_R \cos\zeta_1 \sin\zeta_3 - g' \cos\zeta_1 \sin\zeta_2 \cos\zeta_3 + g' \sin\zeta_1 \sin\zeta_3) Z_1 \\
&+ (g_R \cos\zeta_1 \cos\zeta_3 - g_R \sin\zeta_1 \sin\zeta_2 \sin\zeta_3 - g' \sin\zeta_1 \cos\zeta_3 - g' \cos\zeta_1 \sin\zeta_2 \sin\zeta_3) Z_2 \\
&+ 2 g_R \sin\zeta_1 \cos\zeta_2 A \\
= &\, g_R\big[-2\sin\zeta_1 \sin\zeta_2 \cos\zeta_3 - \cos\zeta_1(1 - \tan^2\zeta_1)\sin\zeta_3\big] Z_1 \\
&+ g_R\big[\cos\zeta_1(1 - \tan^2\zeta_1)\cos\zeta_3 - 2\sin\zeta_1 \sin\zeta_2 \sin\zeta_3\big] Z_2 \\
&+ 2 g_R \sin\zeta_1 \cos\zeta_2 A \\
= &\frac{g_R}{\cos\zeta_1}\big[-(\sin 2\zeta_1 \sin\zeta_2 \cos\zeta_3 + \cos 2\zeta_1 \sin\zeta_3) Z_1
\end{aligned}
$$

$$+ (\cos 2\zeta_1 \cos\zeta_3 - \sin 2\zeta_1 \sin\zeta_2 \sin\zeta_3) Z_2\big] + 2g_R \sin\zeta_1 \cos\zeta_2 A. \tag{A.69}$$

With the phenomenological assumption $v_L \ll \kappa_1, \kappa_2 \ll v_R$, we can approximately write

$$\tan 2\zeta_3 \approx -\frac{g_R^2 \sqrt{g_L^2 g_R^2 + g_L^2 g'^2 + g_R^2 g'^2}(\kappa_1^2 + \kappa_2^2)}{2(g_R^2 + g'^2)^2 v_R^2} \tag{A.70}$$

where $0 < -\zeta_3 \ll 1$. The neutral gauge boson masses can be written as

$$m_{Z_1}^2 \approx \frac{g_L^2 g_R^2 + g_L^2 g'^2 + g_R^2 g'^2}{4(g_R^2 + g'^2)}(\kappa_1^2 + \kappa_2^2 + 4v_L^2) \approx \frac{g_L^2 g_R^2 + g_L^2 g'^2 + g_R^2 g'^2}{4(g_R^2 + g'^2)}(\kappa^2 + \kappa'^2), \tag{A.71}$$

$$m_{Z_2}^2 \approx \frac{g_R^4}{4(g_R^2 + g'^2)}(\kappa_1^2 + \kappa_2^2) + \frac{g'^4}{g_R^2 + g'^2} v_L^2 + (g_R^2 + g'^2) v_R^2 \approx (g_R^2 + g'^2) v_R^2. \tag{A.72}$$

The first approximate approximate expressions are obtained by expanding the gauge boson masses in terms of the small parameters $(\kappa_1^2 + \kappa_2^2)/v_R^2$ and v_L^2/v_R^2 up to the first order. From the second approximate expressions, we can identify the Weinberg angle θ_W from its experimental definition

$$\cos\theta_W \equiv \frac{m_{W_1}}{m_{Z_1}} \approx \cos\zeta_2 \tag{A.73}$$

and also the electric charge from

$$\begin{aligned} e &= g_L \sin\zeta_2 = g_R \sin\zeta_1 \cos\zeta_2 \\ &\approx g_L \sin\theta_W = g_R \sin\zeta_1 \cos\theta_W \end{aligned} \tag{A.74}$$

where we have chosen $e, g_L, g_R, \theta_W > 0$. Now we can rewrite

$$m_{Z_1}^2 \approx \frac{g_L^2(\kappa_1^2 + \kappa_2^2)}{4\cos^2\theta_W}, \qquad m_{Z_2}^2 \approx \frac{g_R^2 v_R^2}{1 - (g_L^2/g_R^2)\tan^2\theta_W}, \tag{A.75}$$

and

$$\zeta_1 = \sin^{-1}\left(\frac{g_L}{g_R}\tan\theta_W\right), \qquad \zeta_2 \approx \theta_W, \qquad \zeta_3 \approx -\frac{g_L\sqrt{g_R^2 - g_L^2\tan^2\theta_W}(\kappa_1^2+\kappa_2^2)}{4\cos\theta_W m_{Z_2}^2}. \tag{A.76}$$

Since $0 < \sin\zeta_1 \le 1$, we must have

$$0 < \frac{g_L}{g_R}\tan\theta_W \le 1 \tag{A.77}$$

where $\tan\theta_W \approx 0.548$. In addition,

$$\tan 2\zeta_3 \approx -\frac{2g_R^2}{\sqrt{g_L^2 g_R^2 + g_L^2 g'^2 + g_R^2 g'^2}}\frac{m_{Z_1}^2}{m_{Z_2}^2} = -2\cos\theta_W\sqrt{g_R^2/g_L^2 - \tan^2\theta_W}\,\frac{m_{Z_1}^2}{m_{Z_2}^2}. \tag{A.78}$$

Now we simply write $\zeta \equiv \zeta_3$. Then, we have

$$\begin{aligned} g_L W^3_{L\mu} - g' B_\mu &= \frac{g_L}{\cos\zeta_2}\left[(\cos\zeta_3 - \tan\zeta_1\sin\zeta_2\sin\zeta_3)Z_1 + (\tan\zeta_1\sin\zeta_2\cos\zeta_3 + \sin\zeta_3)Z_2\right] \\ &\approx \frac{g_L}{\cos\theta_W}\left[\left(1 - \zeta\frac{g_L\sin^2\theta_W}{\sqrt{g_R^2\sin^2\theta_W - g_L^2\cos^2\theta_W}}\right)Z_1 + \left(\frac{g_L\sin^2\theta_W}{\sqrt{g_R^2\sin^2\theta_W - g_L^2\cos^2\theta_W}} + \zeta\right)Z_2\right] \end{aligned} \tag{A.79}$$

and

$$\begin{aligned} g_L W^3_{L\mu} + g' B_\mu &= \frac{g_L}{\cos\zeta_2}\left[(\cos 2\zeta_2\cos\zeta_3 + \tan\zeta_1\sin\zeta_2\sin\zeta_3)Z_1 + (-\tan\zeta_1\sin\zeta_2\cos\zeta_3 + \cos 2\zeta_2\sin\zeta_3)Z_2\right] \\ &\quad + 2g_L\sin\zeta_2 A \\ &\approx \frac{g_L}{\cos\theta_W}\left[\left(\cos 2\theta_W + \zeta\frac{g_L\sin^2\theta_W}{\sqrt{g_R^2\sin^2\theta_W - g_L^2\cos^2\theta_W}}\right)Z_1\right. \\ &\qquad \left. + \left(-\frac{g_L\sin^2\theta_W}{\sqrt{g_R^2\sin^2\theta_W - g_L^2\cos^2\theta_W}} + \zeta\cos 2\theta_W\right)Z_2\right] + 2g_L\sin\theta_W A. \end{aligned} \tag{A.80}$$

For the RH sector,

$$g_R W^3_{R\mu} - g' B_\mu = \frac{g_R}{\cos\zeta_1}(-\sin\zeta_3 Z_1 + \cos\zeta_3 Z_2) \approx \frac{g_R^2}{\sqrt{g_R^2 - g_L^2\tan^2\theta_W}}(-\zeta Z_1 + Z_2) \tag{A.81}$$

and

$$
\begin{aligned}
g_R W^3_{R\mu} + g' B_\mu = {} & \frac{g_R}{\cos\zeta_1}\big[-(\sin 2\zeta_1 \sin\zeta_2 \cos\zeta_3 + \cos 2\zeta_1 \sin\zeta_3) Z_1 + (\cos 2\zeta_1 \cos\zeta_3 - \sin 2\zeta_1 \sin\zeta_2 \sin\zeta_3) Z_2\big] \\
& + 2 g_R \sin\zeta_1 \cos\zeta_2 A \\
\approx {} & \frac{g_L}{\sqrt{g_R^2 - g_L^2 \tan^2\theta_W}} \left[- \left(2\sin\theta_W \tan\theta_W \sqrt{g_R^2/g_L^2 - \tan^2\theta_W} + \zeta \left[g_R^2/g_L^2 - 2\tan^2\theta_W \right] \right) Z_1 \right. \\
& \left. + \left(g_R^2/g_L^2 - 2\tan^2\theta_W - 2\zeta \sin\theta_W \tan\theta_W \sqrt{g_R^2/g_L^2 - \tan^2\theta_W} \right) Z_2 \right] + 2 g_L \sin\theta_W A \\
= {} & \frac{g_L}{\cos\theta_W} \left[- \left(2\sin^2\theta_W + \zeta \frac{\left[g_R^2/g_L^2 - 2\tan^2\theta_W \right] \cos\theta_W}{\sqrt{g_R^2/g_L^2 - \tan^2\theta_W}} \right) Z_1 \right. \\
& \qquad \left. + \left(\frac{\left[g_R^2/g_L^2 - 2\tan^2\theta_W \right] \cos\theta_W}{\sqrt{g_R^2/g_L^2 - \tan^2\theta_W}} - 2\zeta \sin^2\theta_W \right) Z_2 \right] + 2 g_L \sin\theta_W A.
\end{aligned}
\tag{A.82}
$$

Appendix B: Expressions of observables

For the observables discussed here, the expressions presented in reference [12] are mostly used. The exceptions are the form factors $F_R^{Z_1}$ and $B_{RR}^{\mu eee}$: for $F_R^{Z_1}$, a mixed expression from references [12] and [57] is used; for $B_{RR}^{\mu eee}$, the suppression factor $(m_{W_L}/m_{W_R})^2$ is multiplied to the whole expression. The normalized Yukawa couplings $\widetilde{h}_L$ and $\widetilde{h}_R$ are explicitly distinguished in this paper, since they are generally different even with the manifest left-right symmetry.

Charged lepton flavour violation

The normalized Yukawa couplings $\widetilde{h}_L$, $\widetilde{h}_R$ in the charged lepton mass basis are given by [58]

$$\widetilde{h}_L \equiv \frac{2}{g} V_L^{\ell \mathsf{T}} h_L V_L^{\ell} = \frac{2}{g} V_L^{\ell \mathsf{T}} \frac{M_L^* e^{-i\theta_L}}{\sqrt{2} v_L} V_L^{\ell}, \tag{B.1}$$

$$\widetilde{h}_R \equiv \frac{2}{g} V_R^{\ell \mathsf{T}} h_R V_R^{\ell} = \frac{2}{g} V_R^{\ell \mathsf{T}} \frac{M_R}{\sqrt{2} v_R} V_R^{\ell} = V_R^{\ell \mathsf{T}} \frac{M_R}{m_{W_R}} V_R^{\ell}. \tag{B.2}$$

Note that $\widetilde{h}_L \neq \widetilde{h}_R$ in general since $V_L^\ell \neq V_R^\ell$ for nonzero α, although $h \equiv h_L = h_R$ with the parity symmetry. The loop functions of CLFV are given in appendix B.

$\ell_a \to \ell_b\gamma$

For on-shell decay $\ell_a \to \ell_b\gamma$, the branching ratio is given by

$$\mathrm{BR}_{\ell_a\to\ell_b\gamma} = \frac{\alpha_W^3 s_W^2 m_{\ell_a}^5}{256\pi^2 m_{W_L}^4 \Gamma_{\ell_a}}\left(|G_L^\gamma|^2 + |G_R^\gamma|^2\right) \tag{B.3}$$

where $\alpha_W \equiv g^2/(4\pi)$, $s_W \equiv \sin\theta_W$, and Γ_{ℓ_a} is the decay rates of ℓ_a: $\Gamma_\mu = 2.996\cdot 10^{-19}$ GeV and $\Gamma_\tau = 2.267\cdot 10^{-12}$ GeV [59]. The form factors G_L^γ, G_R^γ are given by

$$G_L^\gamma = \sum_{i=1}^{3}\left[V_{\mu i}V_{ei}^*\xi^2 G_1^\gamma(x_i) - S_{\mu i}^* V_{ei}^*\xi e^{-i\alpha} G_2^\gamma(x_i)\frac{m_{N_i}}{m_{\ell_a}} + V_{\mu i}V_{ei}^*\frac{m_{W_L}^2}{m_{W_R}^2}G_1^\gamma(y_i) + \widetilde{h}_{R\mu i}\widetilde{h}_{Rei}^*\frac{2}{3}\frac{m_{W_L}^2}{m_{\delta_R^{++}}^2}\right], \tag{B.4}$$

$$G_R^\gamma = \sum_{i=1}^{3}\left[S_{\mu i}^* S_{ei} G_1^\gamma(x_i) - V_{\mu i}S_{ei}\xi e^{i\alpha}G_2^\gamma(x_i)\frac{m_{N_i}}{m_{\ell_a}} + \widetilde{h}_{L\mu i}\widetilde{h}_{Lei}^*\left(\frac{2}{3}\frac{m_{W_L}^2}{m_{\delta_L^{++}}^2} + \frac{1}{12}\frac{m_{W_L}^2}{m_{H_1^+}^2}\right)\right] \tag{B.5}$$

where $x_i = (m_{N_i}/m_{W_L})^2$ and $y_i = (m_{N_i}/m_{W_R})^2$. The initial and final charged leptons have opposite chiralities, and L or R in $G_{L,R}^\gamma$ denotes the chirality of the initial charged lepton. The Feynman diagrams of on-shell $\mu \to e\gamma$ are given in figure B.1.

$\mu \to eee$

The tree-level contribution to $\mu \to eee$ is

$$\mathrm{BR}_{\mu\to eee}^{\mathrm{tree}} = \frac{\alpha_W^4 m_\mu^5}{24576\pi^3 m_{W_L}^4\Gamma_\mu}\frac{(4\pi)^2}{2\alpha_W^2}\left(\left|\widetilde{h}_{L\mu e}\widetilde{h}_{Lee}^*\right|^2\frac{m_{W_L}^4}{m_{\delta_L^{++}}^4} + \left|\widetilde{h}_{R\mu e}\widetilde{h}_{Ree}^*\right|^2\frac{m_{W_L}^4}{m_{\delta_R^{++}}^4}\right). \tag{B.6}$$

The Feynman diagrams of the tree-level processes are given in figure B.2. The one-loop type-I seesaw contribution is given by [60, 61]

$$
\begin{aligned}
\mathrm{BR}^{\text{type-I}}_{\mu\to eee} = \frac{\alpha_W^4 m_\mu^5}{24576\pi^3 m_{W_L}^4 \Gamma_\mu}\Bigg[& 2\Bigg\{\left|\frac{1}{2}B^{\mu eee}_{LL} + F_L^{Z_1} - 2s_W^2\big(F_L^{Z_1} - F_L^\gamma\big)\right|^2 + \left|\frac{1}{2}B^{\mu eee}_{RR} - 2s_W^2\big(F_R^{Z_1} - F_R^\gamma\big)\right|^2\Bigg\} \\
& + \left|2s_W^2\big(F_L^{Z_1} - F_L^\gamma\big) - B^{\mu eee}_{LR}\right|^2 + \left|2s_W^2\big(F_R^{Z_1} - F_R^\gamma\big) - \big(F_R^{Z_1} + B^{\mu eee}_{RL}\big)\right|^2 \\
& + 8s_W^2\Bigg\{\mathrm{Re}\Big[\big(2F_L^{Z_1} + B^{\mu eee}_{LL} + B^{\mu eee}_{LR}\big)G_R^{\gamma *}\Big] + \mathrm{Re}\Big[\big(F_R^{Z_1} + B^{\mu eee}_{RR} + B^{\mu eee}_{RL}\big)G_L^{\gamma *}\Big]\Bigg\} \\
& - 48s_W^4\Bigg\{\mathrm{Re}\Big[\big(F_L^{Z_1} - F_L^\gamma\big)G_R^{\gamma *}\Big] + \mathrm{Re}\Big[\big(F_R^{Z_1} - F_R^\gamma\big)G_L^{\gamma *}\Big]\Bigg\} \\
& + 32s_W^4\big(|G_L^\gamma|^2 + |G_R^\gamma|^2\big)\Bigg\{\ln\left(\frac{m_\mu^2}{m_e^2}\right) - \frac{11}{4}\Bigg\}\Bigg],
\end{aligned}
\tag{B.7}
$$

and the interference terms are

$$
\begin{aligned}
\mathrm{BR}^{\text{tree+type-I}}_{\mu\to eee} = & \frac{\alpha_W^4 m_\mu^5}{24576\pi^3 m_{W_L}^4 \Gamma_\mu}\frac{2(4\pi)}{\alpha_W}\times \\
& \Bigg[\frac{m_{W_L}^2}{m_{\delta_L^{++}}^2}\mathrm{Re}\Bigg[\widetilde{h}^*_{L\mu e}\widetilde{h}_{Lee}\Bigg\{2s_W^2 F_L^\gamma + 4s_W^2 G_R^\gamma + B^{\mu eee}_{LL} + F_L^{Z_1}(1 - 2s_W^2)\Bigg\}\Bigg] \\
& + \frac{m_{W_L}^2}{m_{\delta_R^{++}}^2}\mathrm{Re}\Bigg[\widetilde{h}^*_{R\mu e}\widetilde{h}_{Ree}\Bigg\{2s_W^2 F_R^\gamma + 4s_W^2 G_L^\gamma + B^{\mu eee}_{RR} - 2s_W^2 F_R^{Z_1}\Bigg\}\Bigg]\Bigg].
\end{aligned}
\tag{B.8}
$$

The form factors for the off-shell photon exchange are

$$
F_L^\gamma = \sum_{i=1}^{3}\left[S^*_{\mu i}S_{ei}F_\gamma(x_i) - \widetilde{h}_{L\mu i}\widetilde{h}^*_{Lei}\left(\frac{2}{3}\frac{m_{W_L}^2}{m_{\delta_L^{++}}}\ln\frac{m_\mu^2}{m_{\delta_L^{++}}} + \frac{1}{18}\frac{m_{W_L}^2}{m_{H_1^+}}\right)\right], \tag{B.9}
$$

$$
F_R^\gamma = \sum_{i=1}^{3}\left[V_{\mu i}V^*_{ei}\left(\xi^2 F_\gamma(x_i) + \frac{m_{W_L}^2}{m_{W_R}^2}F_\gamma(y_i)\right) - \widetilde{h}_{R\mu i}\widetilde{h}^*_{Rei}\frac{2}{3}\frac{m_{W_L}^2}{m_{\delta_R^{++}}}\ln\frac{m_\mu^2}{m_{\delta_R^{++}}}\right]. \tag{B.10}
$$

For the Z_1-exchange diagrams, the form factors are given by

$$F_L^{Z_1} = \sum_{i,j=1}^{3} S_{\mu i}^* S_{ej} \Big[\delta_{ij} \big\{ F_Z(x_i) + 2G_Z(0, x_i) \big\}$$
$$+ (S^\mathsf{T} S^*)_{ij} \big\{ G_Z(x_i, x_j) - G_Z(0, x_i) - G_Z(0, x_j) \big\} + (S^\dagger S)_{ij} H_Z(x_i, x_j) \Big], \tag{B.11}$$

$$F_R^{Z_1} = \sum_{i=1}^{3} V_{\mu i} V_{ei}^* \Bigg[\frac{8\zeta_3 c_W^2}{\sqrt{1 - 2s_W^2}} \bigg\{ F_Z(y_i) + 2G_Z(0, y_i) - \frac{y_i}{2} \bigg\} + 2 \left(\frac{\kappa_1 \kappa_2}{v_{\mathrm{EW}} v_R} \right)^2 D_Z(y_i, x_i)$$
$$+ \left(\frac{\kappa_1^2 - \kappa_2^2}{\sqrt{2} v_{\mathrm{EW}} v_R} \right)^2 D_Z(y_i, z_i) \Bigg] \tag{B.12}$$

where $z_i = (m_{N_i}/m_{H_2^+})^2$, $c_W \equiv \cos\theta_W$, and ζ_3 is the Z_1-Z_2 mixing parameter given by equation 2.18. The Feynman diagrams that contribute to $F_{L,R}^{\gamma}$ and $F_{L,R}^{Z_1}$ are presented in reference [58]. The form factors of the box diagrams are written as

$$B_{LL}^{\mu eee} = -2 \sum_{i=1}^{3} S_{\mu i}^* S_{ei} \big[F_{\mathrm{Xbox}}(0, x_i) - F_{\mathrm{Xbox}}(0, 0) \big]$$
$$+ \sum_{i,j=1}^{3} S_{\mu i}^* S_{ej} \Big[-2S_{ej}^* S_{ei} \big\{ F_{\mathrm{Xbox}}(x_i, x_j) - F_{\mathrm{Xbox}}(0, x_j) - F_{\mathrm{Xbox}}(0, x_i) + F_{\mathrm{Xbox}}(0, 0) \big\}$$
$$+ S_{ei}^* S_{ej} G_{\mathrm{box}}(x_i, x_j, 1) \Big], \tag{B.13}$$

$$B_{RR}^{\mu eee} = -2 \frac{m_{W_L}^2}{m_{W_R}^2} \sum_{i,j=1}^{3} V_{\mu i} V_{ei}^* \big[F_{\mathrm{Xbox}}(0, y_i) - F_{\mathrm{Xbox}}(0, 0) \big]$$
$$+ \frac{m_{W_L}^2}{m_{W_R}^2} \sum_{i,j=1}^{3} V_{\mu i} V_{ej}^* \Big[-2V_{ej} V_{ei}^* \big\{ F_{\mathrm{Xbox}}(y_i, y_j) - F_{\mathrm{Xbox}}(0, y_j) - F_{\mathrm{Xbox}}(0, y_i) + F_{\mathrm{Xbox}}(0, 0) \big\}$$
$$+ V_{ei} V_{ej}^* G_{\mathrm{box}}(y_i, y_j, 1) \Big], \tag{B.14}$$

$$B_{LR}^{\mu eee} = \frac{1}{2} \frac{m_{W_L}^2}{m_{W_R}^2} \sum_{i,j=1}^{3} S_{\mu i}^* S_{ej} V_{ei} V_{ej}^* G_{\mathrm{box}} \left(x_i, x_j, \frac{m_{W_L}^2}{m_{W_R}^2} \right), \tag{B.15}$$

$$B_{RL}^{\mu eee} = \frac{1}{2} \frac{m_{W_L}^2}{m_{W_R}^2} \sum_{i,j=1}^{3} V_{\mu i} V_{ej}^* S_{ei}^* S_{ej} G_{\mathrm{box}} \left(x_i, x_j, \frac{m_{W_L}^2}{m_{W_R}^2} \right). \tag{B.16}$$

Here, the masses of light neutrinos and the momenta of external fields are assumed to be zero. The Feynman diagrams of the box diagrams are presented in figure B.3.

$\mu \to e$

The $\mu \to e$ conversion rate is given by [58, 61–63]

$$\mathrm{R}_{\mu\to e}^{A(N,Z)} = \frac{\alpha_{\mathrm{em}}^3 \alpha_W^4 m_\mu^5}{16\pi^2 m_{W_L}^4 \Gamma_{\mathrm{capt}}} \frac{Z_{\mathrm{eff}}^4}{Z} \left|F_p(-m_\mu^2)\right|^2 \left(\left|Q_L^W\right|^2 + \left|Q_R^W\right|^2\right). \tag{B.17}$$

Here, A, N, and Z are the mass, neutron, and atomic numbers of a nucleus, respectively, and Z_{eff} is the effective atomic number. The parameter F_p is the nuclear form factor, Γ_{capt} is the capture rate, and $\alpha_{\mathrm{em}} \equiv e^2/(4\pi)$. The values of F_p and Γ_{capt} of various nuclei are summarized in table B.1 [63]. The form factors in equation B.17

Nucleus ${}^{A}_{Z}\mathrm{N}$	Z_{eff}	$\lvert F_p(-m_\mu^2)\rvert$	Γ_{capt} (10^6 s^{-1})
${}^{27}_{13}\mathrm{Al}$	11.5	0.64	0.7054
${}^{48}_{22}\mathrm{Ti}$	17.6	0.54	2.59
${}^{197}_{79}\mathrm{Au}$	33.5	0.16	13.07
${}^{208}_{82}\mathrm{Pb}$	34.0	0.15	13.45

Table B.1: Form factors and capture rates of various nuclei associated with $\mu \to e$ conversion.

are given by

$$Q_{L,R}^W = (2Z+N)\left[W_{L,R}^u - \frac{2}{3}s_W^2 G_{R,L}^\gamma\right] + (Z+2N)\left[W_{L,R}^d + \frac{1}{3}s_W^2 G_{R,L}^\gamma\right] \tag{B.18}$$

and

$$W^u_{L,R} = \frac{2}{3}s^2_W F^\gamma_{L,R} + \left(-\frac{1}{4} + \frac{2}{3}s^2_W\right)F^{Z_1}_{L,R} + \frac{1}{4}\left(B^{\mu euu}_{LL,RR} + B^{\mu euu}_{LR,RL}\right), \tag{B.19}$$

$$W^d_{L,R} = -\frac{1}{3}s^2_W F^\gamma_{L,R} + \left(\frac{1}{4} - \frac{1}{3}s^2_W\right)F^{Z_1}_{L,R} + \frac{1}{4}\left(B^{\mu edd}_{LL,RR} + B^{\mu edd}_{LR,RL}\right). \tag{B.20}$$

The box diagram form factors are

$$B^{\mu euu}_{LL} = \sum_{i=1}^{3} S^*_{\mu i} S_{ei}[F_{\rm box}(0, x_i) - F_{\rm box}(0, 0)], \tag{B.21}$$

$$\begin{aligned} B^{\mu edd}_{LL} = \sum_{i=1}^{3} S^*_{\mu i} S_{ei}\big[&F_{\rm Xbox}(0, x_i) - F_{\rm Xbox}(0, 0) \\ &+ |V^q_{Ltd}|^2\{F_{\rm Xbox}(x_t, x_i) - F_{\rm Xbox}(0, x_i) - F_{\rm Xbox}(0, x_t) + F_{\rm Xbox}(0, 0)\}\big], \end{aligned} \tag{B.22}$$

$$B^{\mu euu}_{RR} = \sum_{i=1}^{3} V_{\mu i} V^*_{ei}[F_{\rm box}(0, x_i) - F_{\rm box}(0, 0)], \tag{B.23}$$

$$\begin{aligned} B^{\mu edd}_{RR} = \sum_{i=1}^{3} V_{\mu i} V^*_{ei}\big[&F_{\rm Xbox}(0, x_i) - F_{\rm Xbox}(0, 0) \\ &+ |V^q_{Rtd}|^2\{F_{\rm Xbox}(x_t, x_i) - F_{\rm Xbox}(0, x_i) - F_{\rm Xbox}(0, x_t) + F_{\rm Xbox}(0, 0)\}\big], \end{aligned} \tag{B.24}$$

and $B^{\mu eqq}_{LR} = B^{\mu eqq}_{RL} = 0$ due to their chiral structures. Here, $x_t = m_t^2/m^2_{W_L}$ and $y_t = m_t^2/m^2_{W_R}$ where m_t is the mass of a top quark, and the masses of all the other quarks as well as light neutrinos are assumed to be zero. The matrix V^q_L is the Cabibbo-Kobayashi-Maskawa matrix, and V^q_R is its RH counterpart. Note that $V^q_L \neq V^q_R$ for nonzero α, although $V^q_{Ltd} = V^q_{Rtd}$ is assumed for the numerical analysis in this paper. The momenta of external fields are also assumed to be zero. The Feynman diagrams of the box diagrams are given in figure B.4.

Loop functions

The loop functions of CLFV are

$$F_\gamma(x) = \frac{7x^3 - x^2 - 12x}{12(1-x)^3} - \frac{x^4 - 10x^3 + 12x^2}{6(1-x)^4}\ln x, \tag{B.25}$$

$$G_1^\gamma(x) = -\frac{2x^3 + 5x^2 - x}{4(1-x)^3} - \frac{3x^3}{2(1-x)^4}\ln x, \tag{B.26}$$

$$G_2^\gamma(x) = \frac{x^2 - 11x + 4}{2(1-x)^2} - \frac{3x^2}{(1-x)^3}\ln x, \tag{B.27}$$

$$F_Z(x) = -\frac{5x}{2(1-x)} - \frac{5x^2}{2(1-x)^2}\ln x, \tag{B.28}$$

$$G_Z(x,y) = -\frac{1}{2(1-x)}\left[\frac{x^2(1-y)}{1-x}\ln x - \frac{y^2(1-x)}{1-y}\ln y\right], \tag{B.29}$$

$$H_Z(x,y) = \frac{\sqrt{xy}}{4(x-y)}\left[\frac{x(x-4)}{1-x}\ln x - \frac{y(y-4)}{1-y}\ln y\right], \tag{B.30}$$

$$\begin{aligned} D_Z(x,y) = x\left(2 - \ln\frac{y}{x}\right) + \frac{x(-8+9x-x^2) - x^2(8-x)\ln x}{(1-x)^2} + \frac{xy(1-y+y\ln y)}{(1-y)^2} \\ + \frac{2xy(4-x)\ln x}{(1-x)(1-y)} + \frac{2x(x-4y)\ln\frac{y}{x}}{(1-y)(x-y)}, \end{aligned} \tag{B.31}$$

$$F_{\text{box}}(x,y) = \left(4 + \frac{xy}{4}\right) I_2(x,y,1) - 2xyI_1(x,y,1), \tag{B.32}$$

$$F_{\text{Xbox}}(x,y) = -\left(1 + \frac{xy}{4}\right) I_2(x,y,1) - 2xyI_1(x,y,1), \tag{B.33}$$

$$G_{\text{box}}(x,y,\eta) = -\sqrt{xy}\left[(4 + xy\eta)I_2(x,y,\eta) - (1+\eta)I_1(x,y,\eta)\right] \tag{B.34}$$

where

$$I_1(x,y,\eta) = \left[\frac{x\ln x}{(1-x)(1-\eta x)(x-y)} + (x \leftrightarrow y)\right] - \frac{\eta \ln \eta}{(1-\eta)(1-\eta x)(1-\eta y)}, \tag{B.35}$$

$$I_2(x,y,\eta) = \left[\frac{x^2\ln x}{(1-x)(1-\eta x)(x-y)} + (x \leftrightarrow y)\right] - \frac{\ln \eta}{(1-\eta)(1-\eta x)(1-\eta y)}, \tag{B.36}$$

$$I_i(x,y,1) \equiv \lim_{\eta\to 1} I_i(x,y,\eta). \tag{B.37}$$

Neutrinoless double beta decay

The dimensionless parameter associated with the W_L- and light neutrino exchange is

$$\eta_\nu = \frac{\sum_{i=1}^{3}(U_{ei})^2 m_{\nu_i}}{m_e}. \tag{B.38}$$

For the W_L- and heavy neutrino exchange, we have

$$\eta^L_{N_R} = m_p \sum_{i=1}^{3} \frac{(S_{ei})^2}{m_{N_i}} \tag{B.39}$$

where m_p is the mass of a proton. For the W_R- and heavy neutrino exchange, the parameter is given by

$$\eta^R_{N_R} = m_p \left(\frac{m_{W_L}}{m_{W_R}}\right)^4 \sum_{i=1}^{3} \frac{(V^*_{ei})^2}{m_{N_i}}. \tag{B.40}$$

For the δ_R^{++}-exchange, we have

$$\eta_{\delta_R} = \frac{\sum_{i=1}^{3}(V_{ei})^2 m_{N_i}}{m^2_{\delta_R^{++}} m^4_{W_R}} \frac{m_p}{G_F^2}. \tag{B.41}$$

For the λ-diagram with final state electrons of different helicities, the parameter is written as

$$\eta_\lambda = \left(\frac{m_{W_L}}{m_{W_R}}\right)^2 \sum_{i=1}^{3} U_{ei} T_{ei}^*. \tag{B.42}$$

For the η-diagram with W_L-W_R mixing,

$$\eta_\eta = -\xi e^{-i\alpha} \sum_{i=1}^{3} U_{ei} T_{ei}^*. \tag{B.43}$$

The Feynman diagrams corresponding to those parameters are given in figure B.5. The phase space factors $G_{01}^{0\nu}$ and matrix elements $\mathcal{M}^{0\nu}$ for various processes that lead to $0\nu\beta\beta$ are summarized in table B.2 [12,64–71]. The inverse half-life is written as

$$\begin{aligned}[T_{1/2}^{0\nu}]^{-1} = G_{01}^{0\nu} \left(|\mathcal{M}_\nu^{0\nu}|^2|\eta_\nu|^2 + |\mathcal{M}_N^{0\nu}|^2|\eta_{N_R}^L|^2 + |\mathcal{M}_N^{0\nu}|^2|\eta_{N_R}^R + \eta_{\delta_R}|^2 + |\mathcal{M}_\lambda^{0\nu}|^2|\eta_\lambda|^2 + |\mathcal{M}_\eta^{0\nu}|^2|\eta_\eta|^2\right) \\ + \text{interference terms.}\end{aligned} \tag{B.44}$$

Isotope	$G_{01}^{0\nu}$ (10^{-14} yrs.$^{-1}$)	$\mathcal{M}_\nu^{0\nu}$	$\mathcal{M}_N^{0\nu}$	$\mathcal{M}_\lambda^{0\nu}$	$\mathcal{M}_\eta^{0\nu}$
^{76}Ge	0.686	2.58 – 6.64	233 – 412	1.75 – 3.76	235 – 637
^{82}Se	2.95	2.42 – 5.92	226 – 408	2.54 – 3.69	209 – 234
^{130}Te	4.13	2.43 – 5.04	234 – 385	2.85 – 3.67	414 – 540
^{136}Xe	4.24	1.57 – 3.85	164 – 172	1.96 – 2.49	370 – 419

Table B.2: Phase space factors and matrix elements associated with $0\nu\beta\beta$.

Electric dipole moments of charged leptons

The EDM of the charged lepton ℓ_α ($\alpha = e, \mu, \tau$) is given by [11, 72]

$$d_\alpha = \frac{e\alpha_W}{8\pi m_{W_L}^2} \mathrm{Im}\left[\sum_{i=1}^{3} S_{\alpha i} V_{\alpha i} \xi e^{i\alpha} G_2^\gamma(x_i) m_{N_i}\right]. \tag{B.45}$$

The Feynman diagrams that generate the EDM of an electron are given in figure B.6.

Benchmark model parameters and their predictions

The benchmark model parameters and their predictions are summarized in tables B.3 and B.4. These parameters are chosen to obtain $\mathrm{BR}_{\mu\to e\gamma}$, $\mathrm{BR}_{\mu\to eee}$, $\mathrm{R}_{\mu\to e}$, and $T_{1/2}^{0\nu}$ large enough to be observable in near-future experiments.

The Yukawa coupling matrices f, $\widetilde{f}$ in the symmetry basis calculated from these parameters are

$$f = \begin{pmatrix} -0.117629 & -0.0954074 - 0.303042i & -0.287722 - 0.316317i \\ -0.0954074 + 0.303042i & 0.858098 & -0.581546 - 0.997804i \\ -0.287722 + 0.316317i & -0.581546 + 0.997804i & 1.55438 \end{pmatrix} \cdot 10^{-6}, \tag{B.46}$$

$$\widetilde{f} = \begin{pmatrix} 9.02581 & 0.362808 - 3.15221i & -0.217594 + 0.423914i \\ 0.362808 + 3.15221i & 1.53907 & 3.98014 \cdot 10^{-4} - 0.328771i \\ -0.217594 - 0.423914i & 3.98014 \cdot 10^{-4} + 0.328771i & 0.260124 \end{pmatrix} \cdot 10^{-3}. \tag{B.47}$$

Parameter	Value	Parameter	Value
$\log_{10}(m_{\nu_3}/\mathrm{eV})$	-10.2	$\log_{10}(\kappa_2/\mathrm{GeV})$	-1.12
m_{W_R}	3.60 TeV	α	0.7843093682120977π rad
δ_D	-0.700π rad	$\log_{10}(\lvert A_{11}\rvert/\mathrm{GeV})$	-8.20
δ_{M1}	-0.0640π rad	$A_{11}/\lvert A_{11}\rvert$	1
δ_{M2}	0.850π rad	$A_{22}/\lvert A_{22}\rvert$	-1
θ_{L12}	0.287π rad	$A_{33}/\lvert A_{33}\rvert$	-1
θ_{L13}	0.387π rad	$\theta_{A_{12}}$	-0.5970870460412485π rad
θ_{L23}	0.546π rad	$\theta_{A_{13}}$	0.26505775139215687π rad
δ_{L1}	-0.488π rad	$\theta_{A_{23}}$	-0.6679707059438431π rad
δ_{L2}	-0.953π rad	$\log_{10}\alpha_3$	0.520
δ_{L3}	-0.769π rad	$\log_{10}(\rho_3 - 2\rho_1)$	0.328
δ_{L4}	$-5.30 \cdot 10^{-5}\pi$ rad	$\log_{10}\rho_2$	0.450

Table B.3: Benchmark parameters for large CLFV and $0\nu\beta\beta$. The predictions from these parameters are given in table B.4.

Parameter	Value
m_{W_R}	3.60 TeV
m_{ν_1}	0.0631 eV
m_{ν_2}	0.0637 eV
m_{ν_3}	0.0807 eV
m_{N_1}	0.139 TeV
m_{N_2}	0.280 TeV
m_{N_3}	4.13 TeV
$m_{H_1^+}$	8.08 TeV
$m_{H_2^+}$	10.1 TeV
$m_{\delta_L^{++}}$	8.09 TeV
$m_{\delta_R^{++}}$	18.6 TeV
κ_1	246 GeV
$\kappa_2 e^{i\alpha}$	$0.0759e^{i0.784\pi}$ GeV
α_3	3.31
$\rho_3 - 2\rho_1$	2.13
ρ_2	2.82

The charged lepton and Dirac neutrino mass matrices in the symmetry basis are

$$
\begin{aligned}
M_\ell &= \frac{1}{\sqrt{2}}(f\kappa_2 e^{i\alpha} + \widetilde{f}\kappa_1) \\
&= \begin{pmatrix} 1.57002 - 3.95569 \cdot 10^{-9}i & 0.0631099 - 0.548321i & -0.0378502 + 0.0737391i \\ 0.0631098 + 0.548321i & 0.267718 + 2.88565 \cdot 10^{-8}i & 6.92918 \cdot 10^{-5} - 0.0571891i \\ -0.0378501 - 0.0737391i & 6.92247 \cdot 10^{-5} + 0.0571891i & 0.0452481 + 5.22714 \cdot 10^{-8}i \end{pmatrix} \text{GeV},
\end{aligned}
\tag{B.48}
$$

$$M_D = \frac{1}{\sqrt{2}}(f\kappa_1 + \widetilde{f}\kappa_2 e^{-i\alpha})$$

$$= \begin{pmatrix} -3.97641 - 3.03524i & -1.37761 + 0.668135i & 0.733973 + 0.446252i \\ 0.742466 - 0.912148i & 0.849485 - 0.517565i & -1.12232 - 1.59841i \\ 0.448861 - 0.299905i & -0.901194 + 1.59814i & 2.59511 - 0.0874759i \end{pmatrix} \cdot 10^{-4}\ \text{GeV}. \tag{B.49}$$

The mixing matrices that diagonalize M_ℓ are

$$V_L^\ell = \begin{pmatrix} 0.215620 + 3.59016 \cdot 10^{-5}i & 0.272630 & 0.0353401 + 0.936980i \\ -0.174794 - 0.555520i & 0.00850025 - 0.736518i & -0.340224 + 0.0506041i \\ -0.527503 + 0.579736i & 0.526439 - 0.325580i & 0.0374439 - 0.0332209i \end{pmatrix}, \tag{B.50}$$

$$V_R^\ell = \begin{pmatrix} 0.215620 & 0.272630 & 0.0353401 + 0.936980i \\ -0.174886 - 0.555491i & 0.00850025 - 0.736518i & -0.340224 + 0.0506041i \\ -0.527407 + 0.579824i & 0.526439 - 0.325580i & 0.0374439 - 0.0332209i \end{pmatrix}. \tag{B.51}$$

The neutrino mass matrices in the charged lepton mass basis are written as

$$M_\nu^c = U_{\text{PMNS}} M_\nu^{\text{diag}} U_{\text{PMNS}}^\mathsf{T}$$

$$= \begin{pmatrix} 6.14141 + 0.604007i & -0.641188 + 1.37500i & -0.414134 - 0.161926i \\ -0.641188 + 1.37500i & 5.21993 + 3.90978i & -0.721679 + 2.37952i \\ -0.414134 - 0.161926i & -0.721679 + 2.37952i & 5.35910 + 4.32684i \end{pmatrix} \cdot 10^{-11}\ \text{GeV}, \tag{B.52}$$

$$M_D^c = V_L^{\ell\dagger} M_D V_R^\ell$$
$$= \begin{pmatrix} -0.887458 - 0.00113569i & -0.596983 - 1.80367i & -0.364728 - 0.967911i \\ -0.596682 + 1.80377i & 2.44772 - 0.204264i & 0.650485 - 0.676299i \\ -0.364567 + 0.967972i & 0.650486 + 0.676299i & -3.86700 - 3.43503i \end{pmatrix} \cdot 10^{-4}\ \text{GeV}, \tag{B.53}$$

$$M_R^c = -M_D^{c\mathsf{T}} (M_\nu^c)^{-1} M_D^c$$
$$= \begin{pmatrix} 327.179 - 124.513i & -141.421 - 201.931i & 36.0396 + 816.162i \\ -141.421 - 201.931i & 56.2978 + 60.4971i & 517.744 - 74.6682i \\ 36.0396 + 816.162i & 517.744 - 74.6682i & -2486.91 - 2973.37i \end{pmatrix} \text{GeV}. \tag{B.54}$$

The neutrino mixing matrices are given by

$$U = U_{\text{PMNS}} = \begin{pmatrix} 0.824240 & 0.535780 + 0.109200i & 0.131084 - 0.0667906i \\ -0.365548 + 0.0658493i & 0.632967 + 0.173591i & -0.585126 - 0.298136i \\ 0.420911 + 0.0741679i & -0.516908 + 0.0551401i & -0.659043 - 0.335799i \end{pmatrix}, \tag{B.55}$$

$$S = \begin{pmatrix} -0.492113 - 0.340868i & 0.999284 + 0.0561499i & 0.239615 + 0.0281506i \\ -0.0475962 + 0.503081i & -0.231028 - 1.26661i & -0.00795814 - 0.320325i \\ 0.232020 - 0.00648341i & -0.401571 + 0.125068i & -0.175188 + 0.136668i \end{pmatrix} \cdot 10^{-6}, \tag{B.56}$$

$$T = \begin{pmatrix} -6.53107 - 6.47350i & -8.46370 + 5.72968i & -1.16360 - 8.20634i \\ 2.04202 - 6.05309i & -4.69170 - 5.30774i & 3.49735 - 2.06263i \\ -1.83711 - 0.641098i & 0.0608069 + 1.46932i & 0.103607 - 0.502026i \end{pmatrix} \cdot 10^{-7}, \tag{B.57}$$

$$V = \begin{pmatrix} -0.183724 + 0.375972i & 0.879386 + 0.0740900i & 0.195953 - 0.0876577i \\ -0.881006 + 0.210057i & -0.242230 - 0.320460i & -0.0720947 - 0.114618i \\ -0.0677616 + 0.00212502i & 0.177470 - 0.168300i & -0.408123 + 0.876937i \end{pmatrix}. \tag{B.58}$$

The Yukawa coupling matrix h in the symmetry basis is

$$\begin{aligned} h &= \frac{1}{\sqrt{2}v_R} V_R^{\ell *} M_R^c V_R^{\ell \dagger} \\ &= \begin{pmatrix} 0.206578 + 0.223735i & 0.120506 - 0.0241230i & -0.0469350 - 0.0641918i \\ 0.120506 - 0.0241230i & 0.00351664 - 0.0376782i & -0.0257606 + 0.00173595i \\ -0.046935 - 0.0641918i & -0.0257606 + 0.00173595i & -0.00335158 + 0.0385022i \end{pmatrix}, \end{aligned} \tag{B.59}$$

and the normalized Yukawa couplings $\widetilde{h}_L$, $\widetilde{h}_R$ in the charged lepton mass basis are

$$\begin{aligned} \widetilde{h}_L &= \frac{2}{g} V_L^{\ell \mathsf{T}} h V_L^{\ell} \\ &= \begin{pmatrix} 0.0908945 - 0.0345568i & -0.0392741 - 0.0560986i & 0.00997325 + 0.226713i \\ -0.0392741 - 0.0560986i & 0.0156383 + 0.0168047i & 0.143818 - 0.0207412i \\ 0.00997325 + 0.226713i & 0.143818 - 0.0207412i & -0.690808 - 0.825936i \end{pmatrix}, \end{aligned} \tag{B.60}$$

$$\begin{aligned} \widetilde{h}_R &= \frac{2}{g} V_R^{\ell \mathsf{T}} h V_R^{\ell} \\ &= \begin{pmatrix} 0.0908830 - 0.0345871i & -0.0392835 - 0.0560921i & 0.0100110 + 0.226712i \\ -0.0392835 - 0.0560921i & 0.0156383 + 0.0168047i & 0.143818 - 0.0207412i \\ 0.0100110 + 0.226712i & 0.143818 - 0.0207412i & -0.690808 - 0.825936i \end{pmatrix}. \end{aligned} \tag{B.61}$$

Note that $\widetilde{h}_L \approx \widetilde{h}_R$ since we are considering the cases of $V_L^\ell \approx V_R^\ell$ for the TeV-scale phenomenology.

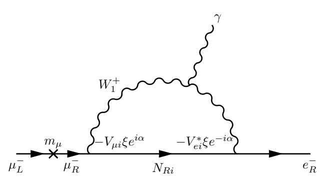

(a) G_L^γ

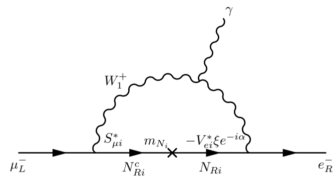

(b) G_L^γ

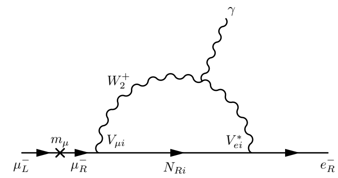

(c) G_L^γ

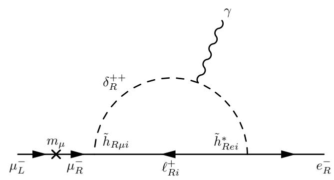

(d) G_L^γ

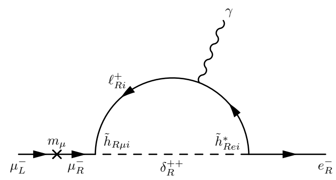

(e) G_L^γ

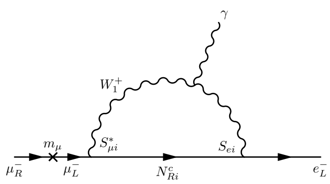

(f) G_R^γ

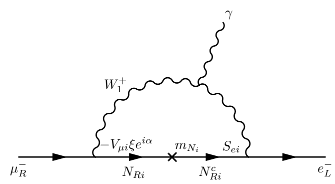

(g) G_R^γ

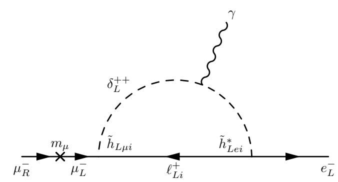

(h) G_R^γ

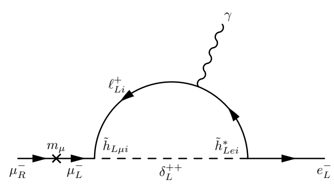

(i) G_R^γ

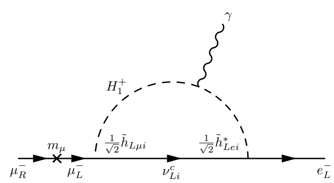

(j) G_R^γ

Figure B.1: Feynman diagrams of on-shell $\mu \to e\gamma$. Here, $W_L^+ \approx W_1^+ + \xi e^{-i\alpha} W_2^+$ and $W_R^+ \approx -\xi e^{i\alpha} W_1^+ + W_2^+$. Figures B.1a−B.1e contribute to G_L^γ, and figures B.1f−B.1j to G_R^γ. The arrows in neutrino propagators denote the directions of the propagation of $N_i = N_{Ri} + N_{Ri}^c$.

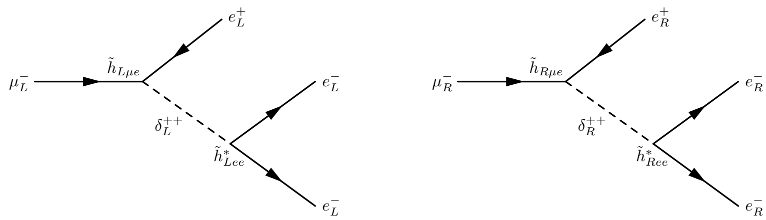

(a) (b)

Figure B.2: Feynman diagrams of the tree-level processes of $\mu \to eee$.

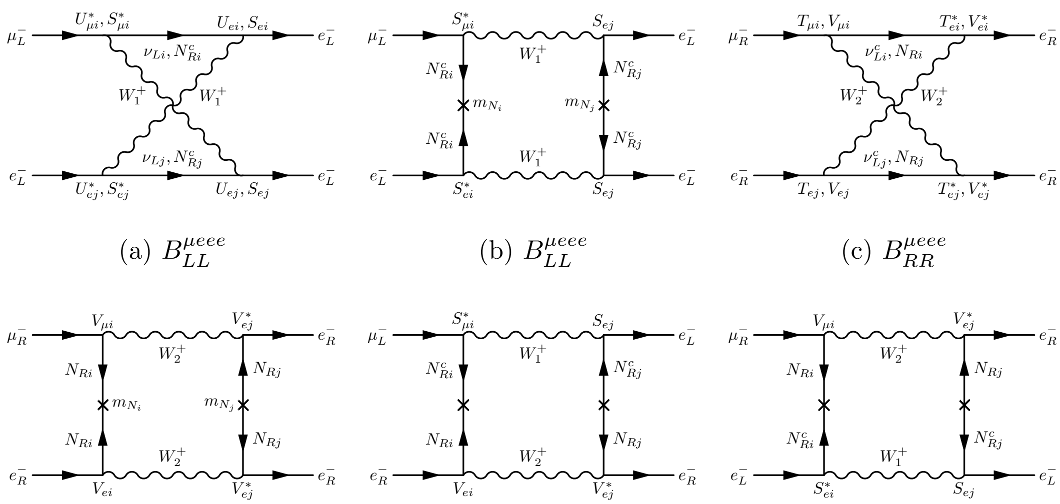

(a) $B_{LL}^{\mu eee}$ (b) $B_{LL}^{\mu eee}$ (c) $B_{RR}^{\mu eee}$

(d) $B_{RR}^{\mu eee}$ (e) $B_{LR}^{\mu eee}$ (f) $B_{RL}^{\mu eee}$

Figure B.3: Feynman diagrams of $B^{\mu eee}$. Note that the arrows in neutrino propagators indicate the directions of the propagation of $\nu_i = \nu_{Li} + \nu_{Li}^c$ or $N_i = N_{Ri} + N_{Ri}^c$.

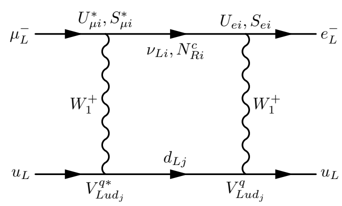

(a) $B_{LL}^{\mu euu}$

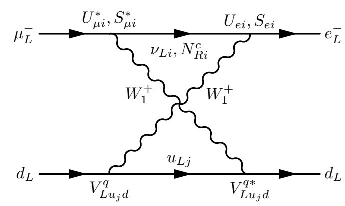

(b) $B_{LL}^{\mu edd}$

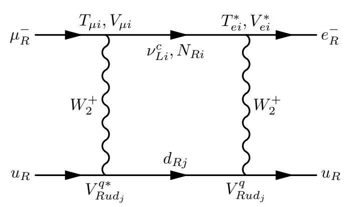

(c) $B_{RR}^{\mu euu}$

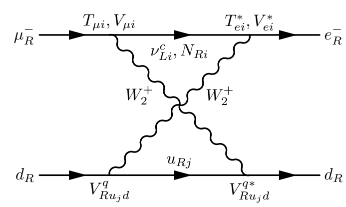

(d) $B_{RR}^{\mu edd}$

Figure B.4: Feynman diagrams of $B^{\mu eqq}$.

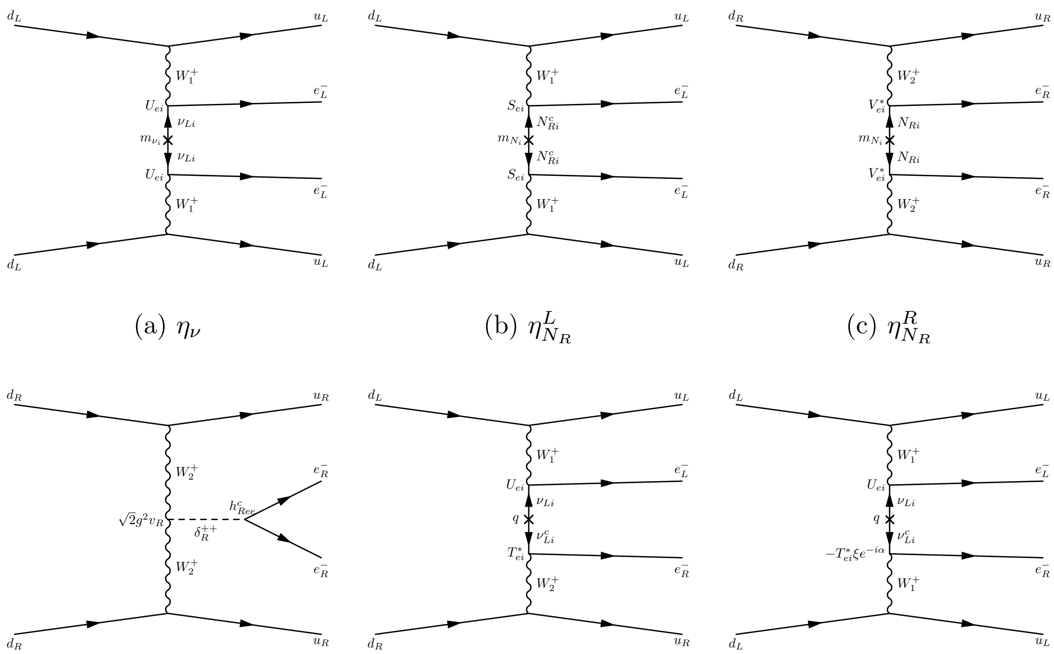

(a) η_ν (b) $\eta_{N_R}^L$ (c) $\eta_{N_R}^R$

(d) η_{δ_R} (e) η_λ (f) η_η

Figure B.5: Feynman diagrams of $0\nu\beta\beta$. Here, $W_L^+ \approx W_1^+ + \xi e^{-i\alpha} W_2^+$ and $W_R^+ \approx -\xi e^{i\alpha} W_1^+ + W_2^+$. The coupling $h_R^c \equiv V_R^{\ell\mathsf{T}} h V_R^\ell = M_R^c/(\sqrt{2}v_R)$ is the Yukawa coupling matrix in the charged lepton mass basis. The typical momentum transfer of the processes is $q \approx 100$ MeV.

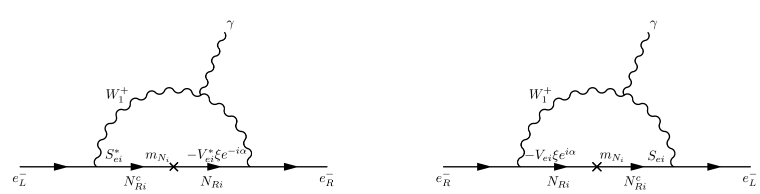

(a) (b)

Figure B.6: Feynman diagrams contributing to the EDM of e.

	Prediction	Near-future sensitivity
$\mathrm{BR}_{\mu\to e\gamma}$	$5.98 \cdot 10^{-14}$	$< 5.0 \cdot 10^{-14}$ (Upgraded MEG)
$\mathrm{BR}_{\tau\to\mu\gamma}$	$1.94 \cdot 10^{-13}$	.
$\mathrm{BR}_{\tau\to e\gamma}$	$4.85 \cdot 10^{-13}$	.
$\mathrm{BR}_{\mu\to eee}$	$8.12 \cdot 10^{-14}$	$< 1.0 \cdot 10^{-15}$ (PSI) [24]
$\mathrm{R}^{\mathrm{Al}}_{\mu\to e}$	$2.17 \cdot 10^{-13}$	$< 3.0 \cdot 10^{-17}$ (COMET)
$\mathrm{R}^{\mathrm{Ti}}_{\mu\to e}$	$4.13 \cdot 10^{-13}$	$< 1.0 \cdot 10^{-18}$ (PRISM/PRIME)
$\mathrm{R}^{\mathrm{Au}}_{\mu\to e}$	$3.98 \cdot 10^{-13}$	.
$\mathrm{R}^{\mathrm{Pb}}_{\mu\to e}$	$3.83 \cdot 10^{-13}$	.
$\lvert\eta_\nu\rvert$	$1.21 \cdot 10^{-7}$	$\lesssim 1.4 \cdot 10^{-7}$ (CUORE)
$\lvert\eta^L_{N_R}\rvert$	$4.97 \cdot 10^{-15}$	.
$\lvert\eta^R_{N_R}\rvert$	$4.77 \cdot 10^{-10}$	.
$\lvert\eta_{\delta_R}\rvert$	$4.24 \cdot 10^{-11}$	.
$\lvert\eta_\lambda\rvert$	$4.61 \cdot 10^{-10}$	.
$\lvert\eta_\eta\rvert$	$2.81 \cdot 10^{-13}$	.
$T^{0\nu}_{1/2}\rvert_{\mathrm{Ge}}$	$2.12 \cdot 10^{26} - 1.31 \cdot 10^{27}$ yrs.	.
$T^{0\nu}_{1/2}\rvert_{\mathrm{Se}}$	$6.11 \cdot 10^{25} - 3.43 \cdot 10^{26}$ yrs.	.
$T^{0\nu}_{1/2}\rvert_{\mathrm{Te}}$	$5.91 \cdot 10^{25} - 2.41 \cdot 10^{26}$ yrs.	$> 2.1 \cdot 10^{26}$ yrs. (CUORE)
$T^{0\nu}_{1/2}\rvert_{\mathrm{Xe}}$	$1.05 \cdot 10^{26} - 5.48 \cdot 10^{26}$ yrs.	.
$\lvert d_e\rvert$	$\lvert -2.98 \cdot 10^{-31}\rvert$ e·cm	.
$\lvert d_\mu\rvert$	$\lvert 1.99 \cdot 10^{-31}\rvert$ e·cm	.
$\lvert d_\tau\rvert$	$\lvert -3.13 \cdot 10^{-31}\rvert$ e·cm	.

Table B.4: Predictions from the benchmark model parameters of table B.3. Only near-future experiments that would detect the corresponding processes are presented here.

Appendix C: Parametrization of the Dirac neutrino mass matrix

In this section, we show that the Casas-Ibarra parametrization [47] of the Dirac neutrino mass matrix is the most general form of M_D for given heavy neutrino masses.

Standard Model with right-handed Majorana neutrinos

For a diagonal matrix D with positive entries, i.e.

$$D = \begin{pmatrix} d_1 & 0 & 0 \\ 0 & d_2 & 0 \\ 0 & 0 & d_3 \end{pmatrix} \tag{C.1}$$

with $d_i > 0$, we define

$$\sqrt{D} \equiv \begin{pmatrix} \sqrt{d_1} & 0 & 0 \\ 0 & \sqrt{d_2} & 0 \\ 0 & 0 & \sqrt{d_3} \end{pmatrix} . \tag{C.2}$$

We write C which satisfies $C^\mathsf{T} C = CC^\mathsf{T} = D$ as $C = \sqrt{D}B$ where $B \equiv \sqrt{D^{-1}}C$. Then, $BB^\mathsf{T} = (\sqrt{D^{-1}}C)(\sqrt{D^{-1}}C)^\mathsf{T} = \sqrt{D^{-1}}CC^\mathsf{T}\sqrt{D^{-1}} = I$, i.e. B is an orthogonal matrix. In other words, any matrix C which satisfies $C^\mathsf{T} C = CC^\mathsf{T} = D$ is orthogonally equivalent to $\sqrt{D^{-1}}$.

Now we go to the basis in the flavour space where the light and heavy neutrino mass matrices are diagonal with positive entries. In that basis, we denote the charged lepton mass matrix as M_ℓ, the Dirac neutrino mass matrix as M_D, the right-handed Majorana neutrino mass matrix as M_R^d, and light neutrino mass matrix as M_ν^d. We assume that the neutrino mass matrices are invertible, which is trivially satisfied as long as the lightest neutrino mass is nonzero. Then, for a matrix C_R which satisfy $C_R C_R^\mathsf{T} = M_R^d$, we can write $C_R = \sqrt{M_R^d} O_R$ for an orthogonal matrix O_R. The neutrino mass matrices satisfy the type-I seesaw formula, and thus

$$
\begin{aligned}
M_\nu^d &= -M_D (M_R^d)^{-1} M_D^\mathsf{T} = -M_D \left(\sqrt{(M_R^d)^{-1}} O_R\right)\left(\sqrt{(M_R^d)^{-1}} O_R\right)^\mathsf{T} M_D \\
&= \left[i M_D \sqrt{(M_R^d)^{-1}} O_R \right]\left[i M_D \sqrt{(M_R^d)^{-1}} O_R \right]^\mathsf{T}.
\end{aligned}
\tag{C.3}
$$

We can therefore write

$$
i M_D \sqrt{(M_R^d)^{-1}} O_R = \sqrt{M_\nu^d} O_\nu \tag{C.4}
$$

for an orthogonal matrix O_ν, and

$$
M_D = -i \sqrt{M_\nu^d} O \sqrt{M_R^d} \tag{C.5}
$$

where $O \equiv O_\nu O_R^\mathsf{T}$ is also an orthogonal matrix.

In the charged lepton mass basis, we have

$$
M_\ell^c = U M_\ell V_R^\ell, \qquad M_\nu^c = U M_\nu^d U^\mathsf{T}, \qquad M_D^c = U M_D, \qquad M_R^c = M_R^d \tag{C.6}
$$

where U and V_R^ℓ are the unitary matrices which transform M_ℓ into the diagonal matrix M_ℓ^c with charged lepton masses as its entries. Note that $U \equiv U_\text{PMNS}$ is the

PMNS matrix. We can write

$$M_D^c = -iU\sqrt{M_\nu^d}O\sqrt{M_R^d}. \tag{C.7}$$

Without loss of generality, the complex orthogonal matrix O can be parametrized as $O = e^S$ where S is a skew-symmetric matrix, i.e. $S^\mathsf{T} = -S$, as the exponential map is surjective.

Left-right symmetric model

We follow the same steps up to the proof of the generality of equations **??** and **??**. In the charged lepton mass basis, we have

$$M_\ell^c = UM_\ell V_R^\ell, \qquad M_\nu^c = UM_\nu^d U^\mathsf{T}, \qquad M_D^c = UM_D V_R^\ell, \qquad M_R^c = V_R^{\ell\mathsf{T}} M_R^d V_R^\ell. \tag{C.8}$$

Hence,

$$M_D^c = -iU\sqrt{M_\nu^d}O\sqrt{M_R^d}V_R^\ell. \tag{C.9}$$

Appendix D: Boltzmann equation

In this section, we explicitly derive the Boltzmann equations for the RH neutrino density and LH lepton doublet asymmetry. Here, we consider the extension of the SM only with three RH neutrinos for simplicity. Note that the relations of collision terms and the correct forms of Boltzmann equations in any other models should be carefully derived in a similar way.

The generic form of the Boltzmann equation is

$$\frac{dn_a}{dt} + 3Hn_a = -\sum_{aX\leftrightarrow Y}\left[\frac{n_a n_X}{n_a^{\rm eq} n_X^{\rm eq}}\gamma(aX\to Y) - \frac{n_Y}{n_Y^{\rm eq}}\gamma(Y\to aX)\right]. \tag{D.1}$$

Since ϕ is a massless scalar field, we have $n_\phi = n_\phi^{\rm eq}$. In addition, $n_{L_i}^{\rm eq} = n_{L_i^c}^{\rm eq} = n_{\ell_i}^{\rm eq}$ where $n_{\ell_i}^{\rm eq} \equiv n_{\ell_{Li}}^{\rm eq} + n_{\ell_{Ri}}^{\rm eq}$ is the total lepton number density of each flavour in equilibrium. The CP-conserving decay term is defined by

$$\gamma_{L_i\phi}^{N_\alpha} \equiv \gamma(N_\alpha\to L_i\phi) + \gamma(N_\alpha\to L_i^c\phi^\dagger), \tag{D.2}$$

and the CP-violating decay term by

$$\delta\gamma_{L_i\phi}^{N_\alpha} \equiv \gamma(N_\alpha\to L_i\phi) - \gamma(N_\alpha\to L_i^c\phi^\dagger). \tag{D.3}$$

By CPT invariance, we have

$$\gamma(L_i\phi\to N_\alpha) = \gamma(N_\alpha\to L_i^c\phi^\dagger) = \frac{1}{2}(\gamma_{L_i\phi}^{N_\alpha} - \delta\gamma_{L_i\phi}^{N_\alpha}), \tag{D.4}$$

$$\gamma(L_i^c\phi^\dagger\to N_\alpha) = \gamma(N_\alpha\to L_i\phi) = \frac{1}{2}(\gamma_{L_i\phi}^{N_\alpha} + \delta\gamma_{L_i\phi}^{N_\alpha}). \tag{D.5}$$

The Boltzmann equation for the RH neutrino density is written as

$$
\begin{aligned}
\frac{dn_{N_\alpha}}{dt} + 3Hn_{N_\alpha} &= -\sum_{j=1}^{3}\left[\frac{n_{N_\alpha}}{n_{N_\alpha}^{\rm eq}}\left\{\gamma(N_\alpha \to L_j\phi) + \gamma(N_\alpha \to L_j^c\phi^\dagger)\right\}\right.\\
&\qquad\left. -\frac{n_{L_j}n_\phi}{n_{L_j}^{\rm eq}n_\phi^{\rm eq}}\gamma(L_j\phi \to N_\alpha) - \frac{n_{L_j^c}n_\phi}{n_{L_j^c}^{\rm eq}n_\phi^{\rm eq}}\gamma(L_j^c\phi^\dagger \to N_\alpha)\right]\\
&= -\sum_{j=1}^{3}\left[\frac{n_{N_\alpha}}{n_{N_\alpha}^{\rm eq}}\gamma_{L_j\phi}^{N_\alpha} - \frac{n_{L_j}}{2n_{\ell_j}^{\rm eq}}(\gamma_{L_j\phi}^{N_\alpha} - \delta\gamma_{L_j\phi}^{N_\alpha}) - \frac{n_{L_j^c}}{2n_{\ell_j}^{\rm eq}}(\gamma_{L_j\phi}^{N_\alpha} + \delta\gamma_{L_j\phi}^{N_\alpha})\right]\\
&= -\sum_{j=1}^{3}\left[\frac{n_{N_\alpha}}{n_{N_\alpha}^{\rm eq}}\gamma_{L_j\phi}^{N_\alpha} - \frac{n_{L_j} + n_{L_j^c}}{2n_{\ell_j}^{\rm eq}}\gamma_{L_j\phi}^{N_\alpha} + \frac{n_{L_j} - n_{L_j^c}}{2n_{\ell_j}^{\rm eq}}\delta\gamma_{L_j\phi}^{N_\alpha}\right]\\
&\approx -\left(\frac{n_{N_\alpha}}{n_{N_\alpha}^{\rm eq}} - 1\right)\gamma_{L\phi}^{N_\alpha} - \sum_{j=1}^{3}\frac{n_{\Delta L_j}}{2n_{\ell_j}^{\rm eq}}\delta\gamma_{L_j\phi}^{N_\alpha}.
\end{aligned}
\tag{D.6}
$$

In addition, the RIS-subtracted CP-conserving scattering terms are defined by

$$\gamma'^{L_i\phi}_{L_j^c\phi^\dagger} \equiv \gamma'(L_i\phi \to L_j^c\phi^\dagger) + \gamma'(L_i^c\phi^\dagger \to L_j\phi), \tag{D.7}$$

$$\gamma'^{L_i\phi}_{L_j\phi} \equiv \gamma'(L_i\phi \to L_j\phi) + \gamma'(L_i^c\phi^\dagger \to L_j^c\phi^\dagger). \tag{D.8}$$

The corresponding CP-violating terms can be written as [49]

$$\gamma'(L_i\phi \to L_j^c\phi^\dagger) - \gamma'(L_i^c\phi^\dagger \to L_j\phi) = \frac{1}{2}\sum_{\alpha=1}^{3}(B_{N_\alpha}^i\delta_{N_\alpha}^j + B_{N_\alpha}^j\delta_{N_\alpha}^i)\gamma_{L\phi}^{N_\alpha}, \tag{D.9}$$

$$\gamma'(L_i\phi \to L_j\phi) - \gamma'(L_i^c\phi^\dagger \to L_j^c\phi^\dagger) = -\frac{1}{2}\sum_{\alpha=1}^{3}(B_{N_\alpha}^i\delta_{N_\alpha}^j - B_{N_\alpha}^j\delta_{N_\alpha}^i)\gamma_{L\phi}^{N_\alpha} \tag{D.10}$$

where

$$\delta_{N_\alpha}^i = \frac{\Gamma(N_\alpha \to L_i\phi) - \Gamma(N_\alpha \to L_i^c\phi^\dagger)}{\sum_{j=1}^{3}\left[\Gamma(N_\alpha \to L_j\phi) + \Gamma(N_\alpha \to L_j^c\phi^\dagger)\right]}, \tag{D.11}$$

$$B_{N_\alpha}^i = \frac{\Gamma(N_\alpha \to L_i\phi) + \Gamma(N_\alpha \to L_i^c\phi^\dagger)}{\sum_{j=1}^{3}\left[\Gamma(N_\alpha \to L_j\phi) + \Gamma(N_\alpha \to L_j^c\phi^\dagger)\right]}. \tag{D.12}$$

We therefore have

$$\gamma'(L_i\phi \to L_j^c\phi^\dagger) = \frac{1}{2}\gamma'^{L_i\phi}_{L_j^c\phi^\dagger} + \frac{1}{4}\sum_{\alpha=1}^{3}(B^i_{N_\alpha}\delta^j_{N_\alpha} + B^j_{N_\alpha}\delta^i_{N_\alpha})\gamma^{N_\alpha}_{L\phi}, \tag{D.13}$$

$$\gamma'(L_i^c\phi^\dagger \to L_j\phi) = \frac{1}{2}\gamma'^{L_i\phi}_{L_j^c\phi^\dagger} - \frac{1}{4}\sum_{\alpha=1}^{3}(B^i_{N_\alpha}\delta^j_{N_\alpha} + B^j_{N_\alpha}\delta^i_{N_\alpha})\gamma^{N_\alpha}_{L\phi}, \tag{D.14}$$

$$\gamma'(L_i\phi \to L_j\phi) = \frac{1}{2}\gamma'^{L_i\phi}_{L_j\phi} - \frac{1}{4}\sum_{\alpha=1}^{3}(B^i_{N_\alpha}\delta^j_{N_\alpha} - B^j_{N_\alpha}\delta^i_{N_\alpha})\gamma^{N_\alpha}_{L\phi}, \tag{D.15}$$

$$\gamma'(L_i^c\phi^\dagger \to L_j^c\phi^\dagger) = \frac{1}{2}\gamma'^{L_i\phi}_{L_j\phi} + \frac{1}{4}\sum_{\alpha=1}^{3}(B^i_{N_\alpha}\delta^j_{N_\alpha} - B^j_{N_\alpha}\delta^i_{N_\alpha})\gamma^{N_\alpha}_{L\phi}. \tag{D.16}$$

The Boltzmann equations for the LH lepton doublet number density are written as

$$\begin{aligned}\frac{dn_{L_i}}{dt} + 3Hn_{L_i} = &-\sum_{\alpha=1}^{3}\frac{n_{L_i}n_\phi}{n^{\text{eq}}_{L_i}n^{\text{eq}}_\phi}\gamma(L_i\phi \to N_\alpha) - \sum_{j=1}^{3}\frac{n_{L_i}n_\phi}{n^{\text{eq}}_{L_i}n^{\text{eq}}_\phi}\gamma'(L_i\phi \to L_j^c\phi^\dagger)\\ &-\sum_{j=1}^{3}\frac{n_{L_i}n_\phi}{n^{\text{eq}}_{L_i}n^{\text{eq}}_\phi}\gamma'(L_i\phi \to L_j\phi) + \sum_{\alpha=1}^{3}\frac{n_{N_\alpha}}{n^{\text{eq}}_{N_\alpha}}\gamma(N_\alpha \to L_i\phi)\\ &+\sum_{j=1}^{3}\frac{n_{L_j^c}n_\phi}{n^{\text{eq}}_{L_j^c}n^{\text{eq}}_\phi}\gamma'(L_j^c\phi^\dagger \to L_i\phi) + \sum_{j=1}^{3}\frac{n_{L_j}n_\phi}{n^{\text{eq}}_{L_j}n^{\text{eq}}_\phi}\gamma'(L_j\phi \to L_i\phi) + \cdots,\end{aligned} \tag{D.17}$$

$$\begin{aligned}\frac{dn_{L_i^c}}{dt} + 3Hn_{L_i^c} = &-\sum_{\alpha=1}^{3}\frac{n_{L_i^c}n_\phi}{n^{\text{eq}}_{L_i^c}n^{\text{eq}}_\phi}\gamma(L_i^c\phi^\dagger \to N_\alpha) - \sum_{j=1}^{3}\frac{n_{L_i^c}n_\phi}{n^{\text{eq}}_{L_i^c}n^{\text{eq}}_\phi}\gamma'(L_i^c\phi^\dagger \to L_j\phi)\\ &-\sum_{j=1}^{3}\frac{n_{L_i^c}n_\phi}{n^{\text{eq}}_{L_i^c}n^{\text{eq}}_\phi}\gamma'(L_i^c\phi^\dagger \to L_j^c\phi^\dagger) + \sum_{\alpha=1}^{3}\frac{n_{N_\alpha}}{n^{\text{eq}}_{N_\alpha}}\gamma(N_\alpha \to L_i^c\phi)\\ &+\sum_{j=1}^{3}\frac{n_{L_j}n_\phi}{n^{\text{eq}}_{L_j}n^{\text{eq}}_\phi}\gamma'(L_j\phi \to L_i^c\phi^\dagger) + \sum_{j=1}^{3}\frac{n_{L_j^c}n_\phi}{n^{\text{eq}}_{L_j^c}n^{\text{eq}}_\phi}\gamma'(L_j^c\phi^\dagger \to L_i^c\phi^\dagger) + \cdots\end{aligned} \tag{D.18}$$

where we have explicitly written only the terms that would contribute to $\delta\gamma^{N_\alpha}_{L_i\phi}$. We can thus write

$$\begin{aligned}\frac{dn_{\Delta L_i}}{dt} + 3Hn_{\Delta L_i} = &-\sum_{\alpha=1}^{3}\frac{n_{L_i}n_\phi}{n^{\text{eq}}_{L_i}n^{\text{eq}}_\phi}\gamma(L_i\phi \to N_\alpha) - \sum_{j=1}^{3}\frac{n_{L_i}n_\phi}{n^{\text{eq}}_{L_i}n^{\text{eq}}_\phi}\gamma'(L_i\phi \to L_j^c\phi^\dagger)\\ &-\sum_{j=1}^{3}\frac{n_{L_i}n_\phi}{n^{\text{eq}}_{L_i}n^{\text{eq}}_\phi}\gamma'(L_i\phi \to L_j\phi) + \sum_{\alpha=1}^{3}\frac{n_{N_\alpha}}{n^{\text{eq}}_{N_\alpha}}\gamma(N_\alpha \to L_i\phi)\\ &+\sum_{j=1}^{3}\frac{n_{L_j^c}n_\phi}{n^{\text{eq}}_{L_j^c}n^{\text{eq}}_\phi}\gamma'(L_j^c\phi^\dagger \to L_i\phi) + \sum_{j=1}^{3}\frac{n_{L_j}n_\phi}{n^{\text{eq}}_{L_j}n^{\text{eq}}_\phi}\gamma'(L_j\phi \to L_i\phi),\end{aligned}$$

$$
\begin{aligned}
&+\sum_{\alpha=1}^{3}\frac{n_{L_i^c}n_\phi}{n_{L_i^c}^{\mathrm{eq}}n_\phi^{\mathrm{eq}}}\gamma(L_i^c\phi^\dagger\to N_\alpha)+\sum_{j=1}^{3}\frac{n_{L_i^c}n_\phi}{n_{L_i^c}^{\mathrm{eq}}n_\phi^{\mathrm{eq}}}\gamma'(L_i^c\phi^\dagger\to L_j\phi)\\
&\quad+\sum_{j=1}^{3}\frac{n_{L_i^c}n_\phi}{n_{L_i^c}^{\mathrm{eq}}n_\phi^{\mathrm{eq}}}\gamma'(L_i^c\phi^\dagger\to L_j^c\phi^\dagger)-\sum_{\alpha=1}^{3}\frac{n_{N_\alpha}}{n_{N_\alpha}^{\mathrm{eq}}}\gamma(N_\alpha\to L_i^c\phi)\\
&\quad-\sum_{j=1}^{3}\frac{n_{L_j}n_\phi}{n_{L_j}^{\mathrm{eq}}n_\phi^{\mathrm{eq}}}\gamma'(L_j\phi\to L_i^c\phi^\dagger)-\sum_{j=1}^{3}\frac{n_{L_j^c}n_\phi}{n_{L_j^c}^{\mathrm{eq}}n_\phi^{\mathrm{eq}}}\gamma'(L_j^c\phi^\dagger\to L_i^c\phi^\dagger)+\cdots\\
=&-\sum_{\alpha=1}^{3}\frac{n_{L_i}}{2n_{\ell_i}^{\mathrm{eq}}}(\gamma_{L_i\phi}^{N_\alpha}-\delta\gamma_{L_i\phi}^{N_\alpha})-\sum_{j=1}^{3}\frac{n_{L_i}}{2n_{\ell_i}^{\mathrm{eq}}}\left[\gamma'^{L_i\phi}_{L_j^c\phi^\dagger}+\frac{1}{2}\sum_{\alpha=1}^{3}(B^i_{N_\alpha}\delta^j_{N_\alpha}+B^j_{N_\alpha}\delta^i_{N_\alpha})\gamma^{N_\alpha}_{L\phi}\right]\\
&\quad-\sum_{j=1}^{3}\frac{n_{L_i}}{2n_{\ell_i}^{\mathrm{eq}}}\left[\gamma'^{L_i\phi}_{L_j\phi}-\frac{1}{2}\sum_{\alpha=1}^{3}(B^i_{N_\alpha}\delta^j_{N_\alpha}-B^j_{N_\alpha}\delta^i_{N_\alpha})\gamma^{N_\alpha}_{L\phi}\right]\\
&\quad+\sum_{\alpha=1}^{3}\frac{n_{N_\alpha}}{2n_{N_\alpha}^{\mathrm{eq}}}(\gamma_{L_i\phi}^{N_\alpha}+\delta\gamma_{L_i\phi}^{N_\alpha})+\sum_{j=1}^{3}\frac{n_{L_j^c}}{2n_{\ell_j}^{\mathrm{eq}}}\left[\gamma'^{L_i\phi}_{L_j^c\phi^\dagger}-\frac{1}{2}\sum_{\alpha=1}^{3}(B^i_{N_\alpha}\delta^j_{N_\alpha}+B^j_{N_\alpha}\delta^i_{N_\alpha})\gamma^{N_\alpha}_{L\phi}\right]\\
&\quad+\sum_{j=1}^{3}\frac{n_{L_j}}{2n_{\ell_j}^{\mathrm{eq}}}\left[\gamma'^{L_i\phi}_{L_j\phi}+\frac{1}{2}\sum_{\alpha=1}^{3}(B^i_{N_\alpha}\delta^j_{N_\alpha}-B^j_{N_\alpha}\delta^i_{N_\alpha})\gamma^{N_\alpha}_{L\phi}\right],\\
&+\sum_{\alpha=1}^{3}\frac{n_{L_i^c}}{2n_{\ell_i}^{\mathrm{eq}}}(\gamma_{L_i\phi}^{N_\alpha}+\delta\gamma_{L_i\phi}^{N_\alpha})+\sum_{j=1}^{3}\frac{n_{L_i^c}}{2n_{\ell_i}^{\mathrm{eq}}}\left[\gamma'^{L_i\phi}_{L_j^c\phi^\dagger}-\frac{1}{2}\sum_{\alpha=1}^{3}(B^i_{N_\alpha}\delta^j_{N_\alpha}+B^j_{N_\alpha}\delta^i_{N_\alpha})\gamma^{N_\alpha}_{L\phi}\right]\\
&\quad+\sum_{j=1}^{3}\frac{n_{L_i^c}}{2n_{\ell_i}^{\mathrm{eq}}}\left[\gamma'^{L_i\phi}_{L_j\phi}+\frac{1}{2}\sum_{\alpha=1}^{3}(B^i_{N_\alpha}\delta^j_{N_\alpha}-B^j_{N_\alpha}\delta^i_{N_\alpha})\gamma^{N_\alpha}_{L\phi}\right]\\
&\quad-\sum_{\alpha=1}^{3}\frac{n_{N_\alpha}}{2n_{N_\alpha}^{\mathrm{eq}}}(\gamma_{L_i\phi}^{N_\alpha}-\delta\gamma_{L_i\phi}^{N_\alpha})-\sum_{j=1}^{3}\frac{n_{L_j}}{2n_{\ell_j}^{\mathrm{eq}}}\left[\gamma'^{L_i\phi}_{L_j^c\phi^\dagger}+\frac{1}{2}\sum_{\alpha=1}^{3}(B^i_{N_\alpha}\delta^j_{N_\alpha}+B^j_{N_\alpha}\delta^i_{N_\alpha})\gamma^{N_\alpha}_{L\phi}\right]\\
&\quad-\sum_{j=1}^{3}\frac{n_{L_j^c}}{2n_{\ell_j}^{\mathrm{eq}}}\left[\gamma'^{L_i\phi}_{L_j\phi}-\frac{1}{2}\sum_{\alpha=1}^{3}(B^i_{N_\alpha}\delta^j_{N_\alpha}-B^j_{N_\alpha}\delta^i_{N_\alpha})\gamma^{N_\alpha}_{L\phi}\right]+\cdots\\
=&-\sum_{\alpha=1}^{3}\frac{n_{L_i}-n_{L_i^c}}{2n_{\ell_i}^{\mathrm{eq}}}\delta\gamma^{N_\alpha}_{L_i\phi}+\sum_{\alpha=1}^{3}\frac{n_{L_i}+n_{L_i^c}}{2n_{\ell_i}^{\mathrm{eq}}}\delta\gamma^{N_\alpha}_{L_i\phi}+\sum_{\alpha=1}^{3}\frac{n_{N_\alpha}}{n_{N_\alpha}^{\mathrm{eq}}}\delta\gamma^{N_\alpha}_{L_i\phi}\\
&-\sum_{j=1}^{3}\frac{n_{L_i}-n_{L_i^c}}{2n_{\ell_i}^{\mathrm{eq}}}\gamma'^{L_i\phi}_{L_j^c\phi^\dagger}-\sum_{j=1}^{3}\frac{n_{L_i}+n_{L_i^c}}{4n_{\ell_i}^{\mathrm{eq}}}\sum_{\alpha=1}^{3}(B^i_{N_\alpha}\delta^j_{N_\alpha}+B^j_{N_\alpha}\delta^i_{N_\alpha})\gamma^{N_\alpha}_{L\phi}\\
&\quad-\sum_{j=1}^{3}\frac{n_{L_i}-n_{L_i^c}}{2n_{\ell_i}^{\mathrm{eq}}}\gamma'^{L_i\phi}_{L_j\phi}+\sum_{j=1}^{3}\frac{n_{L_i}+n_{L_i^c}}{4n_{\ell_i}^{\mathrm{eq}}}\sum_{\alpha=1}^{3}(B^i_{N_\alpha}\delta^j_{N_\alpha}-B^j_{N_\alpha}\delta^i_{N_\alpha})\gamma^{N_\alpha}_{L\phi}\\
&\quad-\sum_{j=1}^{3}\frac{n_{L_j}-n_{L_j^c}}{2n_{\ell_j}^{\mathrm{eq}}}\gamma'^{L_i\phi}_{L_j^c\phi^\dagger}-\sum_{j=1}^{3}\frac{n_{L_j}+n_{L_j^c}}{4n_{\ell_j}^{\mathrm{eq}}}\sum_{\alpha=1}^{3}(B^i_{N_\alpha}\delta^j_{N_\alpha}+B^j_{N_\alpha}\delta^i_{N_\alpha})\gamma^{N_\alpha}_{L\phi}\\
&\quad+\sum_{j=1}^{3}\frac{n_{L_j}-n_{L_j^c}}{2n_{\ell_j}^{\mathrm{eq}}}\gamma'^{L_i\phi}_{L_j\phi}+\sum_{j=1}^{3}\frac{n_{L_j}+n_{L_j^c}}{4n_{\ell_j}^{\mathrm{eq}}}\sum_{\alpha=1}^{3}(B^i_{N_\alpha}\delta^j_{N_\alpha}-B^j_{N_\alpha}\delta^i_{N_\alpha})\gamma^{N_\alpha}_{L\phi}+\cdots\\
\approx&-\sum_{\alpha=1}^{3}\frac{n_{\Delta L_i}}{2n_{\ell_i}^{\mathrm{eq}}}\delta\gamma^{N_\alpha}_{L_i\phi}+\sum_{\alpha=1}^{3}\delta\gamma^{N_\alpha}_{L_i\phi}+\sum_{\alpha=1}^{3}\frac{n_{N_\alpha}}{n_{N_\alpha}^{\mathrm{eq}}}\delta\gamma^{N_\alpha}_{L_i\phi}\\
&-\sum_{j=1}^{3}\frac{n_{\Delta L_i}}{2n_{\ell_i}^{\mathrm{eq}}}\gamma'^{L_i\phi}_{L_j^c\phi^\dagger}-\frac{1}{2}\sum_{j=1}^{3}\sum_{\alpha=1}^{3}(B^i_{N_\alpha}\delta^j_{N_\alpha}+B^j_{N_\alpha}\delta^i_{N_\alpha})\gamma^{N_\alpha}_{L\phi}
\end{aligned}
$$

$$
\begin{aligned}
&\quad - \sum_{j=1}^{3} \frac{n_{\Delta L_i}}{2n_{\ell_i}^{\text{eq}}} \gamma'^{L_i\phi}_{L_j\phi} + \frac{1}{2} \sum_{j=1}^{3} \sum_{\alpha=1}^{3} (B^i_{N_\alpha} \delta^j_{N_\alpha} - B^j_{N_\alpha} \delta^i_{N_\alpha}) \gamma^{N_\alpha}_{L\phi} \\
&\quad - \sum_{j=1}^{3} \frac{n_{\Delta L_j}}{2n_{\ell_j}^{\text{eq}}} \gamma'^{L_i\phi}_{L_j^c\phi^\dagger} - \frac{1}{2} \sum_{j=1}^{3} \sum_{\alpha=1}^{3} (B^i_{N_\alpha} \delta^j_{N_\alpha} + B^j_{N_\alpha} \delta^i_{N_\alpha}) \gamma^{N_\alpha}_{L\phi} \\
&\quad + \sum_{j=1}^{3} \frac{n_{\Delta L_j}}{2n_{\ell_j}^{\text{eq}}} \gamma'^{L_i\phi}_{L_j\phi} + \frac{1}{2} \sum_{j=1}^{3} \sum_{\alpha=1}^{3} (B^i_{N_\alpha} \delta^j_{N_\alpha} - B^j_{N_\alpha} \delta^i_{N_\alpha}) \gamma^{N_\alpha}_{L\phi} + \cdots \\
&= - \sum_{\alpha=1}^{3} \frac{n_{\Delta L_i}}{2n_{\ell_i}^{\text{eq}}} \delta\gamma^{N_\alpha}_{L_i\phi} + \sum_{\alpha=1}^{3} \delta\gamma^{N_\alpha}_{L_i\phi} + \sum_{\alpha=1}^{3} \frac{n_{N_\alpha}}{n_{N_\alpha}^{\text{eq}}} \delta\gamma^{N_\alpha}_{L_i\phi} \\
&\quad - \sum_{j=1}^{3} \frac{n_{\Delta L_i}}{2n_{\ell_i}^{\text{eq}}} \gamma'^{L_i\phi}_{L_j^c\phi^\dagger} - \frac{1}{2} \sum_{\alpha=1}^{3} (B^i_{N_\alpha} \delta\gamma^{N_\alpha}_{L\phi} + \delta\gamma^{N_\alpha}_{L_i\phi}) \\
&\quad - \sum_{j=1}^{3} \frac{n_{\Delta L_i}}{2n_{\ell_i}^{\text{eq}}} \gamma'^{L_i\phi}_{L_j\phi} + \frac{1}{2} \sum_{\alpha=1}^{3} (B^i_{N_\alpha} \delta\gamma^{N_\alpha}_{L\phi} - \delta\gamma^{N_\alpha}_{L_i\phi}) \\
&\quad - \sum_{j=1}^{3} \frac{n_{\Delta L_j}}{2n_{\ell_j}^{\text{eq}}} \gamma'^{L_i\phi}_{L_j^c\phi^\dagger} - \frac{1}{2} \sum_{\alpha=1}^{3} (B^i_{N_\alpha} \delta\gamma^{N_\alpha}_{L\phi} + \delta\gamma^{N_\alpha}_{L_i\phi}) \\
&\quad + \sum_{j=1}^{3} \frac{n_{\Delta L_j}}{2n_{\ell_j}^{\text{eq}}} \gamma'^{L_i\phi}_{L_j\phi} + \frac{1}{2} \sum_{\alpha=1}^{3} (B^i_{N_\alpha} \delta\gamma^{N_\alpha}_{L\phi} - \delta\gamma^{N_\alpha}_{L\phi}) + \cdots \\
&= \sum_{\alpha=1}^{3} \left(\frac{n_{N_\alpha}}{n_{N_\alpha}^{\text{eq}}} - 1 \right) \delta\gamma^{N_\alpha}_{L_i\phi} - \sum_{\alpha=1}^{3} \frac{n_{\Delta L_i}}{2n_{\ell_i}^{\text{eq}}} \delta\gamma^{N_\alpha}_{L_i\phi} \\
&\quad - \sum_{j=1}^{3} \frac{n_{\Delta L_i}}{2n_{\ell_i}^{\text{eq}}} (\gamma'^{L_i\phi}_{L_j^c\phi^\dagger} + \gamma'^{L_i\phi}_{L_j\phi}) - \sum_{j=1}^{3} \frac{n_{\Delta L_j}}{2n_{\ell_j}^{\text{eq}}} (\gamma'^{L_i\phi}_{L_j^c\phi^\dagger} - \gamma'^{L_i\phi}_{L_j\phi}) + \cdots . \qquad \text{(D.19)}
\end{aligned}
$$

Now we simplify the left-hand side of the Boltzmann equation D.1. Since $T \propto a$ where a is the scale factor in the Friedmann-Robertson-Walker metric, we have

$$\frac{1}{T}\frac{dT}{dt} = \frac{\dot{a}}{a} = -H, \qquad \text{(D.20)}$$

and thus

$$\frac{dz}{dt} = -\frac{z}{T}\frac{dT}{dt} = zH. \qquad \text{(D.21)}$$

Hence,

$$\frac{dn_X}{dt} = \frac{dz}{dt}\frac{dn_X}{dz} = zH\frac{dn_X}{dz}, \qquad \text{(D.22)}$$

and for $\eta_X \equiv n_X/n_\gamma$, we have

$$\frac{d\eta_X}{dz} = \frac{1}{n_\gamma}\frac{dn_X}{dz} - \frac{n_X}{n_\gamma^2}\frac{dn_\gamma}{dz} = \frac{1}{n_\gamma}\left(\frac{dn_X}{dz} + \frac{3}{z}n_X\right) = \frac{1}{zHn_\gamma}\left(\frac{dn_X}{dt} + 3Hn_X\right)$$
$$= \frac{z}{H_N n_\gamma}\left(\frac{dn_X}{dt} + 3Hn_X\right). \tag{D.23}$$

Therefore, we can write

$$\frac{dn_X}{dt} + 3Hn_X = \frac{H_N n_\gamma}{z}\frac{d\eta_X}{dz}. \tag{D.24}$$

Reduced scattering cross section

The thermally averaged scattering rate is given by

$$\gamma(ab \to 12) = n_a^{\rm eq} n_b^{\rm eq} \langle \sigma(ab \to 12)|\mathbf{v}|\rangle$$
$$= \frac{T}{64\pi^4}\int_{s_{\rm min}}^{\infty} ds\ \sqrt{s}\ \hat{\sigma}(s)\ K_1\left(\frac{\sqrt{s}}{T}\right). \tag{D.25}$$

Here, $s_{\rm min} \equiv \max[(m_a+m_b)^2, (m_1+m_2)^2]$. The Källén function is defined by

$$\lambda(a,b,c) = a^2 + b^2 + c^2 - 2ab - 2bc - 2ca. \tag{D.26}$$

The scattering cross section is given by

$$\sigma(ab \to Y) = \frac{1}{4\sqrt{\lambda}}\int \left(\prod_{c\in Y}\frac{d^3p_c}{(2\pi)^3 2E_c}\right)(2\pi)^4\delta^{(4)}(p_a + p_b - Y)\sum_{\rm spin}|\mathcal{M}(ab \to Y)|^2. \tag{D.27}$$

In reference [48], the phase space factors are defined as follows:

$$d\pi_X = \prod_{b\in X} d\pi_b, \quad d\pi_b = g_b\frac{d^3p_b}{(2\pi)^3}\frac{1}{2E(\mathbf{p}_b)}. \tag{D.28}$$

Note that equation A7 in that paper has a typo in the expression of $d\pi_b$: $(2\pi)^2 \to (2\pi)^3$. The reduced cross section is defined as

$$\begin{aligned}\hat{\sigma}(s) &\equiv 8\pi\Phi_2(s)\int d\pi_Y(2\pi)^4\delta^4(p_a+p_b-p_Y)|\mathcal{A}(ab\to Y)|^2 \\ &= 8\pi\Phi_2(s)\int\left(\prod_{c\in Y} g_c\frac{d^3p_c}{(2\pi)^3}\frac{1}{2E(\mathbf{p}_c)}\right)(2\pi)^4\delta^4(p_a+p_b-p_Y)|\mathcal{A}(ab\to Y)|^2.\end{aligned} \tag{D.29}$$

Rewriting the multipicative degrees of freedom, g_a, g_b, and g_c as spin sums, we obtain

$$\begin{aligned}\hat{\sigma}(s) &= 8\pi\Phi_2(s)\int\left(\prod_{c\in Y}\frac{d^3p_c}{(2\pi)^3}\frac{1}{2E(\mathbf{p}_c)}\right)(2\pi)^4\delta^4(p_a+p_b-p_Y)\frac{1}{g_ag_b}\sum_{\text{spin}}|\mathcal{M}(ab\to Y)|^2 \\ &= 8\pi\Phi_2(s)\frac{4\sqrt{\lambda}}{g_ag_b}\sigma(ab\to Y)\end{aligned} \tag{D.30}$$

The two-body phase space factor $\Phi_2(s)$ is given by

$$\begin{aligned}\Phi_2(s) &\equiv \int d\pi_a d\pi_b(2\pi)^4\delta^4(p_a+p_b-p_Y) \\ &= \frac{g_ag_b}{8\pi s}\sqrt{[s-(m_a+m_b)^2][s-(m_a-m_b)^2]} \\ &= \frac{g_ag_b}{8\pi s}\sqrt{\lambda}.\end{aligned} \tag{D.31}$$

Therefore, we can write

$$\hat{\sigma}(s) = \frac{4}{s}\lambda\sigma(ab\to Y) \tag{D.32}$$

which is twice the expression below equation 2.8 in reference [48]. The differential cross section is given by

$$\frac{d\sigma}{dt} = \frac{1}{16\pi s\sqrt{\lambda}}\sum_{\text{spin}}|\mathcal{M}(ab\to Y)|^2. \tag{D.33}$$

In principle, the differential scattering cross section is given by

$$\frac{d\sigma}{dt} = \frac{1}{4\sqrt{\lambda}} \int \left(\prod_{c\in Y} \frac{d^3 p_c}{(2\pi)^3 2E_c} \right) (2\pi)^4 \delta^{(4)}(p_a + p_b - Y) \sum_{\text{spin}} |\mathcal{M}(ab \to Y)|^2 \delta(t - (p_a - p_1)^2). \tag{D.34}$$

According to reference [48], the differential reduced scattering cross section is given by

$$\begin{aligned} \frac{d\hat{\sigma}}{dt} &= \frac{g_a g_b g_c g_d}{8\pi s} |\mathcal{A}(ab \to Y)|^2 \\ &\to \frac{1}{8\pi s} \sum_{\text{spin}} |\mathcal{M}(ab \to Y)|^2. \end{aligned} \tag{D.35}$$

$N_\alpha \ell_{R\alpha} \to u^c_R d_R$

The Feynman amplitude for this process is given by

$$\begin{aligned} i\mathcal{M} &= \left(i\frac{g_R}{\sqrt{2}} \right)^2 \overline{v_N}(p_N)\gamma^\mu \mathsf{R} u_\ell(p_\ell) \frac{-i}{(p_N + p_\ell)^2 - m^2_{W_R} + i m_{W_R}\Gamma_{W_R}} \overline{u_d}(p_d)\gamma_\mu \mathsf{R} v_u(p_u) \\ &= i\frac{g_R^2}{2} \overline{v_N}(p_N)\gamma^\mu \mathsf{R} u_\ell(p_\ell) \frac{1}{(p_N + p_\ell)^2 - m^2_{W_R} + i m_{W_R}\Gamma_{W_R}} \overline{u_d}(p_d)\gamma_\mu \mathsf{R} v_u(p_u), \end{aligned} \tag{D.36}$$

and thus

$$\begin{aligned} -i\mathcal{M}^\dagger &= -i\frac{g_R^2}{2} v_u^\dagger(p_u)\mathsf{R}\gamma_\nu^\dagger \gamma^0 u_d(p_d) \frac{1}{(p_N + p_\ell)^2 - m^2_{W_R} - i m_{W_R}\Gamma_{W_R}} u_\ell^\dagger(p_\ell)\mathsf{R}\gamma^{\nu\dagger}\gamma^0 v_N(p_N) \\ &= -i\frac{g_R^2}{2} \overline{v_u}(p_u)\gamma_\nu \mathsf{R} u_d(p_d) \frac{1}{(p_N + p_\ell)^2 - m^2_{W_R} - i m_{W_R}\Gamma_{W_R}} \overline{u_\ell}(p_\ell)\gamma^\nu \mathsf{R} v_N(p_N) \end{aligned} \tag{D.37}$$

where we have used $u^c_s = v_{-s}$. We therefore have

$$\sum_{\text{spin}} |\mathcal{M}|^2 = \frac{g_R^4}{4} \frac{1}{[(p_N + p_\ell)^2 - m^2_{W_R}]^2 + m^2_{W_R}\Gamma^2_{W_R}} \mathrm{tr}[\gamma^\nu \mathsf{R} v_N \overline{v_N} \gamma^\mu \mathsf{R} u_\ell \overline{u_\ell}] \mathrm{tr}[\gamma_\nu \mathsf{R} u_d \overline{u_d} \gamma_\mu \mathsf{R} v_u \overline{v_u}]. \tag{D.38}$$

The trace part is calculated as follows:

$$
\begin{aligned}
&\mathrm{tr}[\gamma^\nu \mathsf{R} v_N \overline{v_N} \gamma^\mu \mathsf{R} u_\ell \overline{u_\ell}]\mathrm{tr}[\gamma_\nu \mathsf{R} u_d \overline{u_d} \gamma_\mu \mathsf{R} v_u \overline{v_u}] \\
&\quad = \mathrm{tr}[\gamma^\nu \mathsf{R}(\not{p}_N + m_N)\gamma^\mu \mathsf{R}\not{p}_\ell]\mathrm{tr}[\gamma_\nu \mathsf{R}\not{p}_d \gamma_\mu \mathsf{R}\not{p}_u] = \mathrm{tr}[\gamma^\nu \not{p}_N \gamma^\mu \not{p}_\ell \mathsf{L}]\mathrm{tr}[\gamma_\nu \not{p}_d \gamma_\mu \not{p}_u \mathsf{L}] \\
&\quad = \mathrm{tr}[\gamma^\nu \gamma^\rho \gamma^\mu \gamma^\sigma \mathsf{L}]\mathrm{tr}[\gamma_\nu \gamma_\alpha \gamma_\mu \gamma_\beta \mathsf{L}] p_{N\rho} p_{e\sigma} {p_d}^\alpha {p_u}^\beta \\
&\quad = \frac{1}{4}\left(\mathrm{tr}[\gamma^\nu \gamma^\rho \gamma^\mu \gamma^\sigma] - \mathrm{tr}[\gamma^\nu \gamma^\rho \gamma^\mu \gamma^\sigma \gamma^5]\right)\left(\mathrm{tr}[\gamma_\nu \gamma_\alpha \gamma_\mu \gamma_\beta] - \mathrm{tr}[\gamma_\nu \gamma_\alpha \gamma_\mu \gamma_\beta \gamma^5]\right) p_{N\rho} p_{\ell\sigma} {p_d}^\alpha {p_u}^\beta \\
&\quad = 4(g^{\nu\rho} g^{\mu\sigma} - g^{\nu\mu} g^{\rho\sigma} + g^{\nu\sigma} g^{\rho\mu} + i\epsilon^{\nu\rho\mu\sigma})(g_{\nu\alpha} g_{\mu\beta} - g_{\nu\mu} g_{\alpha\beta} + g_{\nu\beta} g_{\alpha\mu} + i\epsilon_{\nu\alpha\mu\beta}) p_{N\rho} p_{\ell\sigma} {p_d}^\alpha {p_u}^\beta \\
&\quad = 4[{p_N}^\nu {p_\ell}^\mu - g^{\nu\mu}(p_N \cdot p_\ell) + {p_\ell}^\nu {p_N}^\mu + i\epsilon^{\nu\rho\mu\sigma} p_{N\rho} p_{\ell\sigma}][p_{d\nu} p_{u\mu} - g_{\nu\mu}(p_d \cdot p_u) + p_{u\nu} p_{d\mu} + i\epsilon_{\nu\alpha\mu\beta} {p_d}^\alpha {p_u}^\beta] \\
&\quad = 4[(p_N \cdot p_d)(p_\ell \cdot p_u) - (p_d \cdot p_u)(p_N \cdot p_\ell) + (p_\ell \cdot p_d)(p_N \cdot p_u) + i\epsilon^{\nu\rho\mu\sigma} p_{N\rho} p_{\ell\sigma} p_{d\nu} p_{u\mu} \\
&\qquad - (p_N \cdot p_\ell)(p_d \cdot p_u) + 4(p_N \cdot p_\ell)(p_d \cdot p_u) - (p_\ell \cdot p_N)(p_d \cdot p_u) \\
&\qquad + (p_N \cdot p_u)(p_\ell \cdot p_d) - (p_u \cdot p_d)(p_N \cdot p_\ell) + (p_\ell \cdot p_u)(p_N \cdot p_d) + i\epsilon^{\nu\rho\mu\sigma} p_{N\rho} p_{\ell\sigma} p_{u\nu} p_{d\mu} \\
&\qquad + i\epsilon_{\nu\alpha\mu\beta} {p_N}^\nu {p_\ell}^\mu {p_d}^\alpha {p_u}^\beta + i\epsilon_{\nu\alpha\mu\beta} {p_\ell}^\nu {p_N}^\mu {p_d}^\alpha {p_u}^\beta - \epsilon^{\nu\rho\mu\sigma} \epsilon_{\nu\alpha\mu\beta} p_{N\rho} p_{e\sigma} {p_d}^\alpha {p_u}^\beta] \\
&\quad = 4[(p_N \cdot p_d)(p_\ell \cdot p_u) - (p_d \cdot p_u)(p_N \cdot p_\ell) + (p_\ell \cdot p_d)(p_N \cdot p_u) + 2(p_N \cdot p_\ell)(p_d \cdot p_u) \\
&\qquad + (p_N \cdot p_u)(p_\ell \cdot p_d) - (p_d \cdot p_u)(p_N \cdot p_\ell) + (p_\ell \cdot p_u)(p_N \cdot p_d) + 2(\delta^\rho{}_\alpha \delta^\sigma{}_\beta - \delta^\rho{}_\beta \delta^\sigma{}_\alpha) p_{N\rho} p_{e\sigma} {p_d}^\alpha {p_u}^\beta] \\
&\quad = 4[2(p_N \cdot p_d)(p_\ell \cdot p_u) + 2(p_\ell \cdot p_d)(p_N \cdot p_u) + 2(p_N \cdot p_d)(p_\ell \cdot p_u) - 2(p_N \cdot p_u)(p_\ell \cdot p_d)] \\
&\quad = 16(p_N \cdot p_d)(p_\ell \cdot p_u).
\end{aligned}
\tag{D.39}
$$

Since we have

$$
\begin{aligned}
s &= (p_N + p_\ell)^2 = (p_d + p_u)^2, \\
t &= (p_N - p_u)^2 = (p_d - p_\ell)^2, \\
u &= (p_N - p_d)^2 = (p_u - p_\ell)^2,
\end{aligned}
\tag{D.40}
$$

we can write

$$
\begin{aligned}
2(p_N \cdot p_\ell) &= -(m_N^2 - s), \quad 2(p_d \cdot p_u) = s, \\
2(p_N \cdot p_u) &= m_N^2 - t, \quad 2(p_d \cdot p_\ell) = -t, \\
2(p_N \cdot p_d) &= m_N^2 - u, \quad 2(p_u \cdot p_\ell) = -u.
\end{aligned} \tag{D.41}
$$

Hence, we have

$$
\begin{aligned}
&\mathrm{tr}[\gamma^\nu \mathsf{R} v_N \overline{v_N} \gamma^\mu \mathsf{R} u_\ell \overline{u_\ell}]\mathrm{tr}[\gamma_\nu \mathsf{R} u_d \overline{u_d} \gamma_\mu \mathsf{R} v_u \overline{v_u}] = 4(m_N^2 - u)(-u) = 4(s+t)(s+t-m_N^2) \\
&= 4(s^2 + 2st + t^2 - m_N^2 s - m_N^2 t) = 4[t^2 - (m_N^2 - 2s)t - s(m_N^2 - s)],
\end{aligned} \tag{D.42}
$$

and thus

$$
\sum_{\text{spin}} |\mathcal{M}|^2 = g_R^4 \frac{t^2 - (m_N^2 - 2s)t - s(m_N^2 - s)}{(s - m_{W_R}^2)^2 + m_{W_R}^2 \Gamma_{W_R}^2}. \tag{D.43}
$$

Now the differential reduced scattering cross section is written as

$$
\frac{d\hat{\sigma}}{dt} = \frac{9}{8\pi s} \sum_{\text{spin}} |\mathcal{M}|^2 = \frac{9 g_R^4}{8\pi s} \frac{t^2 - (m_N^2 - 2s)t - s(m_N^2 - s)}{(s - m_{W_R}^2)^2 + m_{W_R}^2 \Gamma_{W_R}^2} \tag{D.44}
$$

where the multiplicative factor 9 is from the numbers of quark flavours and color factors. Note that this is the result for one flavour of RH neutrino. The Mandelstam variable t is written as

$$
\begin{aligned}
t &= (p_N - p_u)^2 = E_N^2 - 2E_N E_u + E_u^2 - |\mathbf{p}_N|^2 - |\mathbf{p}_u|^2 + 2\mathbf{p}_N \cdot \mathbf{p}_u \\
&= m_N^2 - 2(E_N E_u - |\mathbf{p}_N||\mathbf{p}_u| \cos\theta).
\end{aligned} \tag{D.45}
$$

In the center-of-momentum (CM) frame, we have

$$
|\mathbf{p}_N| = \frac{1}{2\sqrt{s}} \sqrt{s^2 - 2m_N^2 s + m_N^4} = \frac{s - m_N^2}{2\sqrt{s}}, \qquad |\mathbf{p}_u| = \frac{\sqrt{s}}{2}, \tag{D.46}
$$

and

$$E_N = \sqrt{|\mathbf{p}_N|^2 + m_N^2} = \frac{s+m_N^2}{2\sqrt{s}}, \qquad E_u = \frac{\sqrt{s}}{2}. \tag{D.47}$$

Hence, we have

$$t = m_N^2 - \frac{1}{2}[s + m_N^2 - (s - m_N^2)\cos\theta], \tag{D.48}$$

and thus

$$t_{\min} = m_N^2 - s, \qquad t_{\max} = 0. \tag{D.49}$$

Therefore, the reduced cross section is

$$\begin{aligned}\hat{\sigma}(s) &= \frac{9g_R^4}{8\pi s[(s-m_{W_R}^2)^2 + m_{W_R}^2\Gamma_{W_R}^2]}\int_{m_N^2-s}^{0} dt\ [t^2 - (m_N^2 - 2s)t - s(m_N^2 - s)] \\ &= \frac{9g_R^4}{8\pi s[(s-m_{W_R}^2)^2 + m_{W_R}^2\Gamma_{W_R}^2]}\frac{1}{6}(m_N^2 - s)^2(m_N^2 + 2s),\end{aligned} \tag{D.50}$$

which is the same as equation 2.15 in [46]. Hence, the CP-conserving reduced cross section is

$$\hat{\sigma}_{u^c d}^{N_\alpha \ell_\alpha}(s) = \frac{9g_R^4}{4\pi s[(s-m_{W_R}^2)^2 + m_{W_R}^2\Gamma_{W_R}^2]}\frac{1}{6}(m_N^2 - s)^2(m_N^2 + 2s). \tag{D.51}$$

$N_\alpha u_R^c \to \ell_{R\alpha} d_R^c$

The Feynman amplitude is written as

$$i\mathcal{M} = i\frac{g_R^2}{2}\overline{u_\ell}(p_\ell)\gamma^\mu \mathsf{R} u_N(p_N)\frac{1}{(p_N - p_\ell)^2 - m_{W_R}^2}\overline{v_u}(p_u)\gamma_\mu \mathsf{R} v_d(p_d), \tag{D.52}$$

and its Hermitian conjugate as

$$\begin{aligned}-i\mathcal{M}^\dagger &= -i\frac{g_R^2}{2}v_d^\dagger(p_d)\mathsf{R}\gamma_\nu^\dagger\gamma^0 v_u(p_u)\frac{1}{(p_N - p_\ell)^2 - m_{W_R}^2}u_N^\dagger(p_N)\mathsf{R}\gamma^{\nu\dagger}\gamma^0 u_\ell(p_\ell) \\ &= -i\frac{g_R^2}{2}\overline{v_d}(p_d)\gamma_\nu \mathsf{R} v_u(p_u)\frac{1}{(p_N - p_\ell)^2 - m_{W_R}^2}\overline{u_N}(p_N)\gamma^\nu \mathsf{R} u_\ell(p_\ell).\end{aligned} \tag{D.53}$$

We thus have

$$\sum_{\text{spin}} |\mathcal{M}|^2 = \frac{g_R^4}{4} \frac{1}{[(p_N - p_\ell)^2 - m_{W_R}^2]^2} \mathrm{tr}[\gamma^\nu \mathsf{R} u_\ell \overline{u_\ell} \gamma^\mu \mathsf{R} u_N \overline{u_N}] \mathrm{tr}[\gamma_\nu \mathsf{R} v_u \overline{v_u} \gamma_\mu \mathsf{R} v_d \overline{v_d}], \tag{D.54}$$

where

$$\begin{aligned}
&\mathrm{tr}[\gamma^\nu \mathsf{R} u_\ell \overline{u_\ell} \gamma^\mu \mathsf{R} u_N \overline{u_N}] \mathrm{tr}[\gamma_\nu \mathsf{R} v_u \overline{v_u} \gamma_\mu \mathsf{R} v_d \overline{v_d}] \\
&\quad = \mathrm{tr}[\gamma^\nu \mathsf{R} \not{p}_e \gamma^\mu \mathsf{R} (\not{p}_N - m_N)] \mathrm{tr}[\gamma_\nu \mathsf{R} \not{p}_u \gamma_\mu \mathsf{R} \not{p}_d] = \mathrm{tr}[\gamma^\nu \not{p}_e \gamma^\mu \not{p}_N \mathsf{L}] \mathrm{tr}[\gamma_\nu \not{p}_u \gamma_\mu \not{p}_d \mathsf{L}] \\
&\quad = 16 (p_N \cdot p_d)(p_\ell \cdot p_u).
\end{aligned} \tag{D.55}$$

Since we have

$$\begin{aligned}
s &= (p_N + p_u)^2 = (p_\ell + p_d)^2, \\
t &= (p_N - p_\ell)^2 = (p_d - p_u)^2, \\
u &= (p_N - p_d)^2 = (p_\ell - p_u)^2,
\end{aligned} \tag{D.56}$$

we can write

$$\begin{aligned}
2(p_N \cdot p_\ell) &= m_N^2 - t, \quad 2(p_d \cdot p_u) = -t, \\
2(p_N \cdot p_u) &= -(m_N^2 - s), \quad 2(p_\ell \cdot p_d) = s, \\
2(p_N \cdot p_d) &= m_N^2 - u, \quad 2(p_\ell \cdot p_u) = -u.
\end{aligned} \tag{D.57}$$

Therefore, we have

$$\begin{aligned}
\mathrm{tr}[\gamma^\nu \mathsf{R} u_\ell \overline{u_\ell} \gamma^\mu \mathsf{R} u_N \overline{u_N}] \mathrm{tr}[\gamma_\nu \mathsf{R} v_u \overline{v_u} \gamma_\mu \mathsf{R} v_d \overline{v_d}] &= 4(m_N^2 - u)(-u) \\
&= 4(s+t)(s+t-m_N^2).
\end{aligned} \tag{D.58}$$

Hence, we have

$$\sum_{\text{spin}} |\mathcal{M}|^2 = g_R^4 \frac{(s+t)(s+t-m_N^2)}{(t-m_{W_R}^2)^2}, \tag{D.59}$$

and the differential reduced scattering cross section is given by

$$\frac{d\hat{\sigma}}{dt} = \frac{9}{8\pi s} \sum_{\text{spin}} |\mathcal{M}|^2 = \frac{9g_R^4}{8\pi s} \frac{(s+t)(s+t-m_N^2)}{(t-m_{W_R}^2)^2} \tag{D.60}$$

where the multiplicative factor 9 is from the numbers of quark flavours and color factors. We have

$$\begin{aligned} t = (p_N - p_\ell)^2 &= E_N^2 - 2E_N E_e + E_e^2 - |\mathbf{p}_N|^2 - |\mathbf{p}_e|^2 + 2\mathbf{p}_N \cdot \mathbf{p}_e \\ &= m_N^2 - 2(E_N E_e - |\mathbf{p}_N||\mathbf{p}_e| \cos\theta). \end{aligned} \tag{D.61}$$

In the CM frame, we can write

$$|\mathbf{p}_N| = \frac{1}{2\sqrt{s}} \sqrt{s^2 - 2m_N^2 s + m_N^4} = \frac{s - m_N^2}{2\sqrt{s}}, \qquad |\mathbf{p}_e| = \frac{\sqrt{s}}{2}, \tag{D.62}$$

and

$$E_N = \sqrt{|\mathbf{p}_N|^2 + m_N^2} = \frac{s + m_N^2}{2\sqrt{s}}, \qquad E_e = \frac{\sqrt{s}}{2}. \tag{D.63}$$

Hence, we obtain

$$t = m_N^2 - \frac{1}{2}[s + m_N^2 - (s - m_N^2)\cos\theta], \tag{D.64}$$

and thus

$$t_{\min} = m_N^2 - s, \qquad t_{\max} = 0. \tag{D.65}$$

Therefore, the reduced cross section is

$$\hat{\sigma}(s) = \frac{9g_R^4}{8\pi s} \int_{m_N^2 - s}^{0} dt \, \frac{(s+t)(s+t-m_N^2)}{(t-m_{W_R}^2)^2}, \tag{D.66}$$

which is the same as equation 2.16 in [46]. Hence, the CP-conserving reduced cross section is

$$\hat{\sigma}_{\ell_\alpha d^c}^{N_\alpha u^c}(s) = \frac{9g_R^4}{4\pi s}\int_{m_N^2-s}^{0} dt\, \frac{(s+t)(s+t-m_N^2)}{(t-m_{W_R}^2)^2}. \tag{D.67}$$

$N_\alpha d_R \to \ell_{R\alpha} u_R$

The Feynman amplitude is

$$i\mathcal{M} = i\frac{g_R^2}{2}\overline{u_\ell}(p_\ell)\gamma^\mu \mathsf{R} u_N(p_N)\frac{1}{(p_N-p_\ell)^2-m_{W_R}^2}\overline{u_u}(p_u)\gamma_\mu \mathsf{R} u_d(p_d), \tag{D.68}$$

and

$$-i\mathcal{M}^\dagger = -i\frac{g_R^2}{2}\overline{u_d}(p_d)\gamma_\nu \mathsf{R} u_u(p_u)\frac{1}{(p_N-p_\ell)^2-m_{W_R}^2}\overline{u_N}(p_N)\gamma^\nu \mathsf{R} u_\ell(p_\ell). \tag{D.69}$$

We thus have

$$\sum_{\text{spin}}|\mathcal{M}|^2 = \frac{g_R^4}{4}\frac{1}{[(p_N-p_\ell)^2-m_{W_R}^2]^2}\text{tr}[\gamma^\nu \mathsf{R} u_\ell\overline{u_\ell}\gamma^\mu \mathsf{R} u_N\overline{u_N}]\text{tr}[\gamma_\nu \mathsf{R} u_u\overline{u_u}\gamma_\mu \mathsf{R} u_d\overline{u_d}], \tag{D.70}$$

where

$$\begin{aligned}
&\text{tr}[\gamma^\nu \mathsf{R} u_\ell\overline{u_\ell}\gamma^\mu \mathsf{R} u_N\overline{u_N}]\text{tr}[\gamma_\nu \mathsf{R} u_u\overline{u_u}\gamma_\mu \mathsf{R} u_d\overline{u_d}]\\
&\quad = \text{tr}[\gamma^\nu \mathsf{R}\not{p}_e\gamma^\mu \mathsf{R}(\not{p}_N - m_N)]\text{tr}[\gamma_\nu \mathsf{R}\not{p}_u\gamma_\mu \mathsf{R}\not{p}_d] = \text{tr}[\gamma^\nu\not{p}_e\gamma^\mu\not{p}_N \mathsf{L}]\text{tr}[\gamma_\nu\not{p}_u\gamma_\mu\not{p}_d \mathsf{L}]\\
&\quad = 16(p_N\cdot p_d)(p_\ell\cdot p_u).
\end{aligned} \tag{D.71}$$

Since we have

$$\begin{aligned}
s &= (p_N+p_d)^2 = (p_\ell+p_u)^2,\\
t &= (p_N-p_\ell)^2 = (p_u-p_d)^2,\\
u &= (p_N-p_u)^2 = (p_\ell-p_d)^2,
\end{aligned} \tag{D.72}$$

we can write

$$
\begin{aligned}
2(p_N \cdot p_\ell) &= m_N^2 - t, \quad 2(p_d \cdot p_u) = -t, \\
2(p_N \cdot p_u) &= m_N^2 - u, \quad 2(p_\ell \cdot p_d) = -u, \\
2(p_N \cdot p_d) &= -(m_N^2 - s), \quad 2(p_\ell \cdot p_u) = s. \qquad \text{(D.73)}
\end{aligned}
$$

We therefore have

$$
\mathrm{tr}[\gamma^\nu \mathsf{R} u_\ell \overline{u_\ell} \gamma^\mu \mathsf{R} v_N \overline{v_N}]\mathrm{tr}[\gamma_\nu \mathsf{R} u_d \overline{u_d} \gamma_\mu \mathsf{R} v_u \overline{v_u}] = -4s(m_N^2 - s). \qquad \text{(D.74)}
$$

Hence, we have

$$
\sum_{\text{spin}} |\mathcal{M}|^2 = -g_R^4 \frac{s(m_N^2 - s)}{(t - m_{W_R}^2)^2}, \qquad \text{(D.75)}
$$

and the differential reduced scattering cross section is given by

$$
\frac{d\hat{\sigma}}{dt} = \frac{9}{8\pi s} \sum_{\text{spin}} |\mathcal{M}|^2 = -\frac{9g_R^4}{8\pi} \frac{m_N^2 - s}{(t - m_{W_R}^2)^2} \qquad \text{(D.76)}
$$

where the multiplicative factor 9 is from the numbers of quark flavours and color factors. As in the previous case, we have

$$
t_{\min} = m_N^2 - s, \qquad t_{\max} = 0. \qquad \text{(D.77)}
$$

Therefore, the reduced cross section is

$$
\begin{aligned}
\hat{\sigma}(s) &= -\frac{9g_R^4}{8\pi} \int_{m_N^2 - s}^{0} dt \, \frac{m_N^2 - s}{(t - m_{W_R}^2)^2} = \frac{9g_R^4}{8\pi}(m_N^2 - s) \left[\frac{1}{t - m_{W_R}^2} \right]_{m_N^2 - s}^{0} \\
&= \frac{9g_R^4}{8\pi}(m_N^2 - s) \left[-\frac{1}{m_{W_R}^2} - \frac{1}{m_N^2 - s - m_{W_R}^2} \right] \\
&= \frac{9g_R^4}{8\pi}(m_N^2 - s) \left[\frac{1}{s + m_{W_R}^2 - m_N^2} - \frac{1}{m_{W_R}^2} \right] \\
&= \frac{9g_R^4}{8\pi} \frac{(m_N^2 - s)^2}{m_{W_R}^2 (s + m_{W_R}^2 - m_N^2)}, \qquad \text{(D.78)}
\end{aligned}
$$

which is the same as equation 2.17 in equation [46]. Hence, the CP-conserving reduced cross section is

$$\hat{\sigma}_{\ell_\alpha u}^{N_\alpha d}(s) = \frac{9g_R^4}{4\pi}\frac{(m_N^2 - s)^2}{m_{W_R}^2(s + m_{W_R}^2 - m_N^2)}. \tag{D.79}$$

Appendix E: Lepton asymmetry

Exact solution

We can also derive the expression 4.41 by directly solving the differential equation 4.39. This equation is in the form

$$\frac{dy}{dx} = Q(x) - P(x)y \tag{E.1}$$

where

$$x \equiv z, \quad y \equiv \eta_{\Delta L_i}, \quad P(x) \equiv \frac{2}{3}W_i(x), \quad Q(x) \equiv \sum_{\alpha=1}^{3} \delta^i_{N_\alpha} \frac{d\eta_{N_\alpha}}{dz} \frac{\widetilde{D}_\alpha(x)}{D_\alpha(x) + S_\alpha(x)}. \tag{E.2}$$

The differential equation E.1 can be rewritten as

$$0 = \big[Q(x) - P(x)y\big]dx - dy. \tag{E.3}$$

In order to solve this differential equation, we need an integrating factor $f(x, y)$:

$$\begin{aligned} d\varphi &= f(x,y)\big[Q(x) - P(x)y\big]dx - f(x,y)dy \\ &= \frac{\partial\varphi}{\partial x}dx + \frac{\partial\varphi}{\partial y}dy \\ &= 0. \end{aligned} \tag{E.4}$$

Then,

$$\frac{\partial^2\varphi}{\partial y\partial x} = \frac{\partial}{\partial y}\Big\{f(x,y)\big[Q(x) - P(x)y\big]\Big\} = \frac{\partial f(x,y)}{\partial y}\big[Q(x) - P(x)y\big] - f(x,y)P(x)$$

$$\frac{\partial^2\varphi}{\partial x\partial y} = \frac{\partial}{\partial x}\big[-f(x,y)\big] = -\frac{\partial f(x,y)}{\partial x}, \tag{E.5}$$

Thus, we need

$$\frac{\partial f(x,y)}{\partial y}\big[Q(x) - P(x)y\big] - f(x,y)P(x) = -\frac{\partial f(x,y)}{\partial x} \tag{E.6}$$

to have an exact differential $d\varphi$. Now we assume $f(x,y) = f(x)$. Then, the condition E.6 is written as

$$f(x)P(x) = \frac{df(x)}{dx}, \tag{E.7}$$

thus we can write

$$P(x)dx = \frac{df(x)}{f(x)}. \tag{E.8}$$

The solution of this equation is given by

$$\int_{x_0}^{x} P(x')dx' = \ln f(x) - \ln f(x_0), \tag{E.9}$$

thus

$$f(x) = f(x_0)\exp\left[\int_{x_0}^{x} P(x')dx'\right]. \tag{E.10}$$

The differential $d\varphi$ is given by

$$d\varphi = f(x)[Q(x) - P(x)y]dx - f(x)dy = 0. \tag{E.11}$$

We choose the integration path $(x_0, y_0) \xrightarrow[x=x_0]{} (x_0, y) \xrightarrow[y=y_0]{} (x, y)$. Then, we obtain

$$
\begin{aligned}
\varphi(x,y) &= C \\
&= \int_{x_0}^{x} f(x')[Q(x') - P(x')y]dx' - f(x_0)\int_{y_0}^{y} dy' \\
&= \int_{x_0}^{x} f(x')[Q(x') - P(x')y]dx' - f(x_0)(y - y_0) \\
&= \int_{x_0}^{x} f(x')Q(x')dx' - \left[\int_{x_0}^{x} f(x')P(x')dx' + f(x_0)\right] y + f(x_0)y_0
\end{aligned}
\tag{E.12}
$$

where $C = \varphi(x_0, y_0) = 0$. Hence, we can write

$$
\begin{aligned}
y(x) &= \frac{f(x_0)y_0 + \int_{x_0}^{x} f(x')Q(x')dx'}{f(x_0) + \int_{x_0}^{x} f(x')P(x')dx'} = \frac{y_0 + \int_{x_0}^{x} \exp\left[\int_{x_0}^{x'} P(x'')dx''\right] Q(x')dx'}{1 + \int_{x_0}^{x} \exp\left[\int_{x_0}^{x'} P(x'')dx''\right] P(x')dx'} \\
&= \frac{y_0 + \int_{x_0}^{x} \exp\left[\int_{x_0}^{x'} P(x'')dx''\right] Q(x')dx'}{1 + \left\{\exp\left[\int_{x_0}^{x} P(x'')dx''\right] - 1\right\}} \\
&= y_0 \exp\left[-\int_{x_0}^{x} P(x'')dx''\right] + \int_{x_0}^{x} \exp\left[-\int_{x'}^{x} P(x'')dx''\right] Q(x')dx'.
\end{aligned}
\tag{E.13}
$$

At $x = x_c$, we have

$$
y(x_c) = y_0 \exp\left[-\int_{x_0}^{x_c} P(x'')dx''\right] + \int_{x_0}^{x_c} \exp\left[-\int_{x'}^{x_c} P(x'')dx''\right] Q(x')dx'. \tag{E.14}
$$

Using the definitions of variables E.2, we can rewrite this as

$$
\begin{aligned}
\eta_{\Delta L_i}(z_c) = \eta_{\Delta L_i}(z_0) &\exp\left[-\frac{2}{3}\int_{z_0}^{z_c} dz'' W_i(z'')\right] \\
&+ \frac{1}{2\zeta(3)}\int_{z_0}^{z_c} dz' z'^2 K_1(z') \sum_{\alpha} \delta^i_{N_\alpha} \frac{\widetilde{D}_\alpha(z')}{D_\alpha(z') + S_\alpha(z')} \exp\left[-\frac{2}{3}\int_{z'}^{z_c} dz'' W_i(z'')\right] \\
= \eta_{\Delta L_i}(z_0) &\exp\left[-\frac{2}{3}\int_{z_0}^{z_c} dz'' W_i(z'')\right] - \sum_{\alpha} \delta^i_{N_\alpha} \kappa^l_{N_\alpha}(z_c)
\end{aligned}
\tag{E.15}
$$

where

$$
\kappa^l_{N_\alpha}(z) \equiv \int_{z_0}^{z_c} dz' \frac{d\eta_{N_\alpha}}{dz'} \frac{\widetilde{D}_\alpha(z')}{D_\alpha(z') + S_\alpha(z')} \exp\left[-\frac{2}{3}\int_{z'}^{z_c} dz'' W_i(z'')\right] \tag{E.16}
$$

is the efficiency factor. Assuming the first term in equation E.15 is much smaller than the second, (i.e. the initial lepton asymmetry is not so large as to be completely washed out at the critical temperature), we can write

$$\eta_{\Delta L_i}(z_c) = -\sum_{\alpha=1}^{3} \delta^i_{N_\alpha} \kappa^i_{N_\alpha}(z_c). \tag{E.17}$$

Approximate solution

Now we derive the approximate solution 4.44 from equations E.16 and E.17. Note that we do not follow mathematically rigorous steps in this derivation. We define

$$A(z) \equiv \frac{2}{3} W_i(z), \tag{E.18}$$

$$B(z) \equiv -\frac{d\eta^{\mathrm{eq}}_{N_\alpha}}{dz} \frac{\widetilde{D}_\alpha(z)}{D_\alpha(z) + S_\alpha(z)} = \frac{1}{2\zeta(3)} z^2 K_1(z) \frac{\widetilde{D}_\alpha(z)}{D_\alpha(z) + S_\alpha(z)}. \tag{E.19}$$

Note that we have $A(z) \gg 1$ in the strong washout regime. We have

$$-\kappa^i_{N_\alpha}(z_c) = \int_{z_0}^{z_c} dz' B(z') \exp\left[-\int_{z'}^{z_c} dz'' A(z'')\right] \approx \int_{z_1}^{z_c} dz' B(z') \exp\left[-\int_{z'}^{z_c} dz'' A(z'')\right] \tag{E.20}$$

for some z_1 which is very close to z_c due to the large suppresion by the exponential factors. Since z_1 is close to z_c, we can also approximately write

$$\begin{aligned} \int_{z_1}^{z_c} dz' B(z') \exp\left[-\int_{z'}^{z_c} dz'' A(z'')\right] &\approx B(z_c) \int_{z_1}^{z_c} dz' \exp\left[-A(z_c) \int_{z'}^{z_c} dz''\right] \\ &= B(z_c) \int_{z_1}^{z_c} dz' \exp\left[-A(z_c)(z_c - z')\right] \\ &= \frac{B(z_c)}{A(z_c)} \left\{1 - \exp\left[-A(z_c)(z_c - z_1)\right]\right\} \\ &\approx \frac{B(z_c)}{A(z_c)}. \end{aligned} \tag{E.21}$$

At the last step, we assumed

$$A(z_c)(z_c - z_1) > 1, \tag{E.22}$$

which can be satisfied when $A(z_c) \gg 1$, i.e. $W_i(z_c) \gg 1$, with appropriate z_1. Then, we obtain

$$-\kappa^i_{N_\alpha}(z_c) = \frac{B(z_c)}{A(z_c)}, \tag{E.23}$$

which gives the expression 4.44. Note that this solution corresponds to

$$y_c = \frac{Q(x_c)}{P(x_c)}. \tag{E.24}$$

In other words, the expression 4.44 is approximately valid solution of the differential equation E.1 when

$$\left|\frac{dy}{dx}(x_c)\right| \ll Q(x_c) \approx P(x_c) y_c, \tag{E.25}$$

which can be satisfied if $P(x_c) \gg 1$, i.e. $W_i(z_c) \gg 1$.

Bibliography

[1] ATLAS Collaboration, *Observation of a new particle in the search for the Standard Model Higgs boson with the ATLAS detector at the LHC*, *Phys. Lett. B* **716** (2012) 1.

[2] CMS Collaboration, *Observation of a new boson at a mass of 125 GeV with the CMS experiment at the LHC*, *Phys. Lett. B* **716** (2012) 30.

[3] P. Minkowski, *$\mu \to e\gamma$ at a rate of one out of 10^9 muon decays? Phys. Lett. B* **67**, 421 (1977).

[4] T. Yanagida, in: A. Sawada and A. Sugamoto *eds.*, *Workshop on Unified Theories and Baryon Number in the Universe*, KEK, Tsukuba (1979).

[5] M. Gell-Mann, P. Ramond, and R. Slansky, in: P. Van Niewenhuizen and D. Freedman *eds.*, *Supergravity*, North Holland, Amsterdam (1980).

[6] R.N. Mohapatra and G. Senjanović, *Neutrino Mass and Spontaneous Parity Nonconservation*, *Phys. Rev. Lett.* **44**, 912 (1980).

[7] J.C. Pati and A. Salam, *Lepton number as the fourth "color"*, *Phys. Rev. D* **10**, 275 (1974).

[8] R.N. Mohapatra and J.C. Pati, *"Natural" left-right symmetry*, *Phys. Rev. D* **11**, 2558 (1975).

[9] G. Senjanović and R.N. Mohapatra, *Exact left-right symmetry and spontaneous violation of parity*, *Phys. Rev. D* **12**, 1502 (1975).

[10] E.Kh. Akhmedov and M. Frigerio, *Duality in Left-Right Symmetric Seesaw Mechanism*, *Phys. Rev. Lett.* **96**, 061802 (2006).

[11] M. Nemevšek, G. Senjanović, and V. Tello, *Connecting Dirac and Majorana Neutrino Mass Matrices in the Minimal Left-Right Symmetric Model*, *Phys. Rev. Lett.* **110**, 151802 (2013).

[12] J. Barry and W. Rodejohann, *Lepton number and flavour violation in TeV-scale left-right symmetric theories with large left-right mixing*, *JHEP* **09** (2013) 153.

[13] G. Bambhaniya, P.S. Bhupal Dev, S. Goswamia, and M. Mitrad, *The scalar triplet contribution to lepton flavour violation and neutrinoless double beta decay in Left-Right Symmetric Model*, *JHEP* **04** (2016) 046.

[14] D. Borah and A. Dasgupta, *Charged lepton flavour violation and neutrinoless double beta decay in left-right symmetric models with type I+II seesaw*, *JHEP* **07** (2016) 022.

[15] C. Bonilla, M.E. Krauss, T. Opferkuch, and W. Porod, *Perspectives for detecting lepton flavour violation in left-right symmetric models*, *JHEP* **03** (2017) 027.

[16] Y. Zhang, H. An, X. Ji, and R.N. Mohapatra, *General CP violation in minimal left-right symmetric model and constraints on the right-handed scale*, *Nucl. Phys. B* **802** (2008) 247.

[17] Planck Collaboration, *Planck 2015 result, XIII. Cosmological parameters*, *Astron. Astrophys.* **594**, A13 (2016).

[18] A. Maiezza, M. Nemevšek, F. Nesti, and G. Senjanović, *Left-right symmetry at LHC*, *Phys. Rev. D* **82**, 055022 (2010).

[19] MEG Collaboration, *Search for the Lepton Flavour Violating Decay $\mu^+ \to e^+\gamma$ with the Full Dataset of the MEG Experiment*, [arXiv:1605.05081v3].

[20] R. Sawada (MEG Collaboration), *MEG: Status and Upgrades*, *Nucl. Phys. B (Proc. Suppl.)* **248-250** (2014) 29.

[21] BaBar Collaboration, *Searches for Lepton Flavor Violation in the Decays $\tau^\pm \to e^\pm\gamma$ and $\tau^\pm \to \mu^\pm\gamma$*, *Phys. Rev. Lett.* **104**, 021802 (2010).

[22] T. Aushev *et al.*, *Physics at Super B Factory*, [arXiv:1002.5012].

[23] SINDRUM Collaboration, *Search for the decay $\mu^+ \to e^+e^+e$*, *Nucl. Phys. B* **299** (1988) 1.

[24] A.-K. Perrevoort (Mu3e Collaboration), *Status of the Mu3e Experiment at PSI*, *EPJ Web of Conferences* **118** (2016) 01028.

[25] P. Dornan, *Mu to electron conversion with the COMET experiment*, *EPJ Web of Conferences* **118** (2016) 01010.

[26] P. Wintz, in: H.V. Klapdor-Kleingrothaus, I.V. Krivosheina (*eds.*), *Proceedings of the First International Symposium on Lepton and Baryon Number Violation*, Institute of Physics Publishing, Bristol and Philadelphia, (1998) 534, unpublished.

[27] Y. Kuno, *PRISM/PRIME*, *Nucl. Phys. B (Proc. Suppl.)* **149** (2005) 376.

[28] SINDRUM II Collaboration, *Improved Limit on the Branching Ratio of $\mu \to e$ Conversion on Lead*, *Phys. Rev. Lett.* **76**, 200 (1996).

[29] A. Garfagnini, *Neutrinoless double beta decay experiments*, *Int. J. Mod. Phys. Conf. Ser.* **31** (2014) 1460286.

[30] A. Pilaftsis, *Radiatively induced neutrino masses and large Higgs-neutrino couplings in the Standard Model with Majorana fields*, *Z. Phys. C* **55**, 275 (1992).

[31] J. Kersten and A.Y. Smirnov, *Right-handed neutrinos at CERN LHC and the mechanism of neutrino mass generation*, *Phys. Rev. D* **76**, 073005 (2007).

[32] J. Gluza, *On teraelectronvolt Majorana neutrinos*, *Acta Phys. Polon.* **B 33** (2002) 1735.

[33] K. Kiers, M. Assis, D. Simons, A.A. Petrov and A. Soni, *Neutrinos in a left-right model with a horizontal symmetry*, *Phys. Rev. D* **73**, 033009 (2006).

[34] Z.-z. Xing, *Naturalness and Testability of TeV Seesaw Mechanisms*, *Prog. Theor. Phys. Suppl.* **180**, 112 (2009).

[35] X.-G. He, S. Oh, J. Tandean and C.-C. Wen, *Large Mixing of Light and Heavy Neutrinos in Seesaw Models and the LHC*, *Phys. Rev. D* **80**, 073012 (2009).

[36] A. Ibarra, E. Molinaro and S. T. Petcov, *TeV Scale See-Saw Mechanisms of Neutrino Mass Generation, the Majorana Nature of the Heavy Singlet Neutrinos and $(\beta\beta)_{0\nu}$-Decay*, JHEP **1009**, 108 (2010).

[37] M. Mitra, G. Senjanović and F. Vissani, *Neutrinoless Double Beta Decay and Heavy Sterile Neutrinos*, *Nucl. Phys. B* **856**, 26 (2012).

[38] N. Haba, T. Horita, K. Kaneta and Y. Mimura, *TeV-scale seesaw with non-negligible left-right neutrino mixings*, [arXiv:1110.2252 [hep-ph]].

[39] M.-C. Chen and J. Huang, *TeV Scale Models of Neutrino Masses and Their Phenomenology*, *Mod. Phys. Lett. A* **26**, 1147 (2011).

[40] M. Fukugita and T. Yanagida, *Baryogenesis Without Grand Unification*, *Phys. Lett. B* **174**, 45 (1986).

[41] A. Pilaftsis, Nucl. Phys. B **504**, 61 (1997) [hep-ph/9702393].

[42] A. Pilaftsis, Phys. Rev. D **56**, 5431 (1997) [hep-ph/9707235].

[43] A. Pilaftsis and T.E.J. Underwood, *Resonant leptogenesis*, *Nucl. Phys. B* **692** (2004) 303.

[44] J. Liu and G. Segrè, *Reexamination of generation of baryon and lepton number asymmetries by heavy particle decay*, *Phys. Rev. D* **48**, 4609 (1993).

[45] L. Covi, E. Roulet and F. Vissani, *CP violating decays in leptogenesis scenarios*, *Phys. Lett. B* **384**, 169 (1996).

[46] J.-M. Frère, T. Hambye, and G. Vertongen, *Is leptogenesis falsifiable at LHC?*, *JHEP* **01** (2009) 051.

[47] J.A. Casas and A. Ibarra, *Oscillating neutrinos and $\mu \to e, \gamma$*, *Nucl. Phys. B* **618** (2001) 171.

[48] M.A. Luty, *Baryogenesis via leptogenesis*, *Phys. Rev. D* **45**, 455 (1992).

[49] A. Pilaftsis and T.E.J. Underwood, *Electroweak-scale resonant leptogenesis*, *Phys. Rev. D* **72**, 113001 (2005).

[50] A. Pilaftsis, *Electroweak resonant leptogenesis in the singlet Majoron model*, *Phys. Rev. D* **78**, 113008 (2008).

[51] W. Buchmüller, P. Di Bari, and M. Plümacher, *Leptogenesis for pedestrians*, *Annals of Physics* **315** (2005) 305.

[52] F.F. Deppisch and A. Pilaftsis, *Lepton flavour violation and θ_{13} in minimal resonant leptogenesis*, *Phys. Rev. D* **83**, 076007 (2011).

[53] ACME Collaboration, *Order of Magnitude Smaller Limit on the Electric Dipole Moment of the Electron*, *Science* **343**, 269 (2014).

[54] D.S. Weiss, F. Fang, and J. Chen, *Measuring the electric dipole moment of Cs and Rb in an optical lattice*, *Bull. Am. Phys. Soc.* APR03, J1.008 (2003).

[55] Muon $(g-2)$ Collaboration, *Improved limit on the muon electric dipole moment*, *Phys. Rev. D* **80**, 052008 (2009).

[56] Belle Collaboration, *Search for the electric dipole moment of the τ lepton*, *Phys. Lett. B* **551**, 16 (2003).

[57] P. Duka, J. Gluza, and M. Zrałek, *Quantization and renormalization of the manifest left-right symmetric model of electroweak interactions*, *Annals Phys.* **280** (2000) 336.

[58] V. Cirigliano, A. Kurylov, M. Ramsey-Musolf and P. Vogel, *Lepton flavour violation without supersymmetry*, *Phys. Rev. D* **70**, 075007 (2004).

[59] C. Patrignani *et al.* (Particle Data Group), *Review of Particle Physics*, *Chin. Phys. C* **40**, 100001 (2016).

[60] A. Ilakovac and A. Pilaftsis, *Flavor violating charged lepton decays in seesaw-type models*, *Nucl. Phys. B* **437**, 491 (1995).

[61] A. Ilakovac, A. Pilaftsis, and L. Popov, *Charged Lepton Flavour Violation in Supersymmetric Low-Scale Seesaw Models*, *Phys. Rev. D* **87**, 053014 (2013).

[62] A. Pilaftsis and T.E. Underwood, *Electroweak-scale resonant leptogenesis*, *Phys. Rev. D* **72**, 113001 (2005).

[63] R. Alonso, M. Dhen, M. Gavela, and T. Hambye, *Muon conversion to electron in nuclei in type-I seesaw models*, *JHEP* **01** (2013) 118.

[64] J. Kotila and F. Iachello, *Phase space factors for double-β decay*, *Phys. Rev. C* **85**, 034315 (2012).

[65] A. Dueck, W. Rodejohann, and K. Zuber, *Neutrinoless Double Beta Decay, the Inverted Hierarchy and Precision Determination of theta(12)*, *Phys. Rev. D* **83**, 113010 (2011).

[66] J. Vergados, H. Ejiri, and F. Simkovic, *Theory of Neutrinoless Double Beta Decay*, *Rept. Prog. Phys.* **75** (2012) 106301.

[67] A. Faessler, A. Meroni, S. Petcov, F. Simkovic, and J. Vergados, *Uncovering Multiple CP-Nonconserving Mechanisms of $\beta\beta$-Decay*, *Phys. Rev. D* **83**, 113003 (2011).

[68] A. Faessler, G. Fogli, E. Lisi, A. Rotunno, and F. Simkovic, *Multi-Isotope Degeneracy of Neutrinoless Double Beta Decay Mechanisms in the Quasi-Particle Random Phase Approximation*, *Phys. Rev. D* **83**, 113015 (2011).

[69] A. Meroni, S. Petcov, and F. Simkovic, *Multiple CP Non-conserving Mechanisms of $\beta\beta$-Decay and Nuclei with Largely Different Nuclear Matrix Elements*, *JHEP* **02** (2013) 025.

[70] G. Pantis, F. Simkovic, J. Vergados, and A. Faessler, *Neutrinoless double beta decay within QRPA with proton-neutron pairing*, *Phys. Rev. C* **53**, 695 (1996).

[71] J. Suhonen and O. Civitarese, *Weak-interaction and nuclear-structure aspects of nuclear double beta decay*, *Phys. Rept.* **300** (1998) 123.

[72] J. Nieves, D. Chang, and P. Pal *Electric Dipole Moment of the Electron in Left-right Symmetric Theories*, *Phys. Rev. D* **33**, 3324 (1986).